COMPACT FORM FITTING SMALL ANTENNAS USING THREE-DIMENSIONAL RAPID PROTOTYPING

by

Bryan Jon Willis

A dissertation submitted to the faculty of
The University of Utah
in partial fulfillment of the requirements for the degree of

Doctor of Philosophy

Department of Electrical and Computer Engineering

The University of Utah

May 2012

The University of Utah Graduate School

STATEMENT OF DISSERTATION APPROVAL

The dissertation of **Bryan Jon Willis**

has been approved by the following supervisory committee members:

Cynthia Furse	, Chair	**3/27/12** Date Approved
Erik Brunvand	, Member	**3/27/12** Date Approved
Om P. Gandhi	, Member	**4/10/12** Date Approved
Steve Blair	, Member	**3/27/12** Date Approved
Joseph Mark Baird	, Member	**3/27/12** Date Approved

and by **Gianluca Lazzi** , Chair of the Department of **Electrical Engineering**

and by Charles A. Wight, Dean of The Graduate School.

ABSTRACT

Three-dimensional (3D) rapid prototyping holds significant promise for future antenna designs. Many complex designs that would be unmanufacturable or costly are realizable on a 3D printing machine. The ability to create 3D designs of virtually any configuration makes it possible to build compact antennas that can form fit to any space. These antennas build on the concept that small antennas can best reach the ideal operating limit when utilizing the entire 3D space in a sphere surrounding the antenna. Antennas require a combination of dielectric and conductive materials. 3D rapid prototyping is already well advanced for plastics and dielectric materials (with more options coming online). Prototyping with conductive materials has lagged behind; due mainly to their higher melting points, but this is advancing as well. This dissertation focuses on 3D rapid prototyping for antenna design. A 3D antenna made from small cubical cells is optimized for 2.4-3GHz using a genetic algorithm (GA). The antennas are built using 3D printing of plastic covered by conductive paint. The effects of the conductivity of the paint and number of layers on the resonance and gain of the antenna are evaluated. These results demonstrate the feasibility of using 3D rapid prototyping for antenna design.

A 3D dipole is also optimized using a GA to function from 510-910MHz. The antenna was built using 3D rapid prototyping from plastic. The 3D antenna was covered with a conductive coating and measured, showing good agreement with simulation. The 3D GA is used to design 3D antennas of random shape to fit inside the empty space in a cell phone case and optimized for cell phone bands 800-900MHz and 1.6-3.7GHz. The research also evaluates methods and materials that can be used to produce 3D antennas. In addition to the flexibility that 3D prototyping brings to antenna design, this paper describes how this new and emerging method for building antennas can provide fast and affordable antennas for testing, teaching, and fast turn-around prototyping.

TABLE OF CONTENTS

LIST OF FIGURES

LIST OF TABLES

ACKNOWLEDGEMENTS

I am grateful to Dr. Cynthia Furse and her tremendous help with this project. Her enthusiasm made this challenge a very fun learning experience. I am grateful to my wife for her support and for the support of my family, especially my father and mother who instilled in me the love for learning.

CHAPTER 1

INTRODUCTION

Small antenna design is a longstanding area of great importance and interest. It is an ever present reality that as electronic devices continue to get smaller, antenna size must continue to decrease. Smaller antennas with improved performance are necessary to keep pace with electronics that are decreasing in size while increasing in memory and processing speed. The planar or wire antennas most commonly used today allow a part of the geometry to decrease in size; however, they do not take advantage of a significant portion of the volume and are therefore necessarily suboptimal in their designs. One way to improve small antenna performance is to use three-dimensional (3D) designs rather than one-dimensional (1D) (wire) or two-dimensional (2D) (planar) designs.

This dissertation will demonstrate how 3D antennas can be built with rapid prototyping methods to create a new opportunity in antenna design. This antenna can be designed with virtually any shape or configuration. They can fill arbitrary 3D spaces, and are easy to build, inexpensive, and light weight. Virtually any antenna can be built in minutes and thus provide a ready supply of test antennas at your fingertips.

Information on the benefits of 3D antenna design begins with the well-known research on small antennas completed by Wheeler [1] and Chu [2]. The definition of a

small antenna is based on the area of a sphere which encompasses the antenna. Future work such as that done by Mclean [3] has refined the small antenna limit; however, the 3D region still defines the antenna size. All good approximations at meeting the small antenna limit attempt to utilize as much of the 3D space as possible.

Some applications (putting an antenna on the skin of an aircraft, for instance) limit thickness, but there are many other applications where a thicker 3D design is practical. There is often a 3D space that goes unused in our electronic devices, and this 3D space could potentially be filled to create a better antenna. Our research is based on filling the available cavity or shape with a conductor whose final shape can be optimized to perform over a variety of requirements. Requirements include impedance, bandwidth, radiation pattern, gain, and polarization. The shape chosen for this research is to divide the available antenna volume into subwavelength cubes, then each cube is composed of air or conductor. The cube size is chosen based on the wavelength at which it is designed to function; our standard is ~1/30 of a wavelength. A representative antenna geometry with the feed centered between two rectangles is optimized to function as a 3D dipole in the 500-900 MHz band. The antenna structure composed of cubes is shown in Figure 1.

A few attempts at true 3D antennas have been made, some of which are shown in Figure 2, and have initially demonstrated the promise of 3D designs [4], [5] . The manufacturing methods required to produce these antennas are so cumbersome that they have been regarded mainly as far-fetched and impractical designs. But now, cutting edge rapid prototyping of conductive materials is creating 3D manufacturing opportunities that have not previously been available in the antenna design world.

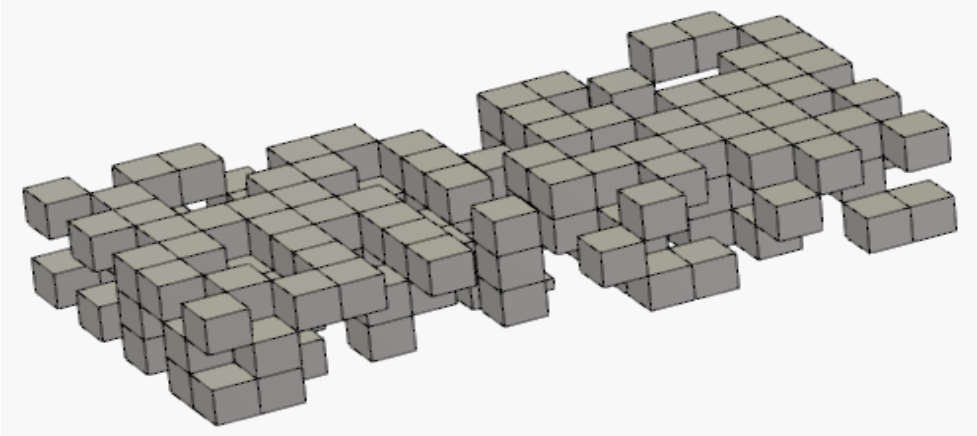

Figure 1: Representation of antenna geometry using subwavelength sections to compose the antenna. This antenna is described in more detail in Chapter 4.

Examples of nonantenna objects are shown in Figure 2, as well. 3D printing [6], [7], selective laser sintering [8], and other high-power melting techniques [9], long available for plastics, are beginning to emerge with effective conductive materials [9], [11].

Silver inks for 3D-type printing have been used along with new designs utilizing a 3D space [15], [16]. Conductive paints commonly used for electromagnetic interference (EMI) shielding are finding their way into the design world [17]. Complicated structures are now easier to machine with tools such as a 5 axis computer numerically controlled CNC mill [18]. Electrical discharge machines (EDM) are also utilized to build complicated structures for microwave devices and are becoming better suited for standard machine shop use [19], [20]. 3D printing or 3D rapid prototyping is an area which has expanded rapidly over the last few years [21]. New 3D printing machines are more common in commercial settings and have found use in areas from medical services to machine shop prototypes [22] .

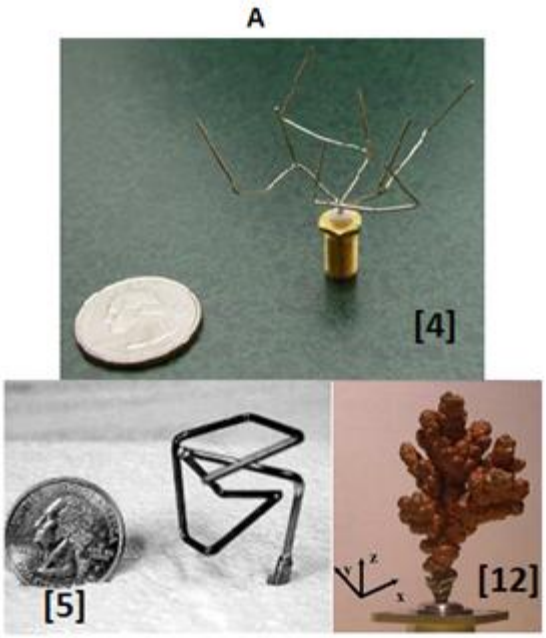

Figure 2: 3D antennas from [4], [5], [12] are optimized and then manufactured by hand and/or using other uncontrolled methods. Antennas are built using controlled 3D rapid prototyping and they indicate the current resolution that is available today. The antenna in [13] is a gold plated plastic cell phone antenna created by laser direct structuring, and [14] provides resolution information on a 2-material 3D printed foot. © 2002, 2007, 2010, IEEE. Reprinted with permission.

One of the great benefits of 3D prototyping machines is the ability to produce complicated 3D geometry and at roughly the cost of the plastic. The basic 3D printers have lower resolution in the 0.5mm range and a slower printing time than their industrial counterparts but are an affordable alternative. 3D printing has developed an online open source community (reprap.org). The community provides links to suppliers for build-it-yourself machines and stores an enormous online repository of available 3D drawings which others have created and shared. 3D printing has the ability to easily create complicated objects quickly and easily in plastic. Our research indicates that using conductive coatings over plastic objects can create antennas that perform quite well.

1.1 Contributions

This dissertation focuses on developing the concepts and design tools necessary to take advantage of the emerging 3D build technology, thus positioning engineers to rapidly design and deploy true 3D antennas that come closer to meeting the optimal designs that theory predicts. This dissertation addresses challenges specifically associated with 3D rapid prototyping for antennas, including design optimization tailored to these methods, and the effects of imperfectly conducting materials. The work here focuses not only on 3D prototyping equipment available today but also the technology that is anticipated to emerge in the next 5 years.

The major contributions of this dissertation are:

1) Introduction of the concept of using 3D rapid prototyping for antenna design. The antennas designed in Chapter 3 are the first of their kind and represent a major shift in antenna design through easy, low-cost 3D manufacturing.
2) Demonstration of the applications where 3D antennas may be most useful. These include the ability to fully utilize the 3D sphere often associated with small antenna theoretical limits [23]. 3D antennas can more closely approach this limit. In addition, the ability to fill random-shaped voids such as those in handheld personal communication devices [24] may provide better antennas for a wide variety of applications. Finally, the advantages of low weight and quick turnaround time are also noted. This information is found in Chapter 4 [24].
3) Evaluation of the impact of conductivity and thickness of the metallic components of the design (typically metal paints or plating) on the efficiency and performance of the antennas [25]. Chapter 5 outlines the requirements as a function of

frequency, and describes the frequency range where 3D rapid prototyping is effective today.

4) Contemplation and evaluation of the future of 3D rapid prototyping for antenna design is found in Chapter 6 [26]. 3D prototyping is rapidly advancing, and this chapter evaluates what changes are coming, what changes are needed, and what these changes may mean for future antenna design and manufacture.

In short, this dissertation provides the tools and methods for a new type of 3D antenna manufacturing that has the potential to revolutionize small to moderate scale antenna design by providing the great flexibility in form and design for 3D manufacturing that has to date been available only for 2D (planar) designs.

CHAPTER 2

BACKGROUND

2.1 Small Antenna Design

Small antenna design and research dates back to early work completed by Wheeler 1947 [1] and Chu [2] in 1948. The small antenna limit (sometimes called the 'Chu Limit') is also known as the Q lower bound. Q is the quality factor and is given in terms of resonance energy. The Q lower bound defined by Chu indicates the size of the sphere (given in terms of wavelength or frequency) that allows the radiated energy mode to exist and to propagate.

$$Q = \frac{1}{(ka)^3} + \frac{1}{ka} \tag{2.1}$$

$$Q_{lb} \geq \eta\left[\frac{1}{(ka)^3} + \frac{1}{ka}\right] \tag{2.2}$$

$$Q_{Lossy} = \eta Q_{Lossless} \tag{2.3}$$

Here *k* is the wave number which is equal to $\omega\sqrt{\varepsilon\mu}$, and *a* is the radius of a sphere which encompasses the entire antenna. For an antenna to be defined as small, typically *ka* is less than 0.5 [27]. The Chu limit was found based on the radiation modes from a capacitor model approximation. This is still utilized today as the absolute minimum size for an antenna that radiates at a specific frequency. Researchers have continued to better define the lower bound, including Chu in [28], and Wheeler in [29], [30]. Hansen further investigates the limits of antennas in 1981 [31], and then proposed a new Chu formula in 2009 [32]. Thal looked at specific spherical antenna geometry and proposes new limits for the antenna spherical antenna [33], [34]. In reality, antennas are not 100% efficient [35], so he added efficiency η to make a more complete lower bound, which is given in [3] and widely accepted as a fundamental limit based on Chu's original work.

In this research, we look at utilizing the 3D space to efficiently use it for an antenna and keep the radius as small as possible. This research also discusses the ability to manufacture complicated 3D geometry and materials that can be used for a highly efficient antenna. Many of the miniaturization techniques utilized today can also be applied to 3D antennas.

Perhaps the most common way to miniaturize an antenna is to reduce its physical size while maintaining its electrical size. This is done by decreasing the wavelength within the antenna structure and/or its very near field using high dielectric materials [36], [37] and/ or electronic band gap (EBG) materials [38]. Higher dielectrics, however, increase the mismatch to free space and decrease radiation efficiency [39] [40]. Metamaterials have also been used to reduce the effective wavelength using materials with a negative index of refraction (NIR). Resonant antennas have been produced with an

impedance matching NIR shell [41], [42]. There has been much interest in this area lately and numerous papers, [41], [42], [43], [44], [45], but the metamaterial antennas that have been produced also have poor radiation efficiency [43], [46] because of the lossy nature of the NIR metamaterial [47]. The latest published research in small antennas at the time this article was written are to decrease the size of the antenna using a composite right- and left-hand material structure with a planer inverted F antenna [48], or a dielectric resonator utilized as an antenna [49].

3D antennas have been reviewed extensively, [5], [15], [33], [34], [50], [51] [52][53][54][55] and indicate promise in utilizing the 3D geometry to lower the operating frequency, increase the bandwidth, and reduce the size of the antenna [56]. For example, Best demonstrates low Q small spherical dipoles [50] and properties of a small spherical helix [51]. The spherical helix antenna is made up of hand-soldered pieces of wire. The design indicates a Q within 1.5 times the fundamental limit $ka < 0.5$ and efficiencies at or above 90%.

It should be noted that before Wheeler and Chu did their work on the small antennas, Schelkunoff was defining the theory for antennas of arbitrary size and shape [57]. Current research on limitations for arbitrary shaped antennas has been completed by Gustafsson [58]. Research completed over a decade ago by Herscovici examines the added efficiency of 3D extrusions for microstrip antennas [59]. He designed the antenna with the ability of a practical single-step build and large-quantity fabrication [59]. A second microstrip antenna is built using layers of etched substrate to add 3D parasitic coupling elements [60]. A stacked microstrip patch makes use of multiple layers of

substrate with different dielectric constants and a coupled 3D feed design. The impedance bandwidth for the stacked microstrip patch is increased to 3:1 using these techniques.

For virtually all wireless applications, effective use of space is an important criterion for antenna design. Over the last decade, wireless handsets in particular have virtually phased out external antennas. Antennas designed for use as internal embedded antennas began to ramp up just over a decade ago. The dilemma over best use of space for maximum performance in a handset is illustrated by David McCartney in April of 2000 [61] and by Skrivervik in 2001 [56].

Some applications strongly prefer planar antennas such as those mounted on the surface of space craft. Others could use available 3D space such as those inside the case of a cell phone [13] or inside the human body, but currently use planar or semiplanar antennas to reduce cost or simplify the analysis. True 3D antennas have been explored in the past for RFID applications [62], multisector antenna designs [63], and for wireless communication [64]. Galehdar [62] has designed an optimal 3D meander line antenna for RFID tag applications. This 3D antenna is shown in Figure 3. Optimizations are performed over various 3D configurations, and the best design is chosen. This 3D antenna even works well when placed close to a ground plane. Altshuler [12] used an optimization method to find the best performing wire antenna within a rectangular size limitation. The antenna in Figure 3 has been optimized for high gain, good impedance match, and minimal resonant frequency (equivalent to maximum effective electrical size). This and similar wire antenna designs [65] gained interest and curiosity, but were clearly impractical to build.

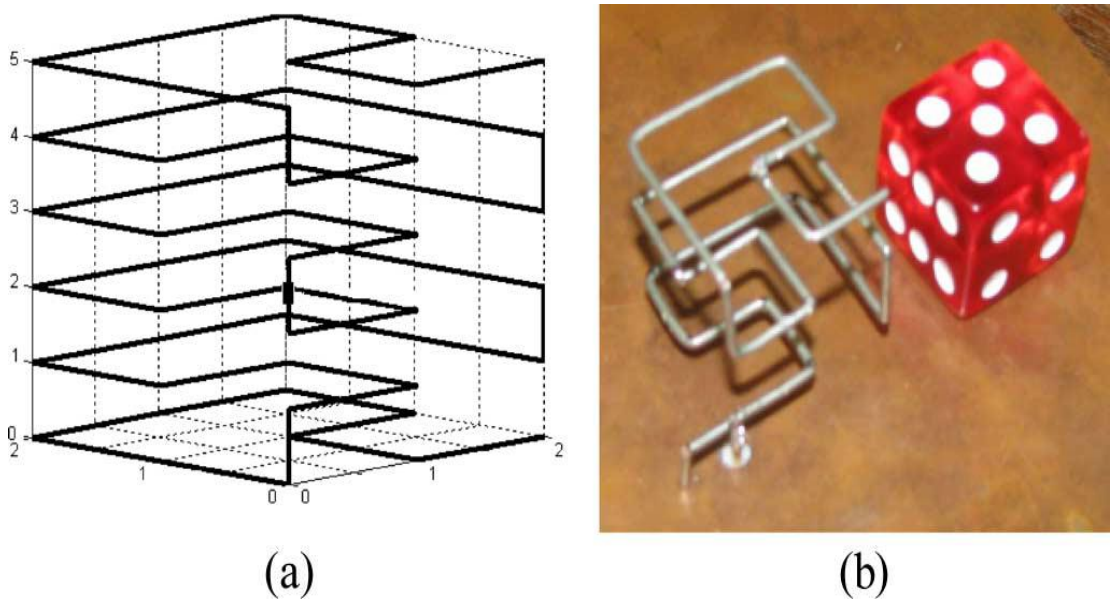

Figure 3: 3D Meander line antenn for passive RFID applications, from [12]. © 2002 IEEE. Reprinted with permission.

Soora [66] designed a 3D triangular and rectangular spiral antenna for a retinal prosthesis. These antennas have helped in achieving small size and enhanced bandwidth as well as achieving broadside radiation pattern. Thevenard [63] provided a conceptually simple 3D multisector antenna based on an original layout of Vivaldi-type antennas, compatible with metalized plastic manufacturing technology. This solution offers great freedom in shape and dimension as well as the potential for mass production of the antenna at low cost, as shown in Figure 4.

Serra [67] simplified the manufacturing of the standard 3D planar inverted F antenna (PIFA) by building the antenna from a single metal sheet, cut and bent to shape. The 3D prototyping methods that are new or emerging provide the opportunity to readily design and build true 3D antennas economically.

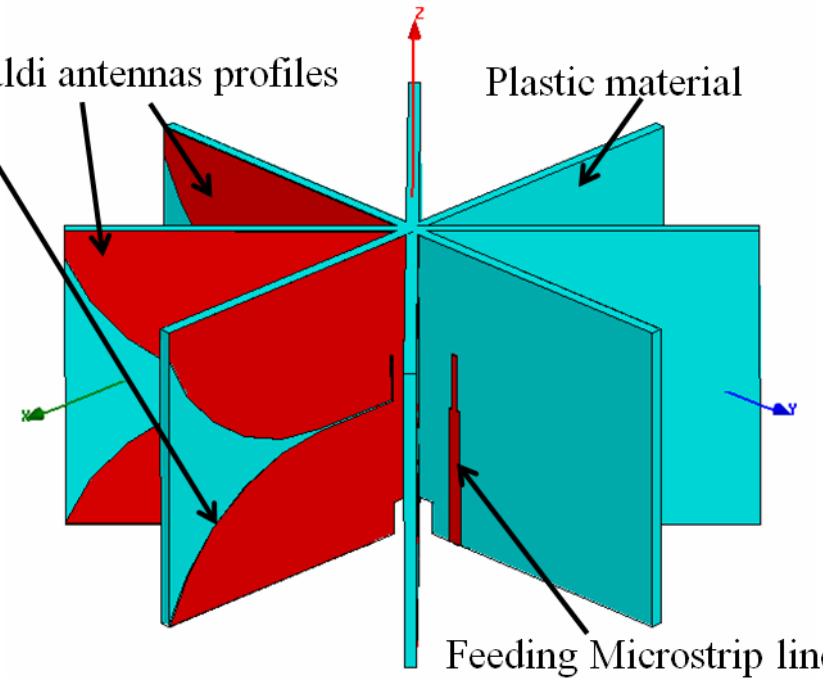

Figure 4: Thevenard Vivaldi type antennas [63]. © 2007 IEEE. Reprinted with permission.

2.2 Next Generation Manufacturing

3D antenna designs are an evolving technology which is becoming more mainstream. The complicated 3D antenna structures are becoming less of a challenge to manufacture. This is in part due to the progress in the mechanical design and manufacturing, including manufacturing which is applicable to good conductors. Rapid prototyping with conductive materials is creating an opportunity for true 3D antenna designs that have previously been impractical. In this research, we evaluate methods and materials which have been used to create 3D antennas or provide the ability to create 3D antennas. There are many methods we did not evaluate which are excellent candidates for building 3D antennas. A few of the methods we believe would be ideal candidates and those we evaluated are described in detail in this section.

There are several promising and emerging 3D prototyping methods that can be used to create metallic and nonmetallic shapes [48]. These include selective laser sintering [8], [9], selective laser melting [9], electroforming [11], and electron beam melting [11] [48]. 3D antenna designs can also be produced by coating a plastic shape with conductive paint [17]. Other unorthodox methods are continually arising; recently, 3D spherical antennas have been built using a process called direct transfer patterning [68]. The process uses a stamp to get the desired pattern onto a curved surface. It then requires a 6-step process including a plasma etch and gold plate to finalize the design on Polyethylene Terephthalate (PET). In [68], the conductor is thickened by the plating process and in [69], it was found that the transfer of thicker metals proved to be difficult, possibly due to wrinkling of the stamp during metal deposition [69]. The research here shows an array of 10 nm thick, 500 micro meter wide Au stripes transferred onto a PET hemisphere. A sheet resistance of 7 ohms/square for 10 nm gold was estimated from measurements made between several points along the metal stripes. This corresponds to 7 X 10^{-6} Ohm·cm, consistent with that of conventional gold thin films [69]. Similarly, 3D antennas have recently been built using conductive silver nano-particles printed on a spherical glass surface [15]. The printing method in [15] uses a small nozzle on a robotic hand to draw a very high conductivity ink on a preshaped glass substrate (in this case, a hemisphere). The ink has reported conductivity of ~1X10^{6}S/m [70]. The 3D nozzle printing method would be more difficult to apply for more complex 3D designs such as those that might be required to fill random-shaped voids.

A method known as laser direct structuring (LDS) is a procedure which requires a multiple-step process. In the process, the plastic where the conductive plating is desired is

typically etched with a laser or chemical etchant. The etched area allows the conductive particles from the polymer to be on the surface and the treated plastic is ready for metallization. The metallization is typically completed by a plating process [13].

Another emerging process uses atomic layer deposition (ALD) to coat a substrate with a nano meter thick conductive layer [71]. Also, a similar technique allows a thin layer to be plated by element sputtering to create thin conductive films [72]. The nanofabrication lab at the University of Utah provided us with an antenna made of gold using ALD on a glass substrate. They also provided one built from sputtering using platinum on a glass substrate. Both of these methods apply a thin conductive film, and are typically used in fabricating micro and nano electronics. It should be noted that it is possible for the films to be plated to a desired thickness.

Electroless plating allows for a conductive layer to be built up by a chemical reaction rather than electrical. The process relies on the presence of a reducing agent which reacts with the metal ions to deposit metal. The base material may be arbitrary shaped and it does not require line of sight [73].

Electroforming is similar to the plating process, but it builds up an object that is much thicker. Typically, electroforming starts with a nonmetallic object. The nonmetallic object is coated with a conductive material, and then built up by electro-plating until it is the desired thickness [9]. Selective laser sintering or melting is similar to electron beam forming. A layer of fine metallic power is spread out, and a high power beam is scanned over the layer to create the 3D geometry. The beam fuses the powder together for that specific layer. When the layer is complete, the build platform is lowered, a new layer of powder is spread, and the beam again hardens that layer [8].

These fusing techniques typically use a 40 micrometer spot beam laser. The laser in combination with the particle size of the powder determines the surface resolution without finishing (typically less than 0.1 mm) [48] Utilizing selective laser sintering as a manufacturing method for antennas is not common. Huang makes use of selective laser sintering to design a plastic mold for wrapping a helix [74]. Sigmarsson uses the process to sinter a layer on a low temperature substrate [75]. Ventis, a wideband antenna manufacture, claims to use selective laser sintering to build complex shapes in their designs [76]. Unfortunately, there are no available references or pictures.

Printing in 3D is becoming more widespread [6], [7], and the cutting edge is printing conductive materials. Using conductive materials with low temperature melting points has been proposed [77]; however, the final product is not thermally stable. 3D conductive printing is making progress; one 3D machine makes use of a separate wire feed printing head to accomplish this [6]. 3D printing is typically accomplished by using an injector that drops a quick hardening resin compound at a precise point for a single layer. The 3D object is then built up in printed layers. This is commonly known as layer deposition modeling (LDM). Initially, 3D printing was done using a powder base and then ink jetting a binder over each layer [9]. 3D printing plastic objects with UV curable plastic stereolithography allows for precise quick builds.

ABS, a common plastic, is used for the LDM type of desktop 3D printer. It is relatively inexpensive and can be found at k-mac-plastics; a 0.25 inch rod costs $1.25 per foot [78]. Botmill sells 5 lbs. of 3mm ABS rod designed for specific 3D printers for $45.00 [79]. A basic 3D printing machines currently costs approximately $1000.00 [79].

The processes vary in the materials they can use and the resolution and complexity they can provide [22]. Today's resolutions for 3D printing are on the order of 0.0006 inches [14]. The resolution provided is common for most low-cost manufacturing methods. One item of note which demonstrates the strong international and economic interest in conductive 3D prototyping, an $80,000 Gada prize (to be given in 2012-2015) was recently announced for the development of advanced 3D printing [77], [80]. One of the requirements for winning is the ability to print useful conductive materials such as those for circuit boards [80].

In this research, selective laser sintering and 3D printing are used to manufacture the initial complicated antenna geometry. Selective laser sintering is used to build a solid conductor and 3D printing is used to build the initial plastic antenna which is then coated with a conductive layer. 3D printing is chosen based upon the background work completed researching next generation manufacturing and a trade study in cost and ease of use. Throughout this project, it has been important to remain abreast of the emerging improvements in 3D rapid prototyping and adapt our designs as needed to keep pace with these capabilities. The open source information will be used to stay up to date with the latest developments in the conductive printing technology. The Objet Connex 500 [14] was graciously hosted by L-3 to build 4 prototype 3D antennas for this research.

2.3 Conductive Materials and Effects of Imperfect Conductors

The effect of imperfect conducting metals on efficiency is a critical parameter when designing small antennas, as efficiency is a parameter in the small antenna equation. One of the chief concerns of this project is to validate the degradation in

radiation efficiency due to manufacturing with a lossy conductor. Recently, there has been much research on imperfectly conducting materials. Applications include replacements for lead-based solder [81],[82], [83], [84], [85], [86], [87], transparent antennas for use over solar panels [88], [89], [90], [91], [92], protective coatings for the high-voltage stator windings on high-power generators [93], [94], flexible and wearable antennas [91], [92], [95], [96], [97], and others. Metals used in fabrication range in conductivity from aluminum 1.0 X 10^6 S/m to silver 6.0 X 10^7 S/m whereas imperfectly conductive materials proposed to replace them can range from paints 1.0 X10^4 S/m to metal mixtures 1.0 X10^6 S/m [98], [93], [97], depending on their compositional makeup. Reducing the electrical conductivity decreases the efficiency and increases losses due to resistance and skin effects [99], [100]. This project will extend the theoretical analysis done for imperfectly conducting transparent antennas [99], [100], to imperfect conducting materials used in 3D prototyping. In [99], [100],we used the Drude model to predict the skin depth and loss effects in detail at multiple frequencies to bound the theoretical antenna efficiency and performance. This project explores the tradeoffs expected when using different 3D prototyping techniques, and will evaluate the implications for antenna design now and as the materials and methods mature.

Imperfectly conducting materials have been used in a variety of electrical and antenna applications. Materials include paints [99], [101], [102], conductive adhesives [81], [82], [83], [84], [85], [86], epoxies [84], [85], polymers [98], [93], [103], [94], [104], [81], [87], [105], optically transparent films [99], [100], [88], [89], [90], thin silicon films [93], [103], nano-fiber [94], [104], [86], [87] powder metals [92], [93], and even conductive fabrics [105], [101], [90], [91], [92], [95], [96], [97]. A material of

particular interest is a metallic flake mixture composed of mostly aluminum with a melting point at approximately 500 degrees Fahrenheit [106]. This metal mixture is currently used for injection molding of metal parts [106]. A similar thermo plastic with carbon fiber and nickel powder is given in [107] and [108]. The lower temperature conductive materials are considered in this research as they may be useful in 3D printing conductive objects.

In order to better understand the importance of the material constraints and how they impact 3D antenna design, this research examines a standard monopole or dipole antenna design using imperfectly conducting materials (with emphasis on paints and printed materials, the most likely near-term materials for rapid prototyping). Skin depth losses and the effect of very thin layers of conductive material, ground effect losses, and surface resistance of the antenna all result in lower efficiency and are evaluated. Once these effects are understood for the dipole antenna, they will be expanded to 3D prototype techniques and materials. The work here evaluates 1) the necessary components and requirements of a conductive material for antenna design, 2) the losses associated with imperfectly conducting materials due to ground and skin effect losses, and manufacturing 3) if 3D optimized antenna designs mitigate these losses and improve efficiency [99], [100].

2.4 Conductivity and Efficiency Measurements

For the measurements, we have selected a sample of materials discussed above. We performed our own characterization of materials using a 4-point probe to measure conductivity and a wheeler cap [109] to measure radiation efficiency. The goal is to

further our understanding between the conductivity of the material, the skin depth, and the efficiency loss for an antenna radiating at a specific frequency. The primary focus is to evaluate the use of emerging techniques and materials which use imperfect conductors. The data are compared to manufactures specifications for conductivity. The measured radiation efficiency is compared to solid copper sheet and to simulated data using lossy materials.

The wheeler cap is designed such that the antenna above a ground plane has its radiated fields shorted out in the near field region. The shape of the cap in this research is constructed to be a rectangular form. Other shapes such as cylinders can be used. The cap also acts as a resonant cavity and it must be designed such that the cavity resonance falls outside the resonance region of the antenna. The fields created inside the cap are then strictly determined by the radiated fields due to the antenna.

The 4-point probe is used to measure conductivity. The thickness of the sample is given by *t*. In the derivation, *t* is required to be much less than the spacing of the probes. The probe spacing on our equipment is given as ~1.5mm. The derivation begins by finding the differential resistance given by the area of the conductive being measured

$$A = 2\pi xt \tag{2.4}$$

Resistance is then

$$R = \int_{x1}^{x2} \rho \frac{\partial \mathrm{x}}{2\pi \mathrm{xt}} \tag{2.5}$$

Substituting for R

$$R = \left(\frac{v}{2I} \right) \tag{2.6}$$

We then solve for the sheet resistivity

$$\rho = \frac{\pi t}{\ln 2}\left(\frac{V}{I}\right) \quad (2.7)$$

In general, sheet resistivity Rs = ρ/t and can be expressed as

$$R_s = k\left(\frac{V}{I}\right) \quad (2.8)$$

where *k* in the case of the semi-infinite thin sheet is *k*=4.53 (which is just *π/ln2)*. The sheet resistivity is given in Ohms/square. To convert to Ohm meters or cm, the thickness of the sample must be factored into the equation. R_s is multiplied by the thickness giving the units of Ohm meters. It is well known that the conductivity is the inverse of the electrical resistivity and is given in Seimens/ meter, which has the units of inverse ohms per meter.

The following materials are measured on the 4-point probe and the results are shown in Table 1. LDS over plastic is designed such that the plastic part is plated with a 40 um layer of gold. Silver and copper conductive paints are sprayed onto a paper substrate. Both are sprayed with three coats of paint. Copper paint is also tested for a single paint layer, and the injection molding material Xyloy® is tested. A standard piece of 17 um copper sheet is used to verify the 4-point probe measurements. Silver epoxy is evaluated and it is used to attach the antennas to the center conductor pin for the antennas. The measurements for gold ALD and platinum sputtering were measured previously by the university of Utah nano-fabrication lab. Other emerging materials have been added to the table as a comparison. The following materials have not been tested on the 4-point probe or for radiation efficiency, and the information included was provided by the available reference. The materials are silver nano-particle ink from [15], and the low temperature carbon fiber melt extrudable thermoplastic from [108].

Table 1: Measured data using the 4-point probe

Material	mV measured	Thickness micro-meters	Ω /□	Resistivity Ω·m	Conductivity S/m
Gold LDS	0.052	40	0.002	$1.17X10^{-8}$	$8.49\ X10^{7}$
1 layer Copper Paint	6.61	16	0.298	$5.27X10^{-6}$	$1.90\ X10^{5}$
Copper Paint	1.97	23	0.089	$2.10X10^{-6}$	$4.77\ X10^{5}$
Silver Paint	1.97	23	0.030	$7.07X10^{-7}$	$1.42\ X10^{6}$
Copper sheet	0.057	17	0.002582	$4.38X10^{-8}$	$2.3\ X10^{7}$
Xyloy	0.024	500	0.001359	$1.69X10^{-7}$	$5.89\ X10^{6}$
Silver Solder (epoxy)	20	125	0.0453	$2.27X10^{-5}$	$4.42\ X10^{4}$

The method described as direct transfer patterning is given in [68]. The material in [68] had an additional thickness from being plated and our information for conductivity was obtained from [69].

The measurements taken had a correction factor applied due to the standard copper sheet measuring ~30% lower than $5.96X10^{7}$. Table 2 presents the data with the correction factor applied. Table 3 provides the skin depth calculations. Figure 5 then indicates how the copper paint compared to the manufacturer's given data. The measured antenna efficiencies are completed using the monopole antennas above a ground plane. The radiation efficiencies are measured using the wheeler cap and are then given in Table 4.

Table 2: Measured data with correction; also included are additional data found in the current literature.

Material	mV measured	Thickness micro-meters	Corrected Ω /□	Corrected Resistivity Ω·m	Corrected Conductivity S/m
Gold LDS	0.052	40	0.00089	4.4910^{-9}	$2.22\ X10^{8}$
1 layer Copper Paint	6.61	16	0.114	$2.01X10^{-6}$	$4.97X10^{6}$
Copper Paint	1.97	23	0.034	$8.0X10^{-7}$	$1.25X10^{6}$
Silver Paint	1.97	23	0.0114	$2.70X10^{-7}$	$3.71X10^{6}$
Copper sheet	0.057	17	0.00098	$1.67X10^{-8}$	$5.96X10^{7}$
Xyloy	0.024	500	0.00051	$6.48X10^{-8}$	$1.54X10^{7}$
Silver Solder (epoxy)	20	125	0.0179	$8.65X10^{-6}$	$1.16X10^{5}$
Premier Carbon fiber	NA	23	0.25	$5.75X10^{-6}$	$1.73X10^{5}$
Silver nano ink	NA	12	NA	$5.2X10^{-7}$	$1.9X10^{6}$
Direct Transfer patterning	NA	0.010	7	$7X10^{-8}$	$1.43X10^{7}$
Gold ALD	NA	0.035	1.2	$4.2X10^{-8}$	$2.38X10^{7}$
Platinum Sputtering	NA	0.190	1.07	$2.0X10^{-7}$	$4.92X10^{6}$

Table 3: Skin depth calculations given in microns at 0.5, 1.6, 2.6, and 15 GHz for the materials of interest.

Material	Corrected Resistivity Ω·m	Skin depth in microns f=0.5 GHz	Skin depth in microns f=1.6GHz	Skin depth in microns f=2.6GHz	Skin depth in microns f=15GHz
Gold LDS	$4.4X10^{-9}$	1.51	0.84	0.66	0.28
Thin Copper Paint over plastic	$2.0X10^{-6}$	31.9	17.84	13.99	5.83
Copper Paint over plastic	$8.0X10^{-7}$	20.13	11.25	8.83	3.68
Silver Paint over plastic	$2.7X10^{-7}$	11.7	6.54	5.13	2.14
Copper sheet standard	$1.6X10^{-8}$	2.91	1.63	1.28	0.53
Xyloy	$6.4X10^{-8}$	5.73	3.2	2.51	1.05
Premier Carbon fiber	$5.7X10^{-6}$	53.97	30.17	23.67	9.85
Silver nano ink	$5.2X10^{-7}$	16.23	9.07	7.12	2.96
Direct Transfer patterning	$7X10^{-8}$	6	3.33	2.61	1.09
Gold ALD	$4.2X10^{-8}$	4.61	2.58	2.02	0.84
Platinum sputtering	$2.0X10^{-7}$	10.07	5.63	4.41	1.84

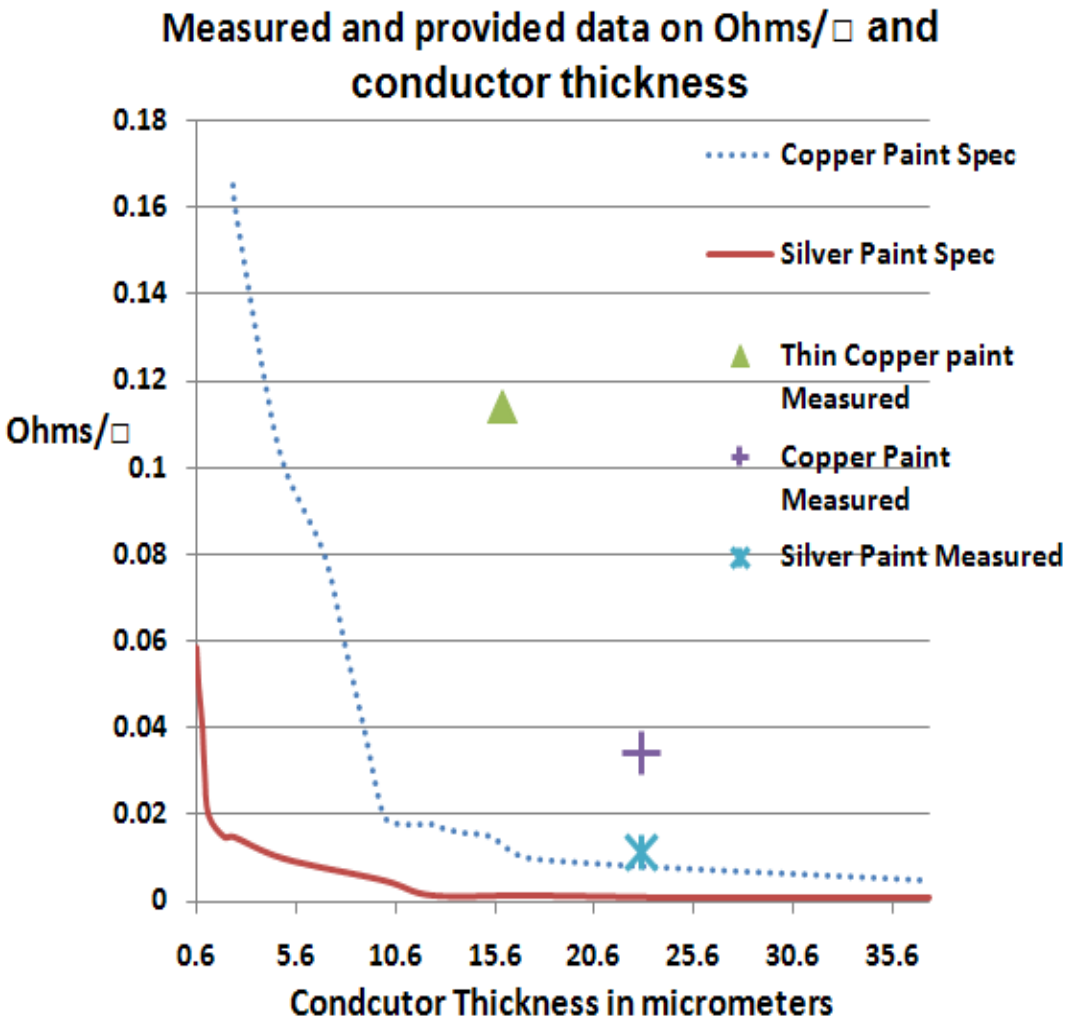

Figure 5: Data from copper paint compared to the manufacturer's data from [110]. © 2012 IEEE. Reprinted with permission.

2.5 Initial Simulation for Background Research

The initial research completed on 3D antenna design for this project began by taking a basic patch antenna and expanding it into 3D space. The basic flat patch was expanded upward to a half height sphere and then to a full half sphere. The design was optimized to have the lowest operating frequency and the widest bandwidth. The antennas and the results are shown in Figure 6.

Table 4: Measured radiation efficiencies for the tested antennas

Material and length	Resonant point in GHz	% Radiation efficiency
Gold plating 35mm	1.79	81 %
Silver Paint 35mm	1.79	75 %
Copper Paint 35mm	1.79	74 %
Copper sheet 35mm	1.79	81 %
Xyloy® 35mm	1.79	81 %
Gold LDS 35mm	2.2	86 %
Titanium 25mm	2.8	41 %
Gold ALD 40mm	2.1	39 %
Silver Paint 70mm	1.64	86 %
Copper Paint 70mm	1.64	74 %
Copper sheet 70mm	1.64	94 %

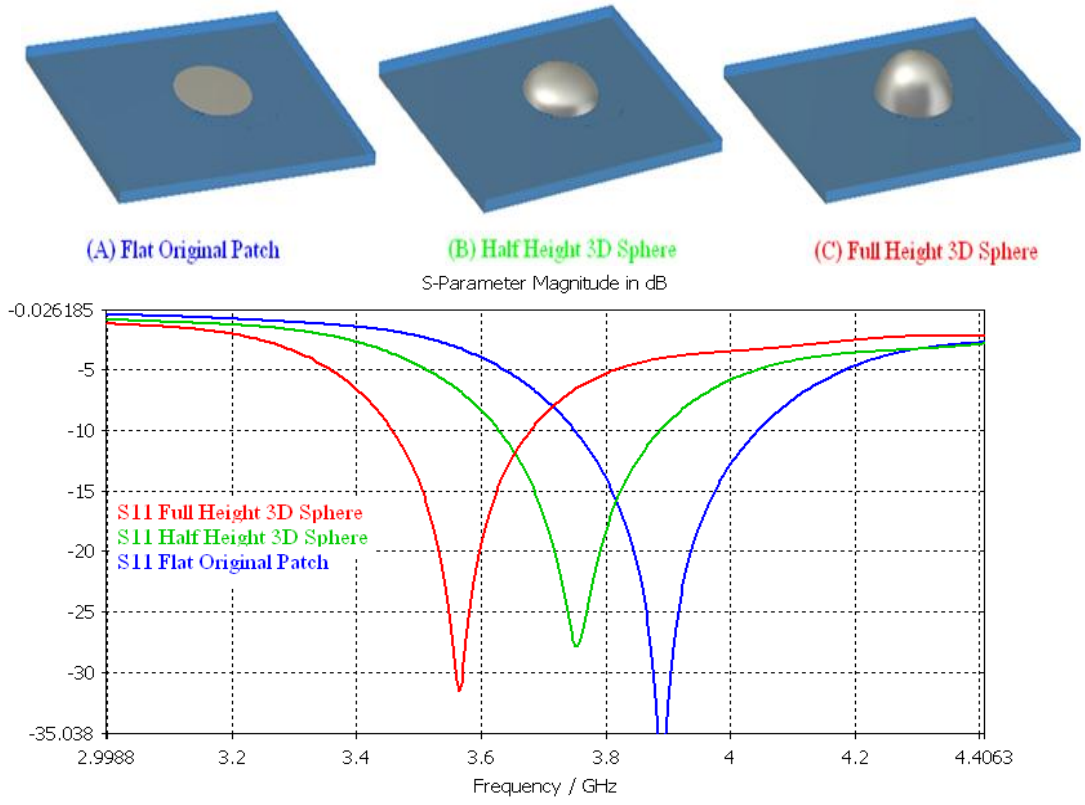

Figure 6: 3D patch antenna and return loss results for preliminary design work.These early results indicated that as we expand in 3D space, we are able to lower the effective operating frequency and maintain the same footprint size. The research was presented in [111].

2.6 References

[1] H. A. Wheeler, “Fundamental limitations of small antennas,” Proce. IRE, vol. 35, pp. 1479–1488, Dec. 1947.

[2] L. J. Chu, “Physical limitations of omni-directional antennas,” J. Appl. Phys., vol. 10, pp. 1163–1175, Dec. 1948.

[3] James S. McLean; “A Re-Examination of the Fundamental Limits on the Radiation Q of Electrically Small Antennas,” IEEE Int. Conf. Communications (ICC) Conf., New York, 5, May 1996

[4] John R Koza "Genetic algrothims and genetic programming" Aug 4th 2004 http://www.genetic-programming.com/coursemainpage.html [Sep. 2, 2010]

[5] H. Rmili, O. E. Mrabet, J.-M. Floc’h, and J.L. Miane, “Study of an Electrochemically-Deposited 3D-Fractal Tree Monopole Antenna,” IEEE Transactions on Antenna and Propagation, vol. 55, no. 4, Apr. 2007, pp. 1045-1050

[6] J. Bayless, M. Chen, B. Dai; “Wire Embedding 3D Printer,” Engineering Physics University of British Columbia April 12, 2010

[7] Ronald L. Hollis, “The Proliferation of 3D Printing Machines”, Product design and development magazine issue 4/12/2010.

[8] RedEye Express "Open Market Rapid Prototype Quotes" http://express.redeyeondemand.com. 2010 [Oct 12 2010]

[9] Dalmar Mfg Co "Dalmar plating information site" http://www.dalmar.net [Oct 9 2010]

[10] Z Corporation " The fastest, most affordable color 3D printing" http://www.zcorp.com/documents/931_9062-ZPrinterBroch.pdf, 2010 [June 2 2010]

[11] Wohlers, T, 2009, Wohlers Report 2009, Rapid Prototyping, Tooling & Manufacturing State of the Industry, Annual Worldwide Progress Report, Wohlers Associates Inc., Colorado, USA

[12] E.E.Altshuler E. E. Altshuler, “Electrically small self-resonant wire antenna optimized using a genetic algorithm,” IEEE Trans. Antennas Propag., vol.50, no. 3, pp. 297–300, Mar. 2002.

[13] Tyco electronics "Laser Direct Structuring" http://www.tycoelectronics.com/mid/lasertech.asp) 2011 [Oct. 9, 2010]

[14] Objet Geometries Inc "Connex 500 3D printer" http://www.objet.com/3D-Printer/Objet_connex500/ 2011, [Jun 2 2010]

[15] J. Bernard, J. Lewis, J. Adams, et al, "Conformal Printing of Electrically Small Antennas on Three-Dimensional Surfaces", Advanced Materials Volume 23, Issue 11, pages 1335–1340, March 18, 2011

[16] J. Lewis B. Ahn M. Motala et al. "Omnidirectional Printing of Flexible, Stretchable, and Spanning Silver Microelectrodes" Science 323, 1590 (2009); DOI: 10.1126/science.1168375

[17] A. Koptioug, P. Jonsson, J. Sidén, T. Olsson and M. Gulliksson, "On The Conductive Behavior of Printed RFID Tag Antennas, Using Conductive Paint", Mid Sweden University, SE-831 25 Östersund, Sweden.

[18] Cha-Soo Jun, Kyungduck Cha, Yuan-Shin Lee "Optimizing tool orientations for 5-axis machining by configuration-space search method" Computer-Aided Design, Volume 35, Issue 6, May 2003, Pages 549-566

[19] Yu, T. Masuzawa, M. Fujino "Micro-EDM for Three-Dimensional Cavities - Development of Uniform Wear Method" CIRP Annals - Manufacturing Technology, Volume 47, Issue 1, 1998, Pages 169-172 Z.Y.

[20] I M.F. DeVries, N.A. Duffie, J.P. Kruth, D.F. Dauw, B. Schumacher, "Integration of EDM within a CIM Environment" CIRP Annals - Manufacturing Technology, Volume 39, Issue 2, 1990, Pages 665-672

[21] [Online Available] http://spectrum.ieee.org/geek-life/hands-on/diy-essentials/2 [Accessed on Aug 20th 2011]

[22] J.R. Honiball "The Application of 3D Printing in reconstructive surgery", PhD Dissertation, University of Stellenbosch , Mar. 2010

[23] (Chapter 3) B. Willis, C. Furse, " Rapid prototyping for small 3D antennas", Submitted paper, IEEE Trans. Antennas and Propagation [2012.]

[24] (Chapter 4) B. Willis, C. Furse, " Design and rapid prototyping for 3D space efficient antennas", Submitted paper, IEEE Trans. Antennas and Propagation [2012.]

[25] (Chapter 5) B. Willis, C. Furse, "A Comparison of Rapid Prototyping Build Techniques" Submitted paper, IEEE Trans. Antennas and Propagation [2012.]

[26] (Chapter 6) B. Willis, C. Furse, "The Fute of 3D Printed Antennas" To Be Submitted paper, IEEE Trans. Antennas and Propagation [2012.]

[27] S Best "A Study of The Performacne Properteis of Small Antennas" [Online avialable]http://www.mitre.org/work/tech_papers/tech_papers_07/07_1131/07_1131.pdf [last accessed Jan. 5, 2012]

[28] R. B. Adler, L. J. Chu, and R. M. Fano, Electromagnetic Energy Transmission and Radiation. New York: Wiley, 1960.

[29] H. A. Wheeler, "Fundamental relations in the design of a VLF transmitting antenna," IRE Trans. Antennas Propagat., vol. 6, pp. 120–122, Jan. 1958.

[30] H. A. Wheeler, "Small antennas," IEEE Trans. Antennas Propagat., vol.23, pp. 462–469, July 1975.

[31] R. C. Hansen, "Fundamental limitations in antennas," Proc. IEEE, vol.69, pp. 170–182, Feb. 1981

[32] Hansen, R.C.; Collin, R.E.; , "A New Chu Formula for Q," Antennas and Propagation Magazine, IEEE , vol.51, no.5, pp.38-41, Oct. 2009

[33] Thal, H.L.; , "New Radiation Limits for Spherical Wire Antennas," Antennas and Propagation, IEEE Transactions on , vol.54, no.10, pp.2757-2763, Oct. 2006

[34] Thal, H.L.; , "A Reevaluation of the Radiation Q Bounds for Loop Antennas," Antennas and Propagation Magazine, IEEE , vol.51, no.3, pp.47-52, June 2009

[35] Yaghjian, A.D.; Best, S.R.; , "Impedance, bandwidth, and Q of antennas," Antennas and Propagation Society International Symposium, 2003. IEEE , vol.1, no., pp. 501-504 vol.1, 22-27 June 2003

[36] Altshuler, E.E.; Best, S.R.; O'Donnell, T.H.; Herscovici, N.; , "An electrically-small multi-frequency genetic antenna immersed in a dielectric powder," Antenna Technology, 2009. iWAT 2009. IEEE International Workshop on , vol.,o.,pp.13, 2-4 March 2009

[37] E. Faruk, C. C. Chen, and J.L.Volakis., " Impedance Matched Ferrite Layers as Ground plane Treatments to improve Wide-Band performance," IEEE Trans. Antennas Propag., Vol 57, No 1, pp. 263-266, Jan 2009.

[38] S. Best, D. Hanna, "Design of a broadband dipole in close proximity to an EBG ground plane," Antennas and Propagation Magazine, IEEE , vol.50, no.6, pp.52-64, Dec. 2008

[39] Best S.R, " A Discussion On Electrically Small Antennas Surrounded By Lossy Dispersive Materials" MITRE, 202 Burlington Road, M/S S230, Bedford, MA 01730 USA Email: sbest@mitre.org 2006

[40] Yoshimi Kawano, Songyoung Bad", Yoshio Koyanagi."', Hisashi Morishita "A study on miniaturization of a handset antenna utilizing magnetic materials" Antenna Technology: Small Antennas and Novel Metamaterials, 2005. IWAT 2005. IEEE International Workshop on, pp. 129- 132, 7-9 March 2005

[41] R. W. Ziolkowski, A. Erentok, "Metamaterial-based efficient electrically small antennas," IEEE Trans. Antennas Propag., vol. 54, no. 7, pp. 2113–2130, Jul. 2006

[42] Vinko Erceg, Hemanth Sampath, and Severine Catreux-Erceg; "Demonstration of Impedance Matching Using a mu-Negative (MNG) metamaterial," IEEE Trans. On Wireless Communications, vol 5, No 1, pp. 28-33, January 2006. 2006

[43] G. Mumcu, K. Sertel, and J. L. Volakis, " Printed Coupled-lines Emulating Anisotropic Materials for Miniature Antenna Design" Department of Electrical and Computer Engineering, ElectroScience Lab. , Ohio State University,

[44] John L. Volakis and Kubilay Sertel, " Periodic Materials & Printed Structures for Miniature Antennas", Loughborough Antennas and Propagation Conference 2 -3 April 2007. Loughborough, UK. 2 -3 April 2007

[45] Aycan Erentok,; Richard W. Ziolkowski; "A Hybrid Optimization Method to Analyze Metamaterial-Based Electrically Small Antennas," IEEE Trans. Antennas and Propagation, vol 55, no 3, pp. 731-741, Mar 2007.

[46] Vinko Erceg, Hemanth Sampath, and Severine Catreux-Erceg; "Demonstration of Impedance Matching Using a mu-Negative (MNG) metamaterial," IEEE Trans. On Wireless Communications, vol 5, No 1, pp. 28-33, January 2006. 2006

[47] Yoshimi Kawano, Songyoung Bad", Yoshio Koyanagi."', Hisashi Morishita "A study on miniaturization of a handset antenna utilizing magnetic materials" IEEE paper from antennas conference 'Depariment of Electrical Engineering, Nutionul Definse Academy, Yokosuka, Japan, 1 Sept. 2004

[48] Cheng-Jung Lee; Wei Huang; Gummalla, A.; Achour, M.; , "Small Antennas Based on CRLH Structures: Concept, Design, and Applications," Antennas and Propagation Magazine, IEEE , vol.53, no.2, pp.10-25, April 2011

[49] Kishk, A.A.; Wei Huang; , "Size-Reduction Method for Dielectric-Resonator Antennas," Antennas and Propagation Magazine, IEEE , vol.53, no.2, pp.26-38, April 2011

[50] S. R. Best, "Low Q electrically small linear and elliptical polarized spherical dipole antennas," IEEE Trans. Antennas Propag., vol. 53, pp. 1047–1053, Mar. 2005.

[51] S. R Best; “The Radiation Properties of Electrically Small Folded Spherical Helix Antennas” IEEE Trans. of Antennas and Propagations, VOL. 52, NO. 4, April 2004 page 953

[52] M. Tariqul Islam*(1), M. N. Shakib(2), N. Misran(2), and B. Yatim(1) “Design of Compact Ultrawideband Patch Antenna for Wireless Communications”

[53] S. Best, D. Hana “Performance Comparison of Fundamental Small Antenna Designs” IEEE Ant & Prop Vol. 52 No. 1, Feb 2010

[54] Elkorany, A.S.; Sharshar, A.A.; Elhalafawy, S.M.; , "Ultra wideband stacked microstrip patch antenna," *Antennas and Propagation, 2009. EuCAP 2009. 3rd European Conference on* , vol., no., pp.1464-1466, 23-27 March 2009

[55] G. Goubau, “Multi-element monopole antenna,” Proceedings of the ECOM-AROWorkshop on Electrically Small Antennas, Fort Monmouth, NJ, pp. 63-67, October

[56] A.K Skrivervik, J.F. Zurcher, O. Staub and J.R Mosig “PCS Antenna Design: The Challenge of Miniaturization”, IEEE Trans. Antennas and propagations Vol 43 No.4 Aug 2001 Page 12

[57] Schelkunoff, S.A.; , "Theory of Antennas of Arbitrary Size and Shape," *Proceedings of the IRE* , vol.29, no.9, pp. 493- 521, Sept. 1941

[58] Gustafsson M., Sohl C., Kristensson G., “Physical limitations on antennas of arbitrary shape” Proc. R. Soc. A (2007) 463.2589-2607 Published online 18 July07

[59] N. Herscovici, " New Considerations in the Design of Microstrip Antennas" IEEE Trans. Antennas and propagations, Vol46 No.6 June 1998.

[60] Arai, H.; Nagatsuka, S.; , "Low-profile dual-mode plate-loop antenna," Antenna Technology, 2009. iWAT 2009. IEEE International Workshop on , vol., no., pp.1-4, 2-4 March 2009

[61] D. McCartney “Embedded antennas technology for next generation handsets”, RF design April of 2000, (www.rfdesign.com)

[62] Amir Galehdar, David V. Thiel, Steven G. O’Keefe, “Design Methods for 3D RFID Antennas Located on a Conducting Ground Plane,” IEEE Trans. Antennas Propag, vol. 57, no. 2, pp. 339-346, Feb. 2009.

[63] J. Thevenard, D. Lo Hine Tong, A. Louzir, C. Nicolas, C.Person, J.P. Coupez, “ 3D multi-sector vivaldi antennas based on metallized plastic technology,” IEEE International Symposium on Antennas and Propagation, 9-15 June 2007.

[64] L. Griffiths, Y.C. Chung, C. Furse, “Integrated Dual Band GSM Microstrip Monopole using GA and FDTD”, IEEE APS, Wash, D.C., July 2005

[65] John R Koza "Genetic algrothims and genetic programming" Aug 4th 2004 http://www.genetic-programming.com/coursemainpage.html [Sep. 2, 2010]

[66] S. Soora, K. Gosalia, M.S. Humayun, G. Lazzi, “A Comparison of Two and Three Dimensional Dipole Antennas for an Implantable Retinal Prosthesis,” IEEE Trans. Antennas Propag, vol. 56, no. 3, pp. 622-629, Mar. 2008.

[67] A.A. Serra, P. Nepa, G. Manara, R. Massini, “A Low-Profile Linearly Polarized 3D PIFA for Handheld GPS Terminals,” IEEE Trans. Antennas Propag., vol. 58, no. 4, pp. 1060-1066, Apr. 2010.

[68] Pfeiffer C. , Grbic A “Novel Methods to Analyze and Fabricate Electrically Small Antennas” Spokane Washington, Antennas and Propagation Conference July 3rd – 8th 2011

[69] X. Xu, M. Davanco, X. Qi, S. R. Forrest, “Direct transfer patterning on three dimensionally deformed surfaces at micrometer resolutions and its application to hemispherical focal plane detector arrays,” *Organic Electronics, vol. 9, no. 6, pp. 1122–1127*, December 2008.

[70] [Online] Available: http://www.mgchemicals.com/products/8331.html

[71] M. Leskelä, M. Ritala, “Atomic Layer Deposition Chemistry: Recent Developments and Future Challenges” Volume 42, Issue 45, pages 5548–5554, November 24, 2003 [Article first published online: 18 NOV 2003]

[72] William D. Westwood (2003). Sputter Deposition, AVS Education Committee Book Series, Vol. 2.

[73] [online available] http://www.electro-coatings.com/electroless-nickel-plating.php [last accessed Jan 4th 2012]

[74] Huang, Haiyu; Nieman, Karl; Hu, Ye; Akinwande, Deji; , "Electrically small folded ellipsoidal helix antenna for medical implant applications," Antennas and Propagation (APSURSI), 2011 IEEE International Symposium on , vol., no., pp.769-771, 3-8 July 2011

[75] Sigmarsson, H.; Kinzel, E.; Chappell, W.; Xianfan Xu; , "Selective laser sintering of patch antennas on FR4," Antennas and Propagation Society International Symposium, 2005 IEEE , vol.1A, no., pp. 280- 283 Vol. 1A, 3-8 July 2005

[76] [Online] Available: http://www.ventistech.com/about.htm [Accessed on Aug 27th 2011]

[77] [Online] Available: http://reprap.org/wiki/Gada_Prize. [Accessed: 11th Jan. 2011].

[78] [Online] Available: http://www.k-mac-plastics.net/abs-rod.htm

[79] [Online] Available: http://botmill.com/index.php/materials.html

[80] [Online] Available: http://www.foresight.org/gadaprize.php. [Accessed: 11th Jan. 2011].

[81] M. Gaynes, R. Kodnani, and M. Pierson, " Flop Chip Attach with Thermoplastic Electrically Conductive Adhesive", in Proc., 3rd Int. Conference of Adhesive Joining and Coating Technology, Sept.1998, pp.244-251.

[82] K. I. Rybakov, V. E. Semenov, S. V. Egorov, A. G. Eremeev, I. V. Plotnikov, and Yu. V. Bykov, "Microwave Heating of Conductive Powder Materials", AIP Journal of Applied Physics, vol. 99, Issue: 2, Jan. 2006, pp. 023506-1 – 023506-8

[83] M.A. Gayness, R. H. Lewis, R. F. Saraf, and J.M. Roldan, " Evaluation of Contact Resistance for Isotropic Electrically Conductive Adhesives," IEEE Transactions on Components, Packaging, and Manufacturing Technology ,vol.18, Issue: 2, May 1995, pp. 299 – 304

[84] R. V. McBean, V. Chiriac, and T. Lee, "Performance Comparisons for Electrically Conductive Epoxies in Wireless Applications", in Proc., The Tenth Intersociety Conference on Thermal and Thermomechanical Phenomena in Electronics Systems, May 2006, pp.288.

[85] Y. Wei and E. Sancakter, "Dependence of Electric Conduction on Film Thickness of Conductive Adhesives", in Proc., 45th Electronic Components and Technology Conference, May 1995, pp. 701-706.

[86] Y. Li, R. Zhang, L. Shu, W. Lin, O. Hilbreth, H. Hiang, J. Lu, Y. Xiu, Y. Liu, J. Moon, and C.P. Wong, "Nano Materials and Composites for Electronic and Photo Packaging", in Proc., 9th IEEE Conference on Nanotechnology, July. 2009, pp.1-3.

[87] Charles M. Krutchen, "Melt Exturdable Polyacetylene Copolymer Blends", U.S. Patent, 3,852,235, Dec. 3, 1974.

[88] N. Guan, H. Furuya, D. Delaune, and K. Ito, "Antennas Made of Transparent Conductive Films," in PIERS Proceedings Online, Vol.4, No. 1, 2008.

[89] N. Outleb, J. Pinel, M. Drissi, and O. Bonnaud, "Microwave Planar Antenna with RF-Sputtered Indium Tin Oxide Films," Microwave and Optical Technology Letters, vol. 24, no. 1, 2000.

[90] Locher, M. Klemm, T. Kirstein, and G. Trster, “Design and Characterization of Purely Textile Patch Antennas,” IEEE Trans. Adv. Packag., vol. 29, pp. 777–788, 2006.

[91] Y. Ouyang and W. J. Chappell, "High Frequency Properties of Electro-Textiles for Wearable Antenna Applications," IEEE Trans. Antennas Propagat. , vol. 56, pp. 381-389, 2008.

[92] Y. Ouyang, E. Karayianni, and W. J. Chappell, “Effect of Fabric Patterns on Electrotextile Patch Antennas,” in Proc. IEEE Antennas and Propag. Soc. Int. Symp., 2005, vol. 2B, pp. 246–249.

[93] K. Bock, “Polytronics-Electronics and Systems on Flexible Substrates”, IEEE VLSI-TSA International Symposium on VLSI Technology, Apr. 2005, pp.53-56

[94] D. Micheli, C. Apollo, R. Pastore, and Mario Marchetti, “Modeling of Microwave Absorbing Structure using Winning Particle Optimization Applied on Electrically Conductive Nano-structured Composite Material”, in Proc., XIX International Conference on Electrical Machines ,Sept. 2010,pp.1-10.

[95] A. Tronquo, H. Rogier, C. Hertleer, and L. Van Langenhove, “Applying Textile Materials for the Design of Antennas for Wireless Body Area Networks”, Proceedings of the European Conference on Antennas and Propagation, EUCAP 2006, Nice, France, p. 159, November 2006.

[96] P. Salonen, Y. Rahmat-Samii, M. Schaffrath, and M. Kivikoski, “Effect of Textile Materials on Wearable Antenna Performance: A case study of GPS antennas,” in Proc. IEEE Antennas Propag. Soc. Int. Symp., 2004, vol. 1, pp. 459–462.

[97] A. Tronquo, H. Rogier, C. Hertleer and L. Van Langenhove, “Robust planar textile antenna for wireless body LANs operating in 2.45 GHz ISM band”, IEEE Electronic Letters, Vol. 42, Issue. 3, February 13,2006, pp. 142-143

[98] R. Malamud and I. Cheremisov, “Anti-Corona Protection of High Voltage Stator Windings and Semi-Conductive Materials for its Realization”, in Proc.,IEEE International Symposium on Electrical Insulation, Apr. 2000, pp.32-35.

[99] J. Saberin; C. Furse; , "Challenges with optically transparent patch antennas for small satellites," Antennas and Propagation Society International Symposium (APSURSI), 2010 IEEE , vol., no., pp.1-4, 11-17 July 2010

[100] R. Gordon, “Criteria for choosing transparent conductors," MRS Bulletin, August 2000.

[101] A. Moscicki, J. Felba, T. Sobierajski, J. Kudzia, A. Arp, and W. Meyer, “Electrically Conductive Formulations Filled Nano Size Silver Filler for Ink-Jet

Technology," in Proc.,5th International Conference on Polymers and Adhesives in Microelectronics and Photonics, October 2009, pp. 40-44.

[102] J. Siden, M. Fein, A. Koptyug, H. Nilsson, "Printed Antennas with Variable Conductive Ink Layer Thickness", IET Microwave and Antennas Propagation, Vol. 1, Issue. 2, 2007, pp. 401 – 407

[103] A. R. Duggal and L. M. Levinson, "A Novel High Current Density Switching Effect in Electrically Conductive Polymer Composite Materials", AIP Journal of Applied Physics, vol. 82, Issue: 11, Dec. 1997, pp. 5532 - 5539.

[104] S. K. Kang and S. Purushothaman, "Development of Low Cost, Low Temperature Conductive Adhesives", in Proc., 3rd Int. Conference of Adhesive Joining and Coating Technology, September 1998, pp. 287.

[105] T. Itano, "Electrically Conductive Thread, Fabric and Fabric Tape", in Proc., International Symposium on Electromagnetic Compatibility, May 1999, pp.809.

[106] [Online]Available: http://www.coolpolymers.com/XyloyM950.asp [Accessed on April 6th 2011]

[107] http://www.rtpcompany.com/products/conductive/

[108] [Online Available] *http://www.chomerics.com/products/premier.htm* [last accessed Sep 15th 2011]

[109] R. H. Johnston, L. P. Ager and J. G. McRory, "A New Small Antenna Efficiency Measurement Method", IEEE Antennas and Propagation Society International Symposium, 1996.

[110] [Online Available] *http://www.spraylat.com/Products/ElectronicMaterials/Technology/ConductiveCoatingTechnology.aspx* [last accessed Sep 15th 2011]

[111] B.Willis , C.Furse,"3D Rapid Prototyping for Small Antenna Design" Spokane Washington, Antennas and Propagation Conference July 3rd – 8th 2011

CHAPTER 3

RAPID PROTOTYPING FOR SMALL 3D ANTENNAS

This paper addresses inexpensive prototyping methods for antennas that can be random or complex in 3D shape. 3D rapid prototyping holds significant promise for future antenna designs. This paper demonstrates how rapid prototyping can be used to create small 3D antennas of random shape optimized for high bandwidth. A 3D antenna made from small cubical cells is optimized using a genetic algorithm (GA) for 2.4-3GHz. The antennas are built using 3D printing of plastic covered by conductive paint. The effects of the conductivity of the paint and number of layers on the resonance and gain of the antenna are evaluated. For comparison, a solid fully metallic antenna is also prototyped using laser sintering. Measurements indicate good agreement with simulation. Conductivity of the paint increases the skin depth by 2 times that of standard copper. These designs are approximately 70 % smaller in planar surface area than corresponding 2D designs. The plastic designs are about 81% lighter weight than a fully metallic antenna built using SLS. The measured and simulated results demonstrate the feasibility of using 3D rapid prototyping for antenna design.

3.1 Introduction

Small antenna design is a longstanding area of great importance and interest. As electronic devices shrink, antenna size must also decrease, yet the demands for higher data rates require improved performance even at these smaller sizes. One way to improve small antenna performance is to use 3D designs rather than 1D (wire) or 2D (planar) designs. This is theoretically supported by the small antenna limit developed by Wheeler [1] and Chu [2] which is based on a spherical volume encompassing the antenna. The Chu limit for quality factor is

$$Q_{lb} = \frac{1}{(ka)^3} + \frac{1}{ka} \tag{3.1}$$

where, *k* is the free space wave number, and a is the radius of the smallest sphere enclosing the entire antenna. Additional work such as that done by Mclean [3] has refined the small antenna limit for lossy antennas:

$$Q_{lossy} = \eta\, Q_{lossless} \tag{3.2}$$

$$Q_{lb} \geq \eta\left[\frac{1}{(ka)^3} + \frac{1}{ka}\right] \tag{3.3}$$

The radiation efficiency η in (3) takes into account the effects of losses as they reduce the quality factor Q. A potential source for loss in antennas produced with rapid prototyping methods is loss in the imperfect conducting materials (such as paints) that

may be used for this application. An important note here is that the calculations for Q in (1)-(3) all consider a 3D area encompassing the antenna.

In practice, if the antenna is a 1D wire antenna, the spherical radius, a, is the total length of the wire antenna, and most of the spherical volume is unused. If the antenna is a 2D planar antenna, *a* is the radius of the sphere enclosing the plane, where again most of the spherical volume is unused. It is true that many applications are best-served by 1D and 2D designs due to a variety of physical and practical constraints. But many applications can support space for 3D antennas. Rarely would this space be truly spherical. Antennas in consumer wireless devices, for instance, may be built into the small, random-shaped voids in the case. For aircraft or unmanned air vehicles, they may be fit into a variety of odd-shaped voids in the body, nose cone, or wings. Classical 3D antennas such as horns, dishes, helices, etc. are not always right for a given application, and more flexibility is often desired. This paper addresses inexpensive prototyping methods for antennas that can be random or complex in 3D shape. The designs in this paper are developed with a genetic algorithm, basically a 3D extension of previous 2D work [4]. This is just one example of a 3D design, and many others would be possible with this or other optimization methods and rapid prototyping.

All good approximations at meeting the small antenna limits ((1)-(3)) attempt to utilize as much of the 3D space as possible for the optimal small antenna design. A few attempts at true 3D antennas have been made in the past and have predicted or demonstrated the potential performance improvements of 3D design [5], [6]. Thal has calculated limits for spherical antennas in [7], and [8] indicating that a spherical helix can better approach the small antenna limit set by Chu. Thal provides a baseline for small

spherical 3D antennas. Best demonstrates low Q small spherical dipoles [9] and properties of a small spherical helix [10]. The spherical helix antenna is made up of hand-soldered pieces of wire. The design indicates a Q within 1.5 times the fundamental limit and efficiencies at or above 90%. Similar complex, hand-soldered antennas are seen in [11], [12], and [13]. It is clear from the photos that these antennas are difficult to build, and [13] specifically mentions that the antenna could be built only approximately like the design due to the difficulty of building it. These antennas do all demonstrate the improvements that may be gained by using the 3D design, especially [13] which uses high dielectric powder surrounding the antenna. The 3D printed antennas described in the sections below could also be further miniaturized by surrounding them with high dielectric material. A 3D hemispherical antenna was recently built by printing a meander-line antenna pattern on a curved glass surface with a silver ink [14]. Another recent 3D spherical antenna was built using a process called direct transfer patterning. The process uses a stamp to transfer the desired pattern onto a curved surface. It then requires a 6-step process including a plasma etch and gold plate to finalize the design on Polyethylene Terephthalate [15]. Both of these antennas again demonstrated the improvement in the 3D design over a planar design with the same footprint. The transfer method is clearly more complex than either the 3D printing method in [14] or the one demonstrated in the sections below. The half sphere designed in [15] provides a more exact and repeatable design of the spherical antenna in [10] and indicates that an antenna with *ka* of 0.26 has efficiency 35%. This design also demonstrated the improvements that can be obtained by going to 3D, but the process is limited to printing on the outer surface of a plastic or

glass substrate and therefore may have less flexibility in antenna design and shape (to fit odd-shaped voids) than the 3D printed antennas demonstrated in Chapter 3.

The printing method in [14] uses a small nozzle on a robotic hand to draw a very high conductivity ink on a preshaped glass substrate (in this case, a hemisphere). The ink has reported conductivity of ~$1X10^{-6}$ S/m similar to the paint when the paint thickness is above 15 um [16]. The 3D nozzle printing method would be more difficult to apply for more complex 3D designs such as those that might be required to fill random-shaped voids. In [5], a 3D fractal tree is randomly grown by an electrochemically deposited conductor. The novel property is the impedance bandwidth improvement over a similar 2D antenna. All of these 3D designs demonstrate improvement over 2D antennas with the same footprint. They are, however, more complicated to build.

Until recently, the manufacturing methods to produce 3D antennas have been so cumbersome or expensive that 3D antennas were practically limited to the classical designs or printing (of potentially complex designs) on simple-shaped substrates. But now, cutting edge rapid prototyping creates 3D manufacturing opportunities that have not previously been available in the antenna design world. The work here assesses these methods, and their relative impact on 3D antenna designs that could be produced in virtually any shape imaginable.

The physical size of an antenna is also often reduced while maintaining its electrical size by decreasing the wavelength within the antenna structure and/or its very near field. This can be done with high dielectric materials [13], [17], [18] and/or electronic band gap (EBG) materials [19]. Other miniaturization techniques include using metamaterials [20], or slotted ground planes [21]. It is worth noting that these and other

antenna miniaturization methods may also be applied to rapid prototyped 3D antennas, although that is beyond the scope of the current research.

This work demonstrates the feasibility of using rapid prototyping to build 3D antennas, and a specific example antenna is used to do this. Section 3.3 discusses 3D rapid prototyping technology in detail and provides a description of most of the well-known 3D rapid prototyping and manufacturing techniques. Also presented are the latest advances in conductive materials.

Section 3.4 demonstrates the effectiveness of these manufacturing methods by constructing and testing an antenna using 3D rapid prototyping. Building on optimization techniques from [4], a genetic algorithm is used to optimize a 3D antenna built on a square footprint from cubical cells (blocks). The antenna is 3D printed from plastic and covered with a conductive paint. The same type of patch is also built using selective laser sintering from steel powder. Both of these are tested and compared against simulation.

3.2 Rapid Prototyping for Antenna Design

3D rapid prototyping provides a novel, easy, and inexpensive manufacturing technique for antennas of arbitrary shape. Most antennas are built out of metals or a combination of metals and insulators (plastics). We will therefore focus on prototyping methods that include metals, high conductivity plastics, or to which metal paints or coatings can be added afterwards. This work demonstrates the feasibility of inexpensive 3D antenna designs that can be optimized with a wide variety of shape and design choices. This section will discuss rapid prototyping options for 3D antenna designs.

Antennas are built from some combination of conductive and insulating components. Chapter 3 provides a table indicating the conductivities and skin depths for the materials used here. There are several promising and emerging 3D prototyping methods that can be used to create metallic and nonmetallic shapes [22] . Methods that can directly produce high conductivity materials include selective laser sintering (SLS) [23], [24], [22], which can use metal or plastics. SLS is similar to selective laser melting [24], which can also use a variety of materials.

Electroforming [23] can also be used to create metallic objects. It is similar to the plating process, but it builds up an object that is relatively thick. Typically, electro-forming starts with a nonmetallic object and coats it with a conductive material. This conductive layer is then built up by electroplating until it is the desired thickness. Resolution for this method is very good and can be less than 1 micrometer [24] .

Selective laser sintering or melting is similar to electron beam forming. A layer of fine metallic power is spread out, and a high-power beam is scanned over the layer to create the 3D geometry. The beam fuses the powder together for that specific layer. When the layer is complete, the build platform is lowered, a new layer of powder is spread, and the beam again hardens that layer [25]. These fusing techniques typically use a 40 micrometer spot beam laser. The laser in combination with the particle size of the powder determines the surface resolution without finishing (typically less than 0.1 mm) [22]. One note is that due to the back filling with bronze required for SLS, the size for a protruding feature must be greater than 0.7mm [22]. Utilizing selective laser sintering as a manufacturing method for antennas is not yet common. Huang makes use of selective laser sintering to design a plastic mold for wrapping a helix [26]. Sigmarsson uses a

similar process to sinter a layer on a low temperature substrate [27]. Selective laser sintering is also used to build broadband antenna designs [28]; unfortunately, there are no publications or pictures for these antennas.

Stereolithography [24], commonly called 3D printing, can be done with multiple plastics or a combination of both [29], [23]. If printing is done with only plastic, a metallic coating or paint can be added afterwards to produce the conductive part of the design, which is the method used in this research. 3D printing is typically accomplished by using an injector that drops a quick hardening resin compound at a precise point for a single layer. The 3D object is then built up in printed layers. This is commonly known as layer deposition modeling (LDM). Initially, 3D printing was done using powder base and then ink jetting a binder over each layer, but now printing can be done by LDM. This method is becoming inexpensive enough for home or teaching applications [30]. LDM is also found in a few commercial 3D printers such as Dimensions 1200es, which has a resolution of 0.33 mm [31]. Other commercial 3D printers such as the Objet® Connex 500 uses 3D printing and stereolithography to UV cure the material. For this paper, we used the Connex 500 with resolution (0.015mm) [32]. There is a wide selection of available materials with various mechanical properties. For our printing, we used a plastic which Objet® refers to as Vero White.

3D printing has been used for insulating materials (plastics) extensively, and it is believed that the next generation 3D printers will print conductive materials as well. This has been demonstrated using conductive materials with low temperate melting points; however, the final products are not thermally stable [33].

3D conductive printing is making progress. One 3D machine makes use of a separate wire feed printing head for conductive materials [34]. A good candidate for a printable conductive material is a metallic flake mixture composed mostly of aluminum with a melting point at approximately 500 degrees Fahrenheit [35]. This metal mixture is currently used for injection molding of metal parts [35].

3D rapid prototyping processes vary in the materials they can use and the resolution and complexity they can provide [36]. Today's resolutions for 3D printing are on the order of 0.015mm [29]. One item of note which demonstrates the strong international and economic interest in conductive 3D prototyping is an $80,000 Gada prize (to be given in 2012-2015) recently announced for the development of advanced 3D printing [33], [37]. One of the requirements is the ability to print useful conductive materials such as those for circuit boards [37]. These materials would also probably be useful for antennas. 3D printers are becoming more mainstream [38] and are recommended in the IEEE do-it-yourself guide as an excellent accessory [39].

Rather than printing conductive materials, they can be added later as coatings. These may include paints [17], [40], [41], conductive adhesives (epoxies) [42], [43], [44], polymers [45], [46], optically transparent films[47], [48], thin silicon films [49], [50], nano-fiber [51], [52], powdered metals [53], [54], and even conductive fabrics [55], [56], [57], [58]. In this research, we evaluate the manufacturing and electrical tradeoffs for a space-efficient antenna design using 3D plastic that was printed and then coated with conductive silver or copper paint.

The paints used in our design are produced by Spraylat® and are commonly used for EMI shielding. The conductivity varies by thickness (number of layers) and paint type.

3.3 3D Antenna Design for Rapid Prototyping

In addition to the ease and low cost of manufacturing, rapid prototyping opens the door for much more diverse 3D antenna designs. Genetic algorithms (GA) [59], [49] , particle swarm [60], and other types of modern antenna design and optimization methods have been used to design 2D antennas of semirandom design, or to optimize more conventional designs. These optimization methods can be readily adapted from 2D [4] to 3D antenna design. Rather than designing with small square plates of metal as in [4], we can optimize for cubes of metal that are built up like a random pile of blocks to create a 3D antenna to fit a given volume of space. In this paper, we have used a GA , but other optimization methods (least squares, particle swarm, classic powell, etc.) would work as well. The design could also be done for more random shaped spaces which do not need to have 90º edges. The purpose of this section is to demonstrate and compare rapid prototyping methods and the materials used in them for a relatively simple antenna design. This demonstrates the feasibility of using simple rapid prototyping methods to enable much more complex 3D antenna designs than have been feasible with more traditional manufacturing techniques.

Our first objective is to demonstrate the usefulness of using a 3D volume. This will be done by designing antennas with single, double, and quadruple layers of cubes using a genetic algorithm (GA) such as those shown in Figure 7.

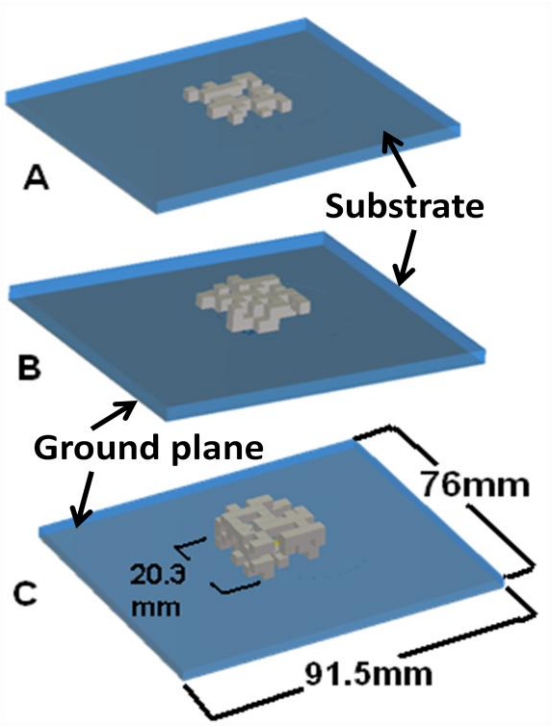

Figure 7: The 3D GA antenna optimized for 1 layer (A), 2 layers (B), and 4 layers (C)

The antennas in Figure 7 are similar to microstrip antennas [61]. The conductive cubes are placed above an insulating dielectric with a ground plane below. The layout of the cubes is optimized by dividing the space into cubes 1/30th wavelength (2.9mm) on a side at approximately 3.7 GHz. Each layer is made up of a pattern of 7x7 of these cubes for a total size of 7/30 wavelength on a side. The resolution of the cubes is chosen based on previous research [4], [59]. The 4-layer antenna is printed using a resolution of 0.015mm, and it took approximately 20 minutes to print.

For the simulated design in Figure 7, the footprint is 20.3 mm square, and each layer has a height of 2.9 mm. The ground plane is 91.5 mm long and 76mm wide. The dielectric substrate is 3.53mm thick Taconic® TLA-6 which has εr =2.62 and (assumed) zero conductivity. The resonance with dielectric for a 1/4 wave 2D patch with this

footprint would be approximately 3.7 GHz. The *ka* with the ground plane is 4.02, which is much larger than 1, and it does not fall under the typical definition for small antennas. The *ka* with a 20.3mm square ground plane is 0.91 and the antenna is resonant at ~2.6GHz when the antenna is fed with a 50 ohm coax. The simulated antenna using lossy materials is 95% efficient.

The GA used to optimize these designs was programmed similar to [4]. The antenna radiating element is divided into a 7x7 grid for each of 1, 2, or 4 layers. Each of these grid locations is one chromosome for the GA. If the chromosome is 'on', the cube at that location will be metallic. If the chromosome is 'off', the cube will be air. The length of the chromosome is 196, the mutation rate is 0.3, and the population size is 2. The chromosome was initially a randomly generated sequence of ones and zeros, but after only a few generations (each with a simple population of 2 and mutation rate of 0.3), the antenna begins to take on a shape that more or less fills the available volume.

The forward solution used to determine the performance and hence the fitness of the antennas was done with a commercial finite integral technique (FIT) solver, CST Microwave Studio [62]. The optimization required 1500-4500 design iterations for this example antenna. This was controlled outside of CST with an additional Matlab® script interfaced to CST with a visual basic (VBA) script. The cost function is calculated in CST. For this test, we optimized by minimizing the S11 (in dB) from 2.2-3.2GHz. The cost function is evaluated by taking each discrete frequency point and comparing it to the minimum value. The frequency band of 1-3GHz is sampled at 1000 points, then added up and averaged for the total cost. The optimization was tested 3 times, for 1,500, 3,000, and 4,500 iterations to ensure convergence. It did converge each time.

An individual simulation of the 7x7x4 GA cube antenna shown in Figure 7 C took approximately 30 seconds on a quad core 3.1 GHz processor with 8 GB of RAM. The total simulation and optimization took approximately 36 hours for 4500 iterations. Methods to speed up both the simulation and optimization exist [4], but the focus of this paper is on the prototyping, not the simulation and optimization approaches, so we did not make any major efforts to speed up this design process. The flow chart detailing the GA optimization is shown in Figure 8.

Using a larger portion of the 3D sphere surrounding the antenna would be expected to produce a lower frequency antenna [1], [2] and was demonstrated for semispherical volumes in [9], [63]. To demonstrate the effectiveness of using a 3D cubical design rather than 2D space, the GA antennas in Figure 7 were optimized for lowest operating band and largest bandwidth. As expected, the antennas resonate at a lower frequency as the volume is increased, as shown in Figure 9.

It is also interesting to compare the 3D cubical antennas to traditional 2D patch antennas [61] with the same footprint ($20.3mm^2$). The bandwidth for the larger volume GA cubical antennas is significantly higher than for a planar patch. For instance, the planar ¼ wavelength patch has a -10 dB resonance from 3.79 GHz to 4.12GHz (a bandwidth of 0.33 GHz) for this case.

The 1-layer GA antenna has a resonant frequency of 3.28GHz (bandwidth of 0.37 GHz). The 2-layer GA antenna has a resonant frequency of 2.88 GHz (bandwidth of 0.34 GHz). The 4-layer GA antenna has a resonant frequency of 2.19GHz (bandwidth of 0.32GHz).

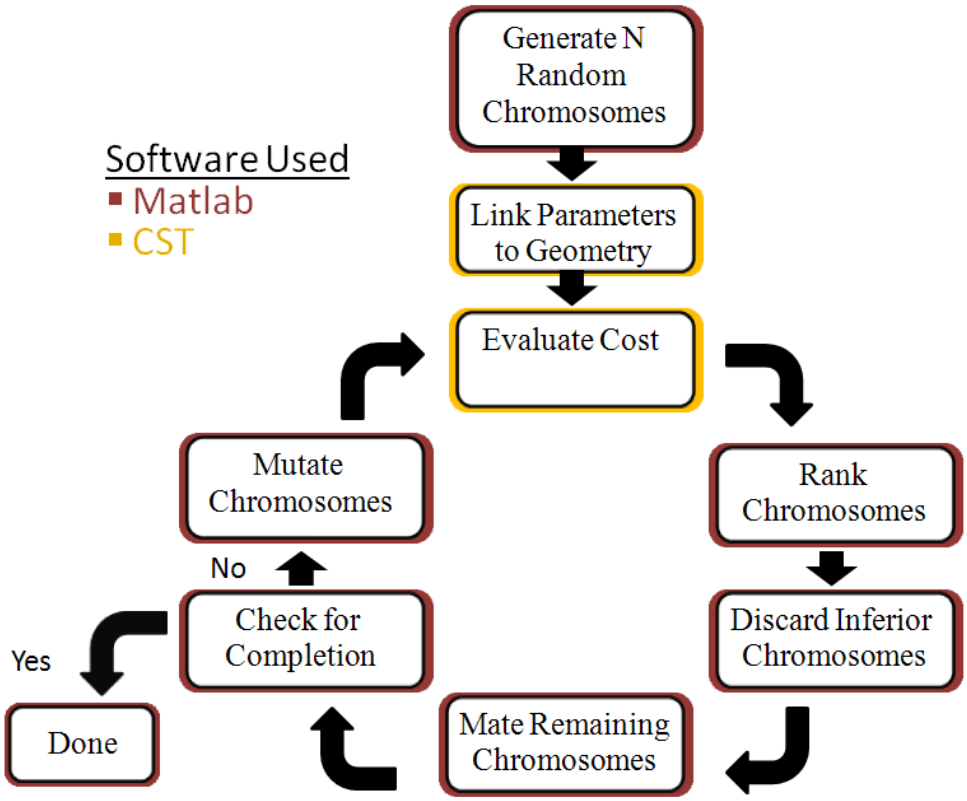

Figure 8: Flow chart indicating the software used for the GA optimziation.

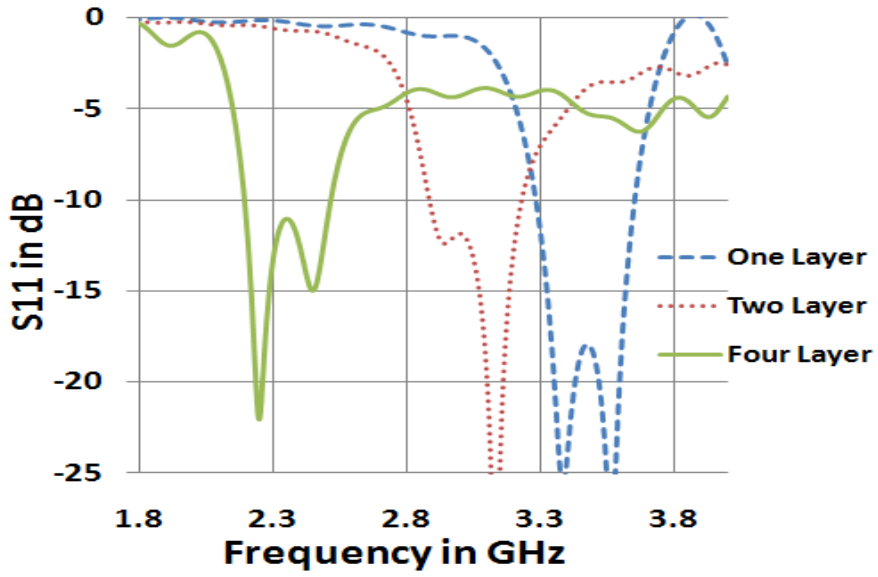

Figure 9: S11 for the 1-, 2-, and 4-layer GA antennas shown in Figure 7 simulated assuming they are built from perfect electric conductors (PEC).

The closer the antenna is to filling the spherical volume, the lower the resonant frequency and the higher the bandwidth, as predicted by theory [2].

Another way to look at this size reduction is to see what size patch is needed to obtain the same resonant frequency as the GA antennas. The size of the patch and the location of the feed point were optimized using a simple classic Powell optimization to create the widest band antenna with S11<= -10dB at the lowest frequency that matches the -10 dB point of the corresponding 3D GA antenna.

One might also wonder if the complex GA-generated shape is necessary or if this improvement is strictly from increasing the volume occupied by the antenna. If the 4-layer GA antenna in Figure 7 C is replaced by a simple cube of the same size, its resonant frequency is approximately 3.5 GHz, which means that it appears electrically smaller than the GA design and justifies continuing with the more complex GA designs. In the next section, we will demonstrate how the 3D GA antennas can be built using rapid prototyping methods.

3.4 Building the Antennas

In this section, we will describe the manufacturing details and measurements of the 4-layer antenna from Figure 7 C. First, the antenna was printed of Vero white plastic using an Object® Connex 500 3D printer. The printing time was approximately 20 minutes. The printed antenna is shown in Figure 10.

Table 5 shows the additional length required for the planar antenna, and its reduction in bandwidth compared to the 3D GA antennas. One might also wonder if the

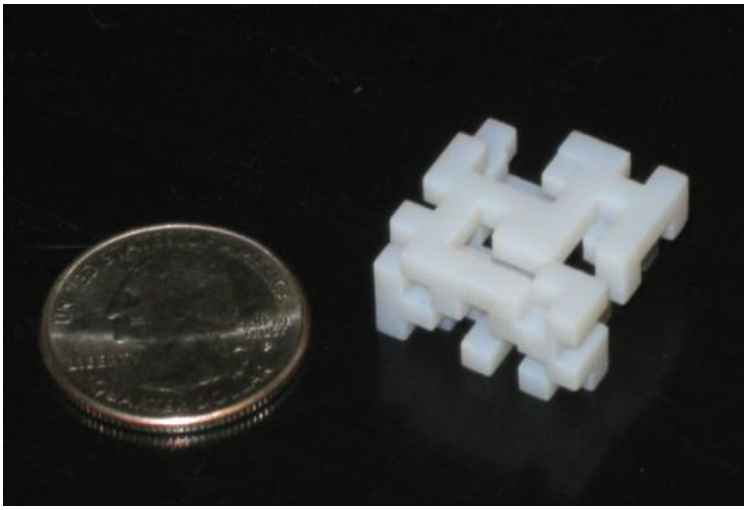

Figure 10: 3D printed 4-layer GA antenna before painting, shown with a US quarter. The antennas were metalized with paint using a Preval® self-loading spray gun

Table 5: Resonant frequency and bandwidth for the 3D GA antennas in Figure 7 or a standard planar patch antenna [61]

Antenna type	Length of side	Low band Resonant Frequency	% larger than 3D counterpart	-10dB Bandwidth
Flat	23.6mm	3.28 GHz	14%	6%
Figure 7, A	20.3 mm	3.28 GHz	0	11%
Flat	27.7mm	2.88 GHz	27%	4%
Figure 7, B	20.3 mm	2.88 GHz	0	12%
Flat	38.1mm	2.19 GHz	46%	3%
Figure 7, C	20.3 mm	2.19 GHz	0	14%

complex GA-generated shape is necessary or if this improvement is strictly from increasing the volume occupied by the antenna.

The antenna was metalized with paint using a Preval® self-loading spray gun using 1, 2 or 3 layers of silver or copper conductive paint [16]. The properties of the paint (and also selective laser sintering) are given in Table 6.

For simplicity and speed of simulation, the antennas were initially designed as PEC. Several rapid prototyping methods can be used to build in 3D with metals, including electroless plating, selective laser sintering, and electron beam forming. We used selective laser sintering to build an antenna from tool steel with bronze. Another very promising method for producing the metallic part of the antenna is to print the antenna with plastic and then metalize only the surface by spraying it with metallic paint. The 4-layer patch antenna shown in Figure 7 C (simulation), Figure 10 (plastic print), and Figure 11 (metalized with copper paint) was printed of Vero white plastic using an Object® Connex 500 3D printer. The printing time was approximately 20 minutes. The plastic was metalized using 2 or 3 layers of silver or copper conductive paint [16].

The measured S11 values for the patch are shown in Figure 12 compared to the simulated results. Here the simulation was updated to represent the new dielectric constant and thickness. Good but not perfect correspondence between simulated and measured results indicates that the PEC simulation probably does not represent the skin depth effects of the high-frequency patch antenna.

Since this has lower conductivity than the PEC simulated and that of the metal antenna produced using the selective laser sintering method, several different

Table 6: Paint thickness, skin depth, and conductivity for the built antennas.

Material	Paint thickness in microns	Skin depth in microns at 2GHz	σ (S/m)
1 layer Silver paint	7.5	4.36	6.67×10^6
2 layer Silver paint	15	3.08	1.33×10^7
3 layer Silver paint	23	1.71	4.3×10^7
1 layer Copper paint	7.5	9.25	1.48×10^6
2 layer Copper paint	15	6.16	3.33×10^6
3 layer Copper paint	23	5.4	4.35×10^6
SLS Steel & Bronze	NA	3.4	1.1×10^7

Figure 11: Final built and tested 3D printed antenna metalized with copper paint

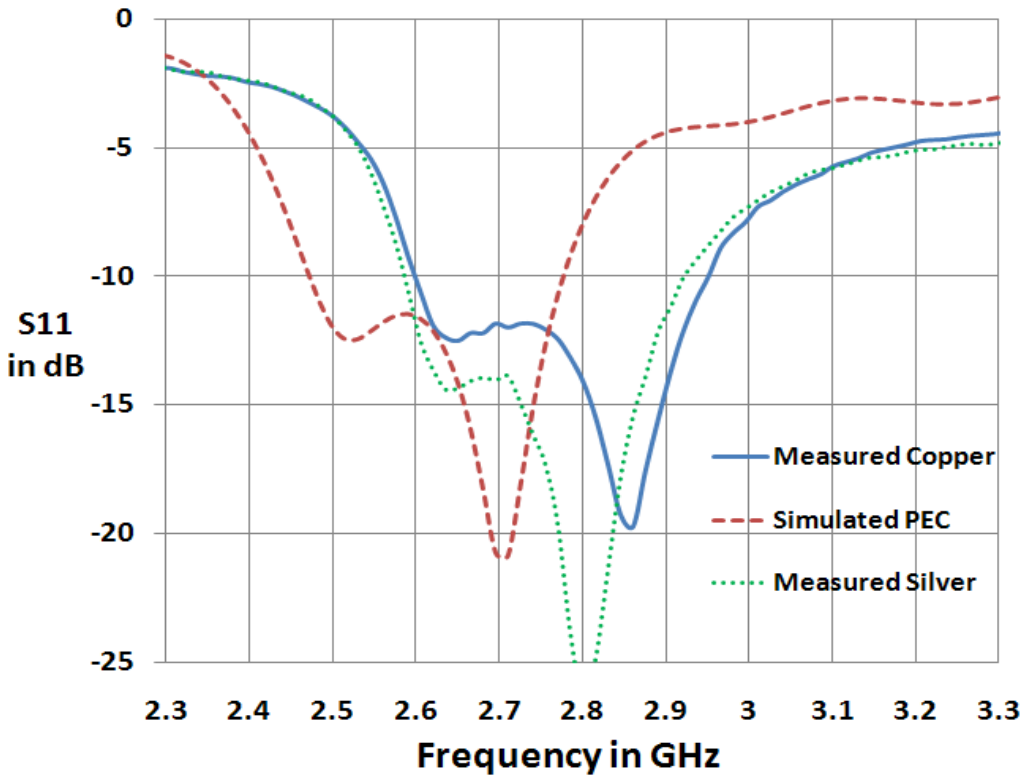

Figure 12: S11 simulation and measurement for the 4-layer 3D GA antenna with 3 layers of silver or copper paint.

metallization options were compared in order to determine if paint would act as a suitable metallization, and if it made any difference what type and number of layers of paint were used. Both silver and copper paint are evaluated in this paper. Based on the manufacturer's data sheet [16], the conductivity and skin depth are given in Table 6.

The skin depths are calculated at 2GHz. In order to minimize losses in the antenna, it is important to make the paint or coating 1-2 skin depths thick [47].

The substrate used in the actual build was 3.1 mm thick Rogers® 5870 substrate with $\varepsilon r = 2.33$. The connector was soldered to the copper ground plane with the center conductor left protruding through the substrate. The painted plastic antenna was then

attached to the feed-point using conductive epoxy [44]. The final antenna with 1-layer of copper paint is shown in Figure 11.

The measured S11 values for the prototyped antennas are shown in Figure 12 compared to the simulated results (using the Rogers substrate but assuming PEC metals). Good but not perfect correspondence between simulated and measured results indicates that the PEC simulation probably does not represent the skin depth effects in the antenna.

The thickness and dielectric constant of the substrate changed from the Taconic® used in simulation to Rogers® for the built antenna. The built 4-layer patch was fed with a 50 ohm SMA connector over a Rogers® 5870 substrate with an $\varepsilon r = 2.33$, that is 3.1 mm thick.

The connector was soldered to the copper ground plane with the center conductor left protruding through the substrate. The painted plastic antenna was then attached using conductive epoxy [44]. The final antenna is shown in Figure 11.

The 4-layer 3D GA antenna was also built using selective laser sintering (SLS). The SLS antenna needed to have some of the finer corner features enlarged in order to be built with that method. The antenna was simulated including the enlargement of the corner features but still assuming PEC. The SLS antenna is shown next to a 3D printed antenna in Figure 13. The comparison of simulated and S11 is shown in Figure 14 . The SLS is a solid conductor and the antenna acts more like the PEC-simulated antennas than the painted plastic antennas whose results are shown in Figure 12.

One item to note is the difference in weight between the plastic (2.5g) and SLS (13.7 g) antennas. The low weight of the plastic antenna is a very desirable feature for many applications.

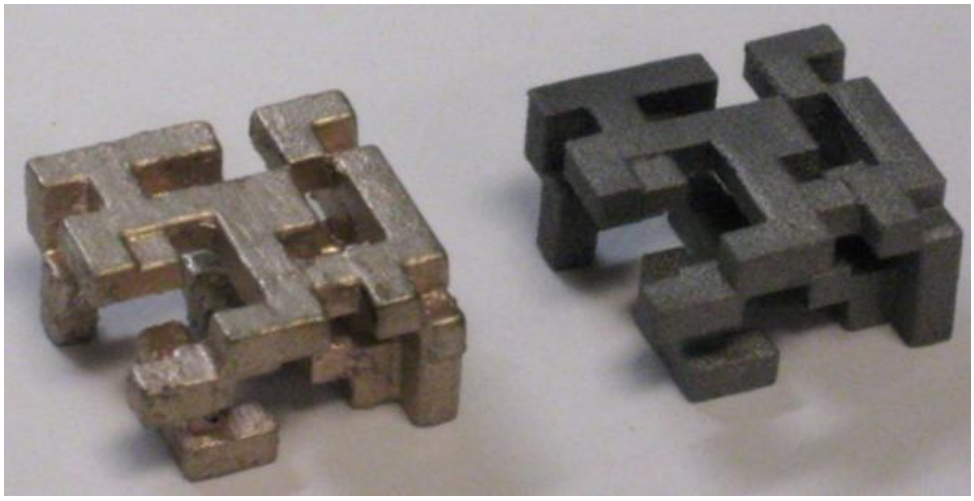

Figure 13: The 3D cubical patch is built from steel and bronze using selective laser sintering shown on the right, in comparison to the 3D printed patch coated with copper paint shown left.

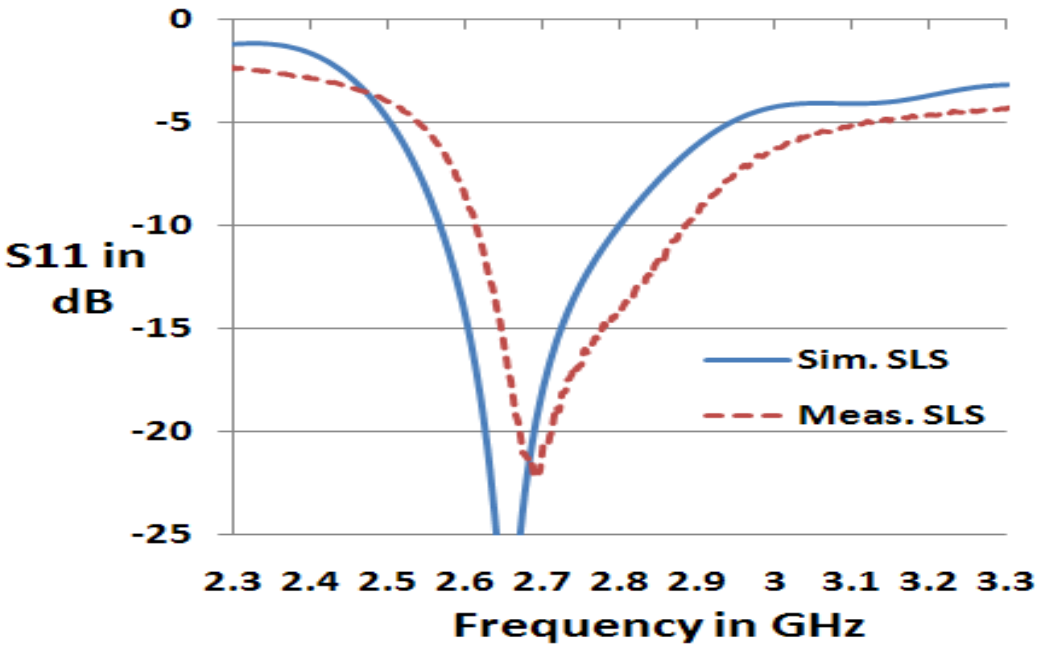

Figure 14: Comparison of the simulated and measured 4-layer 3D GA antenna, manufactured using selective laser sintering (SLS)

Both 4-layer 3D cube patches are simulated and built with corner regions that are electrically connected. The simulation also requires an edge contact and then a review of the final geometry for build.

The simulated results are compared against several standard antenna designs. Here each antenna is designed to fit inside the same cubical volume 20.3mm X 20.3mm X 11.6mm and each used the same size ground plane. The antennas are shown in Figure 15. The S11 results for each antenna are plotted for comparison and shown in Figure 16. The antennas are compared against various S11 data for each. They also exhibit other specific traits due to the shape of the geometry such as radiation pattern. The radiation pattern for the bi-cone , monopole, and solid cube, each have a typical monopole above a ground plane radiation pattern.

The wire helix has a circular polarized radiation pattern directed above the ground plane similar to a patch antenna but with circular polarization. The 4-layer cubical patch has a linear polarized radiation pattern directed above the ground plane which is most like a typical patch antenna.

We next simulated the 4-layer 3D GA antenna as Vero™ plastic ($\varepsilon r = 2.9$) with a 0.05 mm thick conductive layer over the surface of the antenna, representing 3 layers of paint or plating.

The conductivity of the copper plating used in the simulation is $5.96X10^7$ S./m. The manufacturer's provided data on conductivity of the copper paint is $1.4X10^6$ S/m and the silver paint is $6.6X10^6$ S/m [29].

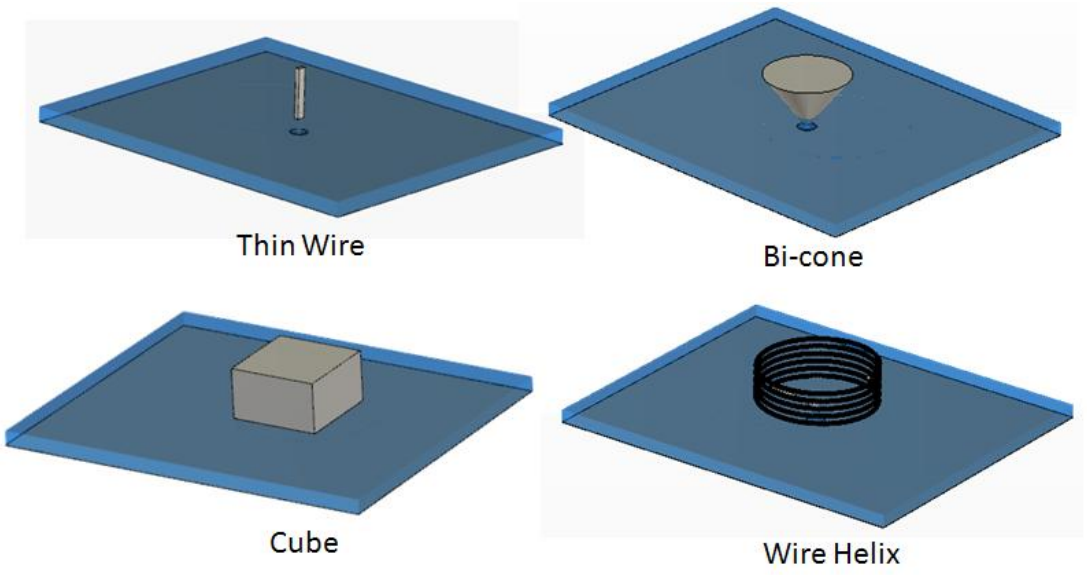

Figure 15: The 4-layer cubical patch is compared to a selection of standard antenna geometries.

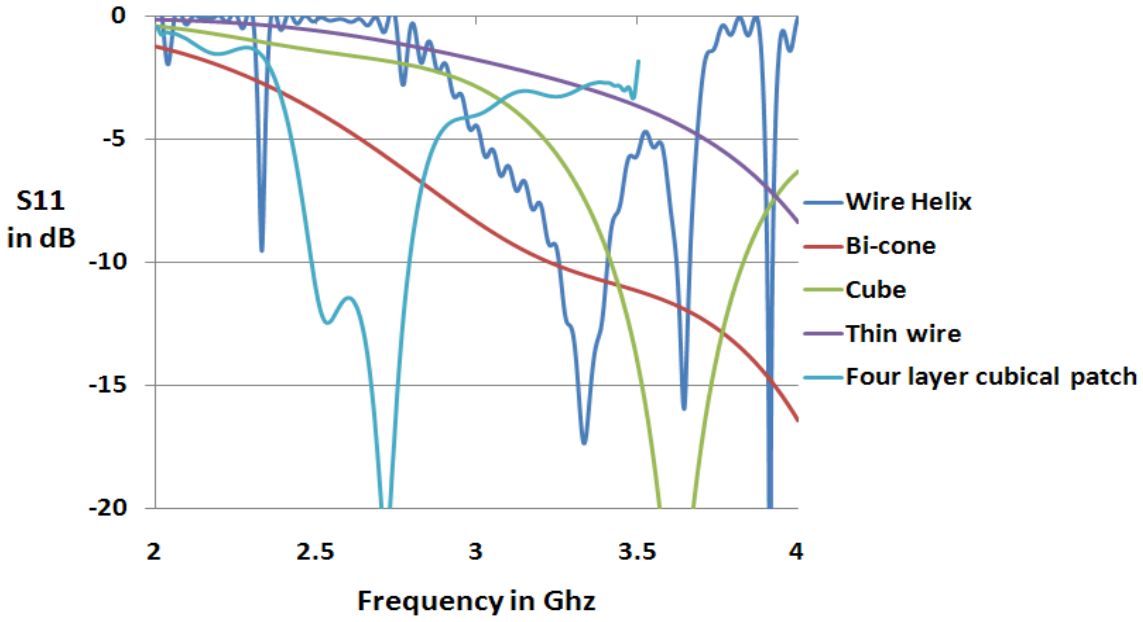

Figure 16: S11 data comparing the 4-layer cubical patch with a selection of standard antenna geometries, the cubical patch operates at a lower frequency with comparable bandwidth.

The more realistic simulations with thin layers of good but imperfect conductors agree with the measured data better than the idealized PEC results, as shown in Figure 17.

Perhaps in the future a good design methodology would be to design the antenna using the simplified PEC until it converges to a good candidate antenna and then refine it using a more complete model, including the skin effects of thin, imperfectly conducting materials.

The conductivity of the paint is sufficiently high that it acts as a good conductor. The challenge is that the paint layer of 8 microns is less than the skin depth at 2GHz. To better quantify the number of paint layers needed, the 4-layer 3D GA antenna was measured using a network analyzer for it S11 values with 1, 2 and 3 layers of silver paint as shown in Figure 18.

Also included is the PEC simulation. The thinner the conductive layer, the more the skin depth effects are seen. The simulation also indicated that once the skin depth is sufficiently thick, which implies greater than ~4 skin depths, the loss is negligible. When the thickness grows larger than necessary, the individual cube features begin to diminish and the S11 values for the antenna begin to vary.

The 4-layer 3D GA antenna was then simulated as a solid conductive material with various conductivities. Figure 19 shows the realized peak gain of the 4-layer 3D patch as a function of conductivity. The datum in Figure 19 illustrates that the conductivity can decrease to about 1% that of copper and still maintain efficiency near that of the copper antenna.

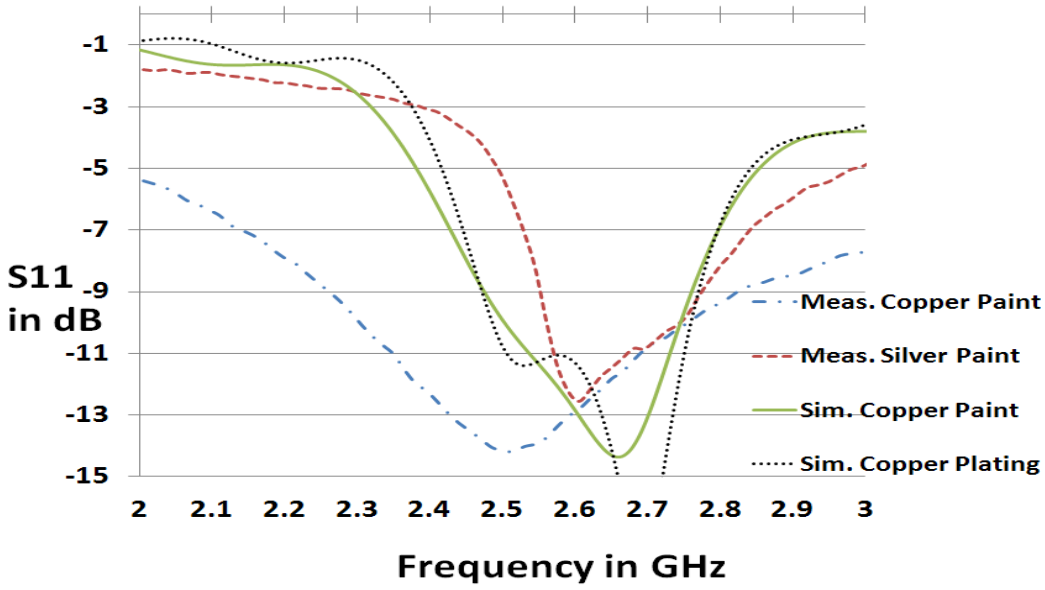

Figure 17: Measured S11 for the 4-layer 3D GA antenna (Vero plastic coated with 1 layer of copper or silver paint approximately 10 micrometers thick) compared to the antenna simulated with 1 layer of copper paint (10 micrometer thickness, conductivity $5X10^6$ S/m) and copper plating (thickness 0.1 um, conductivity $5.96X10^7$ S/m). The skin depth of the paint material is approximately between 2 and 10 microns at 2 GHz, depending on the material.

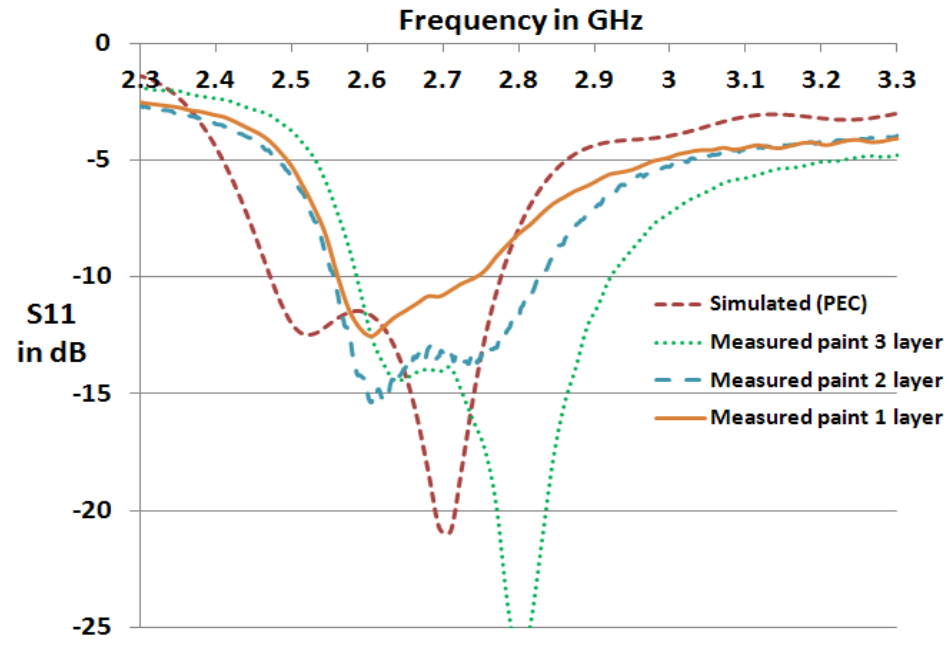

Figure 18: A comparison of return loss and the thickness of conductive paint for the 4-layer patch antenna.

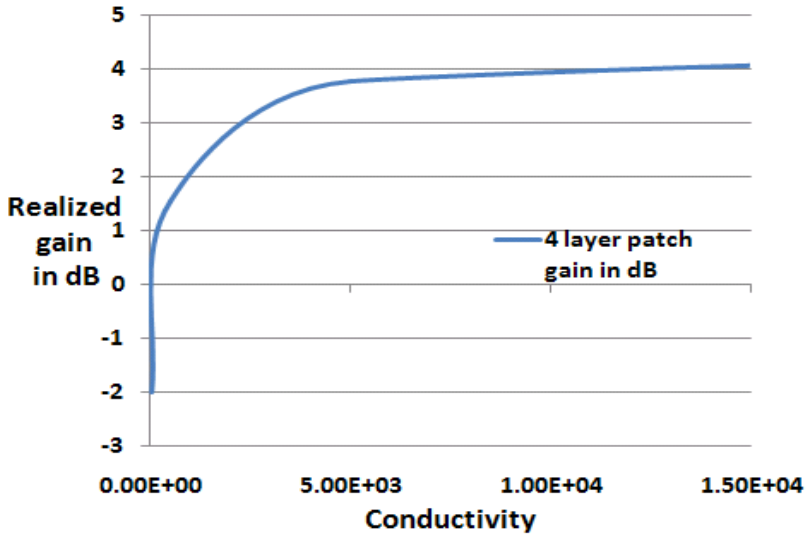

Figure 19: Simulated data of gain vs. conductivity for the 4 layer cubical patch antenna, showing extreme drop off occurring with conductivity less than $5X10^3$

The measured gains of the patch with 3 layers of copper or silver paint and the idealized PEC simulation are shown in Figure 20. The gain is based on the gain available from the isotropic radiator and is given in dBi. Each gain plot is measured across the azimuth plane with elevation at 0 degrees. The peak gain was measured for each antenna at its resonant frequency (2.7 GHz for the measured antennas, 2.6 GHz for simulated). The peak measured gain for the silver paint is 4.9 dBi, and copper paint is 4.71dBi. The SLS antenna has simulated gain using PEC at 5.24 dBi and measured at 5.21dBi. The silver painted antenna is ~6% less efficient than the solid SLS antenna.

A simulation was performed to find the total dissipated power in the antenna. The simulation indicated how much power the plastic antenna could accept before deforming. The simulated data are given in Table 7.

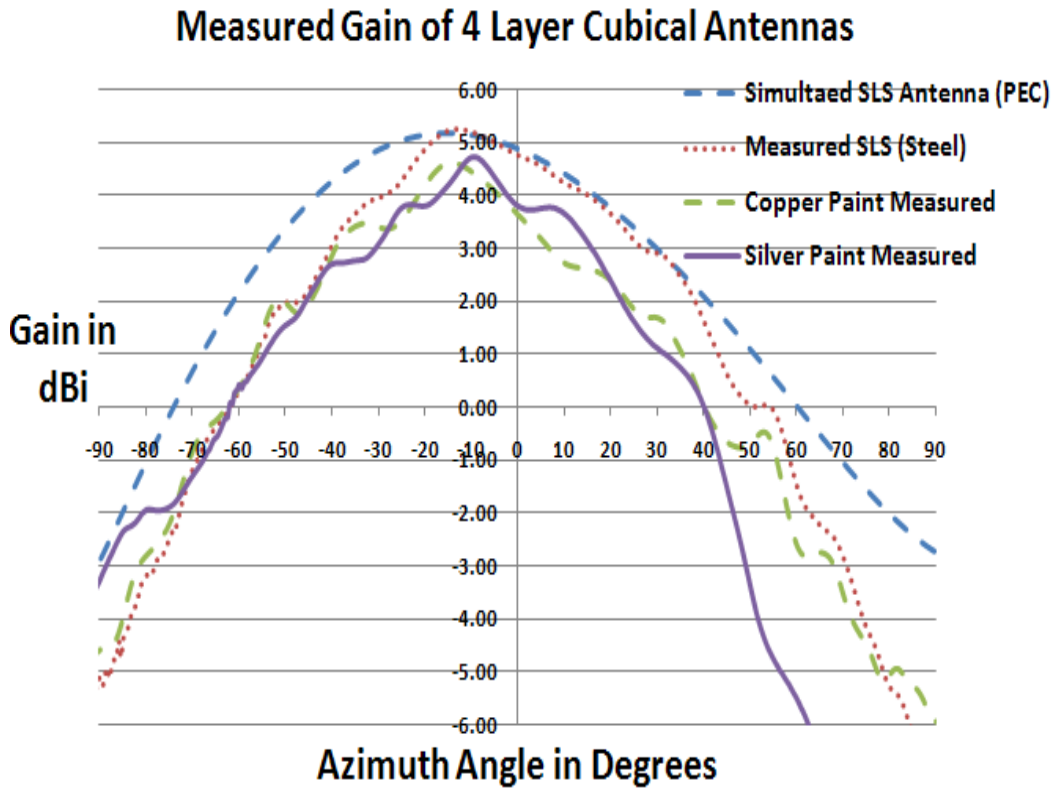

Figure 20: Comparison of gain for the 4 layer 3D GA antenna measured with 3 layers of copper or silver paint and simulated with PEC. Gain is reported at the resonant frequency of the antenna (2.7 GHz for the measured antennas and 2.6 GHz for the simulated PEC antenna)

Table 7: Power loss in the cubical patch antenna

Frequency in GHz	Power loss density in Watts/m^3	Volume in m^3	Watts dissipated	Watts input	Temperature in C°
2.5	28,744	0.000103	2.97	20	113

3.5 Conclusion

This paper has demonstrated that GA design and rapid prototyping can be used as a viable method for manufacturing 3D antennas.

Both 3D printed plastic coated with metallic paint and metal antennas produced by selective laser sintering were viable options. The skin depth effects must be taken into account in these designs. Antennas with 3 layers of paint were better than those with 1 or 2.

As expected, the 3D designs had lower frequencies and higher bandwidth than a 2D antenna with the same footprint. The GA design has a ka of 1.1 when the full size ground plane is removed.

3D rapid prototyping opens up a wide array of potential antenna designs. This paper demonstrated the use of a GA to optimize the designs, but any good optimization method could also be used. The designs in this paper were limited to simple cubical volumes for convenience. Other, much more complex volumes could be used instead. In addition to flexibility of design, the antennas produced using printed plastics coated with metallic paint are much lighter than metal antennas produced using either SLS or (if it were possible to build them at all) traditional metals.

The use of SLS or 3D printing for antenna designs opens up many options in simple, cost-effective 3D antenna design. Both of these methods can be used to produce antennas that have metal or metal-like bodies, and they can be used above a substrate material (as in this paper) if back radiation is not desired. The conductivity of the paint is sufficiently high that it acts as a good conductor. The challenge is that the paint layer of 8 microns is less than the skin depth at 2GHz. They are also lighter weight than

equivalent antennas built of metal. Antennas with a combination of conductors and insulators could be more difficult to build this way. The emerging ability to print conductive materials could soon open up the option to build antennas with a wider variety of distributed materials, perhaps even printing circuits along with the antenna. 3D rapid prototyping provides an opportunity to pursue complicated 3D antenna designs that would otherwise be impractical. It enables a new, wide array of potential antenna designs.

3.6 References

[1] H. A. Wheeler, "Fundamental Limitations of Small Antennas," *Proc. IRE*, vol. 35, pp. 1479–1488, Dec. 1947.

[2] L. J. Chu, "Physical limitations of omni-directional antennas," *J. Appl. Phys*., vol. 10, pp. 1163–1175, Dec. 1948.

[3] J. S. McLean; "A Re-Examination of the Fundamental Limits on the Radiation Q of Electrically Small Antennas," *IEEE Trans. Antennas Propag.*,Vol. 44, No. 5, May 1996, pp. 672-676

[4] L.Griffiths, C.Furse, "Performing 3-D FDTD Simulations in Less than 3 Seconds on a Personal Computer and its Application to Genetic Algorithm Antenna Optimization," *Applied Computational Electromagnetics Society Journal, Vol. 20, No. 2*, pp. 128-135, July 2005

[5] H. Rmili, O. E. Mrabet, J.-M. Floc'h, J.L. Miane, "Study of an Electrochemically-Deposited 3D-Fractal Tree Monopole Antenna," *IEEE Trans. Antennas Propag.*,vol. 55, no. 4, Apr. 2007, pp. 1045-1050

[6] S. R. Best, "Low Q Electrically Small Linear and Elliptical Polarized Spherical Dipole Antennas," *IEEE Trans. Antennas Propag.*, vol. 53, pp. 1047–1053, Mar. 2005.

[7] H.L. Thal,, "New Radiation Limits for Spherical Wire Antennas," *IEEE Trans. Antennas Propag.*,vol.54, no.10, pp.2757-2763, Oct. 2006

[8] H.L.Thal,, "A Reevaluation of the Radiation Q Bounds for Loop Antennas," *IEEE Antennas and Propagation Magazine*, vol.51, no.3, pp.47-52, June 2009

[9] S. R. Best, "Low Q Electrically Small Linear and Elliptical Polarized Spherical Dipole Antennas," *IEEE Trans. Antennas Propag.*,vol. 53, pp. 1047–1053, Mar. 2005.

[10] S. R Best, "The Radiation Properties of Electrically Small Folded Spherical Helix Antennas" *IEEE Trans. Antennas Propag.,Vol. 52, no. 4*, April 2004 page 953-960

[11] E. E. Altshuler, "Electrically small self-resonant wire antenna optimized using a genetic algorithm," *IEEE Trans. Antennas Propag., vol.50*, no. 3, pp. 297–300, Mar. 2002.

[12] [Online available] *http://www.geneticprogramming.com/coursemainpage.html* [Sep. 2, 2010]

[13] E. Altshuler, T. O'Donnell, 'An Electrically Small Multi-Frequency Genetic Antenna Immersed in a Dielectric Powder,' *IEEE Antennas and Propagation Magazine,* vol. 53, no. 5, Oct. 2011, pp.33-40

[14] J. Bernard, J. Lewis, J. Adams, et al, "Conformal Printing of Electrically Small Antennas on Three-Dimensional Surfaces", *Advanced Materials,* Vol. 23, Issue 11, pp. 1335–1340, March 18, 2011

[15] C.Pfeiffer, A.Grbic, "Novel Methods to Analyze and Fabricate Electrically Small Antennas" Spokane Washington, *IEEE Antennas and Propag. Soc. Int. Symp., July 3rd – 8th 2011*

[16] [Online Available] *http://www.spraylat.com/Products/ElectronicMaterials/Technology/ConductiveCoatingTechnology.aspx* [Accessed Sep 15th 2011]

[17] E.E.Altshuler, S.R.Best, T.H.O'Donnell, N.Herscovici, "An Electrically-Small Multi-Frequency Genetic Antenna Immersed in a Dielectric Powder," *Antenna Technology, 2009. iWAT 2009. IEEE International Workshop on* , vol.,o.,pp.13, 2-4 March 2009

[18] E. Faruk, C.C. Chen,J.L.Volakis, " Impedance Matched Ferrite Layers as Ground plane Treatments to improve Wide-Band Performance," *IEEE Trans. Antennas Propag.,* vol 57, no. 1, pp. 263-266, Jan 2009.

[19] S. Best, D. Hanna, "Design of a broadband dipole in close proximity to an EBG ground plane," *IEEE Antennas and Propagation Magazine,* vol.50, no.6, pp.52-64, Dec. 2008

[20] Kawano, Y.; Songyoung Bae; Koyanagi, Y.; Morishita, H.; , "A study on miniaturization of a handset antenna utilizing magnetic materials," Antenna Technology: Small Antennas and Novel Metamaterials, 2005. IWAT 2005. IEEE International Workshop on , pp. 129- 132, 7-9 March 2005

[21] H. Arai, S.Nagatsuka, "Low-profile Dual-mode Plate-loop Antenna," *Antenna Technology, 2009. iWAT 2009. IEEE International Workshop on* , pp.1-4, 2-4 March 2009

[22] MTT Manufacturing Technologies group " Direct Metals Manufacturing Technology " *http://www.mtt-group.com/selective-laser-melting.html* Dec. 22 2010 [Oct 9 2010]

[23] [Online] RedEye Express "Open Market Rapid PrototypeQuotes"*http://express.redeyeondemand.com.* 2010 [Oct 12 2010]

[24] [Online]Dalmar Mfg Co "Dalmar plating information site" *http://www.dalmar.net* [Oct 9 2010]

[25] T. Wohlers, Wohlers Report 2009, "Rapid Prototyping, Tooling & Manufacturing State of the Industry," *Annual Worldwide Progress Report, Wohlers Associates Inc.,* Colorado, USA

[26] H.Huang, K.Nieman, Y.Hu, D.Akinwande, "Electrically Small Folded Ellipsoidal Helix Antenna for medical Implant applications," *IEEE Antennas and Propag. Soc. Int. Symp*.,, vol., no., pp.769-771, July 3-8,201110.1109/APS.2011.5996826

[27] H. Sigmarsson, E.Kinzel, W.Chappell, X.Xianfan , "Selective Laser Sintering of Patch Antennas on FR4," *IEEE Antennas and Propag. Soc. Int. Symp*., vol.1A, pp. 280- 283 July 3-8, 2005

[28] [Online Available] :*http://www.ventistech.com/about.htm* [Accessed on Aug 27th 2011]

[29] [Online] Objet Geometries Inc "Connex 500 3D printer"*http://www.objet.com/3DPrinter/Objet_connex500/ 2011*, [Jun 2 2010]

[30] [Online available] http://store.makerbot.com/ ; last accessed Jan 22 2012;

[31] [Online available] www.dimensionprinting.com; last accessed Nov 16 2011;

[32] [Online] Z Corporation "The Fastest, Most Affordable Color 3D Printing" *http://www.zcorp.com/documents/931_9062-ZPrinterBroch.pdf,* 2010 [June 2 2010]

[33] [Online Available] h*ttp://reprap.org/wiki/Gada_Prize.* [Accessed: 11th Jan. 2011].

[34] J. Bayless, M. Chen, B. Dai; "Wire Embedding 3D Printer," *Engineering Physics University of British Columbia* April 12, 2010

[35] [Online]Available:*http://www.coolpolymers.com/XyloyM950.asp* [Accessed on April 6th 2011]

[36] J.R. Honiball "The Application of 3D Printing in reconstructive surgery", *PhD Dissertation, University of Stellenbosch* , Mar. 2010

[37] [Online]Available:*http://www.foresight.org/gadaprize.php.* [Accessed: 11th Jan. 2011].

[38] Ronald L. Hollis, "The Proliferation of 3D Printing Machines", *Product Design and Development Magazine,* 4/12/2010.

[39] [Online]Available:*http://spectrum.ieee.org/geek-life/hands-on/diy-essentials/2* [Accessed on Aug 20th 2011]

[40] A. Moscicki, J. Felba, T. Sobierajski, J. Kudzia, A. Arp, W. Meyer, "Electrically Conductive Formulations Filled Nano Size Silver Filler for Ink-Jet Technology," *in Proc.,5th International Conference on Polymers and Adhesives in Microelectronics and Photonics*, October 2009, pp. 40-44.

[41] A. Koptioug, P. Jonsson, J. Sidén, T. Olsson M. Gulliksson, " On the Behavior of Printed RFID Tag Antennas using Conductive Paint," in the Proceedings of Antenna-03, Kalmar, Sweden, 2003.

[42] K. I. Rybakov, V. E. Semenov, S. V. Egorov, A. G. Eremeev, I. V. Plotnikov, Y.V. Bykov, "Microwave Heating of Conductive Powder Materials", *AIP Journal of Applied Physics*, vol. 99, Issue. 2, Jan. 2006, pp. 023506-1 – 023506-8

[43] M.A. Gayness, R. H. Lewis, R. F. Saraf, J.M. Roldan, " Evaluation of Contact Resistance for Isotropic Electrically Conductive Adhesives," *IEEE Trans. on Components, Packaging, and Manufacturing Technology* ,vol.18, Issue: 2, May 1995, pp. 299 – 304

[44] [Online]*http://www.mgchemicals.com/products/8331.html* [Accessed Nov 12 2011]

[45] R. Malamud, I. Cheremisov, "Anti-Corona Protection of High Voltage Stator Windings and Semi-Conductive Materials for its Realization*", IEEE International Symposium on Electrical Insulation,* Apr. 2000, pp.32-35.

[46] K. Bock, “Polytronics-Electronics and Systems on Flexible Substrates”, *IEEE VLSI-TSA International Symposium on VLSI Technology*, Apr. 2005, pp.53-56

[47] J. Saberin,C. Furse, “Challenges with Optically Transparent Patch Antennas”, *IEEE Antennas and Propagation Magazine*, in press

[48] R. Gordon, “Criteria for choosing transparent conductors," *MRS Bulletin*, August 2000.

[49] K. Bock, “Polytronics-Electronics and Systems on Flexible Substrates”, *IEEE VLSI-TSA International Symposium on VLSI Technology*, Apr. 2005, pp.53-56

[50] A. R. Duggal, L. M. Levinson, “A Novel High Current Density Switching Effect in Electrically Conductive Polymer Composite Materials”, *AIP Journal of Applied Physics*, vol. 82, Issue 11, Dec. 1997, pp. 5532 – 5539

[51] D. Micheli, C. Apollo, R. Pastore, Mario Marchetti, “Modeling of Microwave Absorbing Structure using Winning Particle Optimization Applied on Electrically Conductive Nano-structured Composite Material”, XIX *International Conference on Electrical Machines* ,Sept. 2010,pp.1-10.

[52] Y. Li, R. Zhang, L. Shu, W. Lin, O. Hilbreth, H. Hiang, J. Lu, Y. Xiu, Y. Liu, J. Moon, C.P. Wong, “Nano Materials and Composites for Electronic and Photo Packaging”, 9th *IEEE Conference on Nanotechnology*, July. 2009, pp.1-3.

[53] H.Huang,K.Nieman, Y.Hu, D.Akinwande, , "Electrically Small Folded Ellipsoidal Helix Antenna for Medical Implant Applications," *IEEE Antennas and Propag. Soc. Int. Symp*.,pp.769-771, July 3-8, 2011

[54] H. Sigmarsson, E.Kinzel, W.Chappell, X.Xianfan, "Selective Laser Sintering of Patch Antennas on FR4," *IEEE Antennas and Propag. Soc. Int. Symp*., vol.1A, pp. 280- 283 July 2005

[55] Y. Ouyang, E. Karayianni, W. J. Chappell, “Effect of Fabric Patterns on Electrotextile Patch Antennas,” *IEEE Antennas and Propag. Soc. Int. Symp*., 2005, vol. 2B, pp. 246–249.

[56] A. Tronquo, H. Rogier, C. Hertleer, L. Van Langenhove, “Applying Textile Materials for the Design of Antennas for Wireless Body Area Networks”, *Proceedings of the European Conference on Antennas and Propagation, EUCAP 2006*, Nice, France, p. 159, November 2006.

[57] P. Salonen, Y. Rahmat-Samii, M. Schaffrath, M. Kivikoski, “Effect of Textile Materials on Wearable Antenna Performance: A case study of GPS Antennas,” *in Proc. IEEE Antennas Propag. Soc. Int. Symp*., 2004, vol. 1, pp. 459–462.

[58] A. Tronquo, H. Rogier, C. Hertleer, L. Van Langenhove, "Robust planar textile antenna for wireless body LANs operating in 2.45 GHz ISM band", *IEEE Electronic Letters*, Vol. 42, Issue. 3, February 13,2006, pp. 142-143

[59] R.Haupt , D. Werner, Genetic Algorithms in Electromagnetics *John Wiley & Sons*, Hoboken, New Jersey 2007.

[60] R.Eberhart, J.Kennedy, "A New Optimizer using Particle Swarm Theory," Micro Machine and Human Science, 1995. MHS '95., *Proceedings of the Sixth International Symposium on , vol., no.,* pp.39-43, 4-6 Oct 1995

[61] C. Balanis, Antenna Theory Analysis and Design, 3rd edition, John Wiley and Sons, Hoboken New Jersey, 2005, page 811.

[62] [Online Available] *http://www.cst.com/* [Accessed: 11th Dec. 2011].

[63] B.Willis , C.Furse,"3D Rapid Prototyping for Small Antenna Design" Spokane Washington, *Antennas and Propagation Conference July 3rd – 8th 2011*

CHAPTER 4

DESIGN AND RAPID PROTOTYPING FOR 3D SPACE EFFICIENT ANTENNAS

3D rapid prototyping holds significant promise for future antenna designs. This paper demonstrates how rapid prototyping can be used to create 3D antennas of random shape which are optimized for high bandwidth. An antenna of random shape is optimized to function above a dielectric and ground plane. The antenna was optimized using a Genetic Algorithm (GA) to form layers of cubical blocks. The antenna was built using plastic 3D rapid prototyping and metalized with conductive paint. A 3D dipole is also optimized using a GA to function from 510-910MHz. The antenna was built using 3D rapid prototyping from plastic. The 3D antenna was covered with a conductive coating and measured showing good agreement with simulation. The 3D GA is used to design 3D antennas of random shape to fit inside the empty space in a cell phone case and optimized for cell phone bands 800-900MHz and 1.6-3.7GHz.

4.1 Introduction

The work in this paper focuses on how to easily design, develop, and manufacture small 3D antennas. Small antenna theoretical limits set forth by Wheeler [1] and Chu [2]

show that antennas can be optimized when they fill the 3D spherical space encompassing their maximum dimension. Thal has calculated limits for spherical antennas in [3], and [4]. Best demonstrates low Q small spherical dipoles [5] and properties of a small spherical helix [6].

3D antennas that approach the Chu limit have typically been difficult or impossible to build. Complicated soldering of bent pieces of wire has been used to produce some intriguing 3D antennas including the spherical antenna in [7] and an antler-shaped antenna in [8]. In [9], a 3D fractal tree is randomly grown by an electrochemically deposited conductor. Unfortunately, the manufacturing methods required to produce these 3D antennas have previously been so cumbersome or expensive that they were regarded as far-fetched and impractical. More recently, a 3D hemispherical antenna was built by printing a meander-line antenna pattern on a curved glass surface with a silver ink [10]. Another recent 3D spherical antenna was built using a process called direct transfer patterning [11]. The process uses a stamp to get the desired pattern onto a curved surface. It then requires a 6-step process including a plasma etch and gold plate to finalize the design on polyethylene terephthalate. These antennas do utilize the exterior of the 3D space, but they are not easily adapted to random-shaped spaces and still have limitations in the types of antennas that can be built using these methods. But now, cutting edge rapid prototyping creates 3D manufacturing opportunities that have not previously been available in the antenna design world. This paper assesses these methods, and their application to realistic 3D antenna designs.

We recently demonstrated the feasibility of using 3D printing to print the antenna shape in plastic and then coat it with metallic paint to produce an inexpensive 3D antenna

that randomly utilized the 3D space [12], [13]. The antenna was built from small cubes whose layout is optimized using a genetic algorithm (GA) originally used to design 2D patch antennas [14]. The cost function is calculated by setting a minimum value as the goal; in this case, the value is -200. The cost function is evaluated by taking each discrete frequency point and comparing it to the minimum value; each point over the frequency band is then added up and averaged for the total cost.

Metallization could also be done by prototyping with metallic materials such as selective laser sintering (SLS), which was also demonstrated in [13] for a cell phone type antenna. In the case of paint over plastic, the skin depth of the paint must be taken into account, and the conductivity of the surface determines the efficiency and performance of the antenna. This determines how many layers and what kind of paint is needed for a given frequency range.

This chapter demonstrates three different kinds of printed 3D antennas. A 3D monopole above a ground plane, a 3D dipole-type design, and an antenna designed to fit the relatively random-shaped void available in a commercial cell phone. The manufactured antennas are built from 3D cubes of printed plastic coated with paint. The specific layout of the cubes is optimized using a genetic algorithm (GA). Other layouts, shapes, and configurations could be designed, and other optimization methods could be used [15], but these example designs demonstrate the feasibility of using emerging 3D rapid prototyping tools and simple optimization methods to create 3D antennas that are quick and easy to build. In addition, antennas that are printed in this way are very light weight and inexpensive. And they are handy; even traditional 3D antennas such as horns

and helices could be built with 3D rapid prototyping, thus providing virtually any antenna at your fingertips.

One of the particular designs that is demonstrated in this paper is for a cellular telephone, where the somewhat random-shaped void in the handset can be filled with the antenna. The sleek look and high capability of today's smart phones has increased demands for PCB real estate while shrinking the volume available for the antenna(s), and demanding efficient multiband performance. 3D antennas that efficiently utilize small, random-shaped volumes can provide increased performance for future phones.

This chapter demonstrates the application of 3D prototyping for realistic antenna design. Section 4.2 describes the GA-optimized cube-based antennas built with 3D plastic printing coated with conductive paint. Section 4.2 gives the example of a monopole-type antenna (2.6-2.95GHz), and Section 4.3 describes a dipole for the UHF band (500-900 MHz). Both of these examples demonstrate the power of 3D antenna design in general.

Section 4.4 introduces a real-world application for optimized 3D antennas. A cell phone antenna is optimized to fill the random-shaped void in a commercial cell phone case, thus demonstrating the viability of fitting antennas in places that have previously been wasted space.

4.2 3D Rapid Prototyping for Antennas

3D rapid prototyping provides a novel, easy, and inexpensive manufacturing technique for antennas of arbitrary shape. Most antennas are built out of metals or a combination of metals and insulators (plastics). In [13], we focused on prototyping

methods that include metals, or metal paints or coatings over a 3D printed plastic base. The antenna is built of small cubical cells filling the available space, optimized with a genetic algorithm (GA) adapted from a method used for 2D planar antenna design [14]

The GA used divided the antenna into a grid; each of these grid locations is one chromosome for the GA. If the chromosome is 'on', the cube at that location will be metallic. If the chromosome is 'off', the cube will be air. The length of the chromosome is 196, the mutation rate is 0.3, and the population size is 2. The chromosome was initially a randomly generated sequence of ones and zeros, but after only a few generations (each with a simple population of 2 and mutation rate of 0.3), the antenna begins to take on a shape that more or less fills the available volume.

The forward solution used to determine the performance and hence the fitness of the antennas was done with a commercial finite integral technique (FIT) solver, CST Microwave Studio [16]. The optimization required 1500-4500 design iterations for this example antenna. This was controlled outside of CST with an additional Matlab® script interfaced to CST with a visual basic (VBA) script. The cost function is calculated in CST. For this test, we optimized by minimizing the S11(in dB) from 2.2-3.2GHz. The cost function is evaluated by taking each discrete frequency point and comparing it to the minimum value. The frequency band of 1-3GHz is sampled at 1000 points, then added up and averaged for the total cost. The optimization was tested 3 times, for 1,500, 3,000, and 4,500 iterations to ensure convergence. It did converge each time.

Figure 21 shows the optimized cubical antenna above a ground plane. The antenna is printed using an Objet Connex 500 [17] in Vero white. The printing time took approximately 20 minutes. The printed patch is then coated with copper paint [13].

Figure 21: 3D printed cubical antenna above a ground plane. From [13]. © 2012 IEEE. Reprinted with permission.

The paints used in [13] are produced by Spraylat® and are commonly used for EMI shielding. The conductivity varies by thickness and paint type. Both silver and copper paint were evaluated in [13]. In order to minimize losses in the antenna, it is important to make the paint or coating at least 1-2 skin depths thick [18]. Based on the manufacturer's data sheet [19], 20 micrometer thick silver paint has conductivity of $1x10^7$ S/m and skin depth of 3.5 micrometers at 2 GHz. Copper paint has conductivity of $5x10^6$ S/m and a skin depth of 5 micrometers. The effect of the finite conductivity of the copper paint is seen in Figure 22, which shows the gain of the antenna in Figure 21 with silver or copper paint or built from metal using a SLS process. The plastic antenna had a significant weight reduction; the plastic with paint weighted (2.5g) and SLS (13.7 g).

This antenna demonstrates the feasibility of building a randomized-antenna with 3D rapid prototyping, but it was not designed for a specific application [13]. The design indicated that there is 46% reduction in planar surface area and 4.5 times the bandwidth over its 2D counterpart.

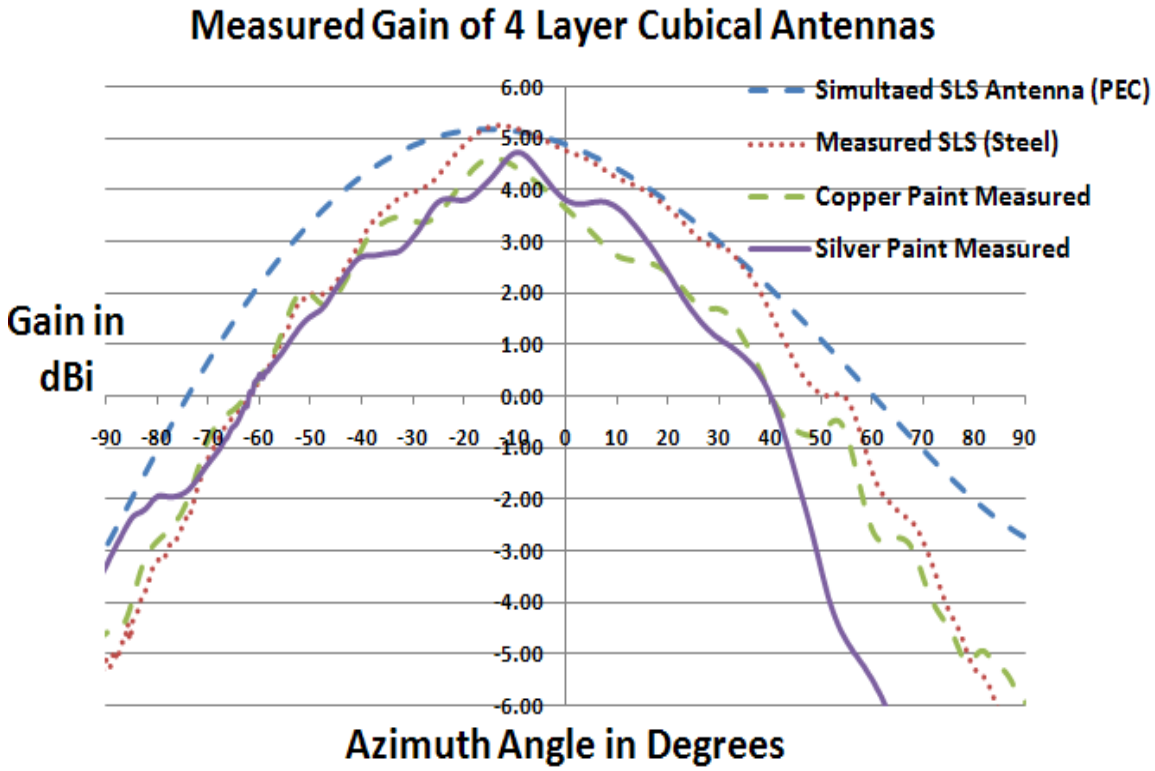

Figure 22: Measured gain for the cubical antenna in Figure 21 compared to the simulated design with perfect conductivity (PEC). The lower conductivity of the paint coating reduces the gain of the antenna. Silver painted antenna is ~6% less efficient than the solid SLS antenna.

The next two sections demonstrate the application of the method to two realistic antennas. Section 4.3 covers a UHF dipole-type antenna for maritime UHF radio or mobile UHF radio application, and Section 4.4 describes an antenna that is designed to fill the random-shaped void in a cell phone case.

The UHF antenna was then 3D printed and metalized with 3 layers of Preval® silver conductive paint [19]. The 50 ohm connector was soldered with conductive epoxy [20] into a small bracket that was 3D printed as part of the antenna design, and is shown in Figure 23. The built UHF antenna weighed 242 grams. By comparison, a selective laser sintered antenna would weigh ~1326.16 grams.

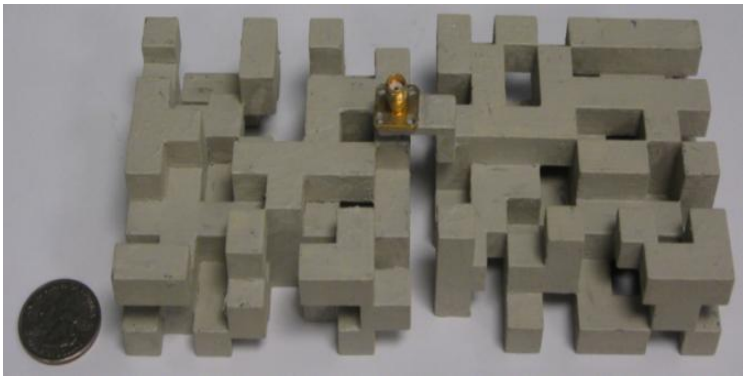

Figure 23: UHF dipole bottom view with silver paint shown next to a US quarter

4.3 UHF Dipole-Type Antenna

In this section, we will describe the manufacturing details and measurements of the UHF dipole antenna shown in Figure 23. For simplicity and speed of simulation, the antennas were initially designed as perfect electric conductors. The antennas were then printed in plastic and then metalized by spraying it with 3 layers of silver metallic paint. The details on paint thickness, skin depth, and conductivity are shown for UHF in Table 8. This shows that 2-3 layers of paint are needed in order to have the thickness greater than 2-3 skin depths.

The research in this paper used the GA from [13] to optimize a dipole antenna. The antenna design method is similar to earlier work; however, this antenna has no ground plane, and was designed to function at a lower frequency (540 MHz).

The antenna is shown in Figure 23. This antenna is fed with a 50 ohm SMA connector in the center. At 610 MHz (UHF), a half-wave dipole would be ~170 mm long. This is the maximum dimension of the 3D antenna optimized with the GA.

Table 8: Paint thickness, skin depth, and conductivity for 500 MHz

Material	Paint thickness (microns)	Skin depth (microns)	σ (S/m)
Silver paint (1 layer)	7.5	8.7	$6.67X10^6$
Silver paint (2 layers)	15	6.1	$1.33X10^7$
Silver paint(3 layers)	23	3.4	$4.35X10^7$
Copper paint (1 layer)	7.5	18.5	$1.48X10^6$
Copper paint (2 layers)	15	12.3	$3.33X10^6$
Copper paint (3 layers)	23	10.8	$4.35X10^6$

The 3D dipole is built in a 81.2 x 30.48 x 170 mm space. The feed point is in the center of the antenna, with a 7mm gap between the two sections of the antenna. The antenna volume was then subdivided into two sets (each side) of 3 layers of 8x8 cubes, each 10.1 mm (approximately 1/60th of a wavelength at 600MHz). The UHF dipole was optimized to function at the lowest possible frequency (in this case, it turns out to be 540 MHz) and over as large a bandwidth as possible (540-910MHz). The optimization was tested 3 times, for 1,500, 3,000, and 4,500 iterations to ensure convergence. It did converge each time, starting with a cost of 189; after about 300 iterations the cost was 125. The lower operating frequency of the GA antenna (541 MHz) compared to a flat dipole (610 MHz) shows the advantage in performance per size that can be obtained with 3D antennas.

The measured S11 values for the UHF dipole are shown in Figure 24. The UHF dipole shows much better agreement with simulated PEC results than did the GA

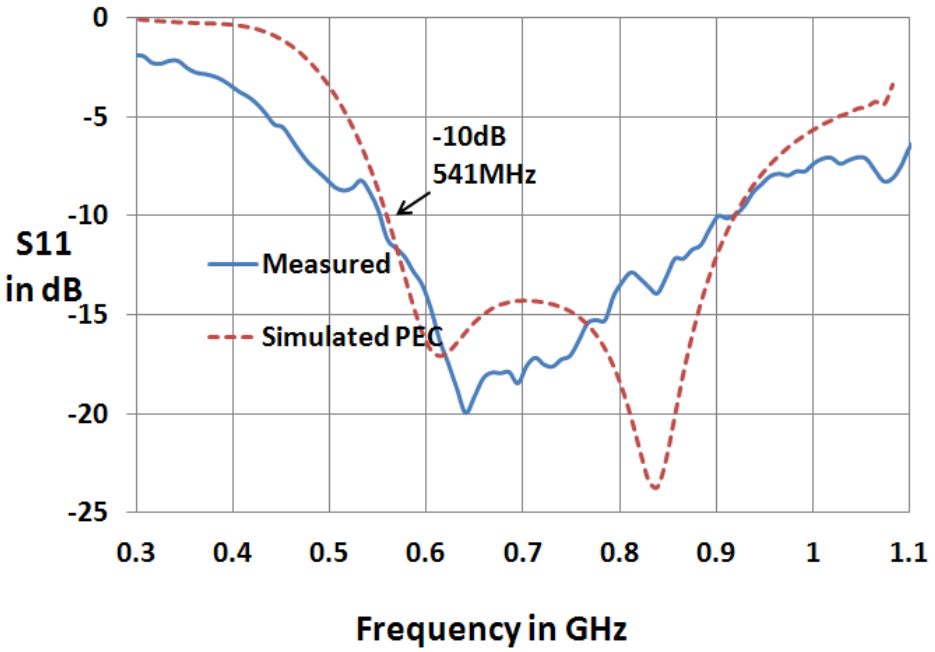

Figure 24: Measured (plastic silver paint) and simulated PEC S11 values for the UHF dipole antenna shown in Figure 23

monopole shown in Section 4.2 [13]. The difference is not due to the conductivity or thickness of the paint. It is believed the dielectric above a ground plane for the GA monopole is slightly different in simulation than with the measured antenna at 2.5GHz, causing the slight shift.

The UHF dipole optimized with the GA is wide band and approaches the small antenna size at its lower frequency resonance. The frequency of operation and bandwidth compare well with the Goubau antenna which is well referenced in the open literature [21]. The *ka* value is calculated for the UHF dipole antenna. Here k is $2\pi / \lambda$, with λ the free space wavelength and a the radius of an imaginary sphere inclosing the entire antenna. Because of the wide bandwidth of this antenna, we utilize a similar comparison from Best completed on work intended for a conference [22]. The research initiates a comparison for cylindrical shaped antennas which are wideband. The *ka* comparison does

not use the center frequency because the *ka* would be much larger than 1 at the center and at the lower frequency, the *ka* is less than 1. The Q is calculated based on the inverse relationship between the fractional matched VSWR bandwidth FBW [22] shown in equation 1 and 2. Using the comparison factor in equation 3 from research completed by Best [22], we compare our design to the Goubau antenna.

$$Q(\omega_o) \approx \frac{2\sqrt{\beta}}{FBW_v(\omega_o)}, \tag{4.1}$$

$$\sqrt{\beta} \approx \frac{s-1}{2\sqrt{s}} \leq 1 \tag{4.2}$$

$$CF = \frac{BWR}{(ka)^3}\frac{d}{l} \tag{4.3}$$

The Goubau antenna has a *ka* of 0.76 and a CF of 11.1; the UHF dipole which was optimized with a GA has a *ka* of 0.96 and a CF of 11.0. The antenna was easily built using 3D printed plastic and coated with conductive paint. The painted antenna matched very well with the PEC simulated data.

4.4 Mobile Phone Antenna

In this section, we demonstrate how the method of using a 3D GA antenna to fill a random-shaped space can be applied to a mobile device with limited, odd-shaped interior cavities. A simple feature phone has been chosen for demonstration purposes, because it was handy and easy for us to measure the interior space. The same technique can be used for designing antennas for more advanced devices. This is an application where low cost and weight are critical, as well as in multiband design to accommodate the various communication standards.

A flip phone was disassembled, and the interior area measured to determine the potential space available where there will also be minimal blockage from the hand, as shown in Figure 25.

We would like to emphasize that this was not a collaboration with the manufacturer of the phone, and no special care was taken to be sure the antenna would actually work in this phone (location of feed point, for instance). This was a phone we had available, and our goal was to demonstrate the potential for a light weight, low cost 3D antenna for applications where the cavity space available for the antenna may be odd in shape.

The phone geometry, particularly the interior space, was modeled as realistically as possible. The plastic case was hypothetically changed to be a radome composed of Acetal [23], a lower loss plastic material, with ε_r =2.9, since we did not know the actual plastic used. The circuit board was modeled as Rogers™ 4003 with a ε_r = 3.6 and a thickness of 0.25mm. The LCD display and camera were modeled with ε_r = 11.6, and a thickness of 2.5mm. The speaker and its subassembly where modeled as PEC.

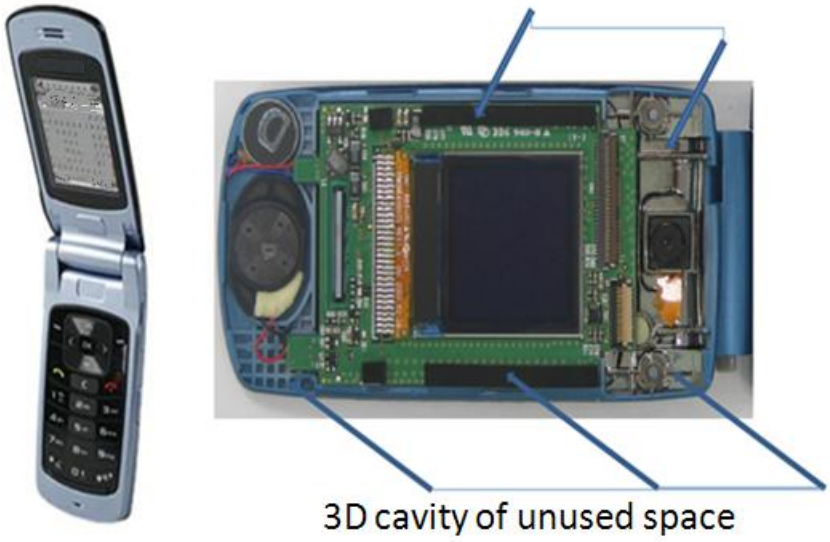

Figure 25: Flip phone showing the small, unused spaces inside the case.

We did not model the head or hand, although this would need to be done for an actual cellular telephone design. The antenna design shown in Figure 26 is designed to operate in the well-known cell phone bands of 800-900 MHz and 1.8 to 3.0 GHz. The cost function is calculated by taking the discrete frequency points and averaging them out to the minimum value desired, similar as to what was done for the antennas in Sections 4.2 and 4.3.

Linear polarization was desired, and the radiation pattern was to have a near omni-directional pattern. The optimization is then used to create a return loss less than -10 dB in the typical cellular bands 800-900 MHz, and 1.8-3.5GHz. The frequency bands here are chosen to be similar to actual bands in use today. In some cases, multiple antennas will be needed and are not taken into account in this feasibility example.

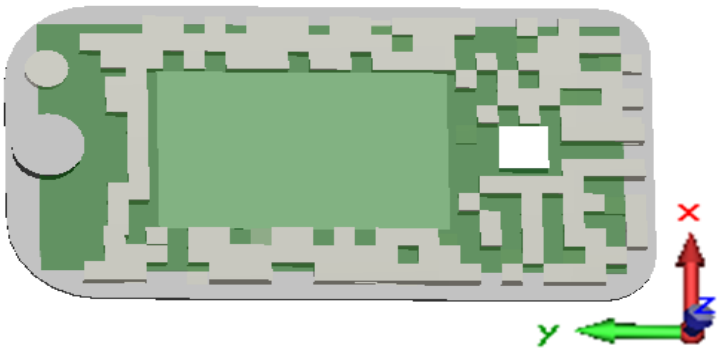

Figure 26: Top view with plastic cover of the phone removed, showing the antenna and phone geometry based on empty space in the Samsung cellular phone. Optimized to functioning in 800-900MHz and 1.8-3.8 GHz

The GA simulation took approximately 3 minutes and the conductor layout converged to the design shown in Figure 27. The (PEC) simulations results of the S11 impedance are given in Figure 28. The radiation patterns are shown in Figure 29. The radiation patterns are measured from zero to 360 degrees for the antenna as it is rotated around the X axis.

The optimization demonstrates that it is possible to utilize the 3D empty space of an electronic device for an antenna. The simulated antenna has efficiency of 83% and above in the resonance bands.

Similar optimizations can be done in the same space for a different frequency band such as 1.4-3GHz.

The estimated weight of a 3D printed antenna based on the built antenna in Section 4.2 would be ~1.78 grams. Applying the comparison factor used for the UHF dipole over the 1.6-3.55GHz bandwidth, the cell phone antenna has a *ka* of 1.31 and a CF of 15.66

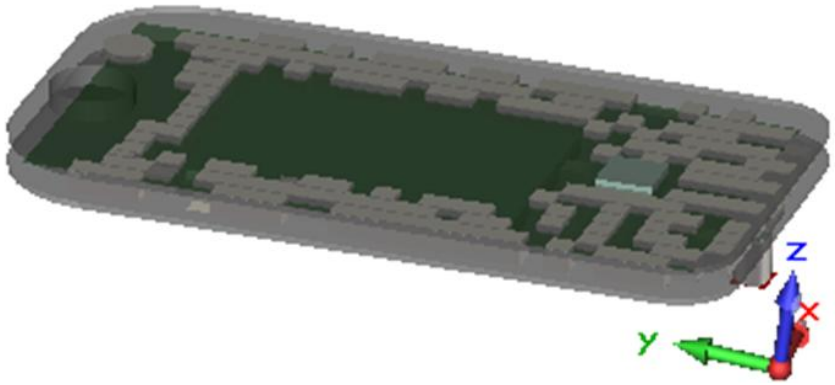

Figure 27: Cell phone simulation showing a transparent plastic cover and the optimized antenna functioning in 800-900MHz and 1.8-3.8 GHz

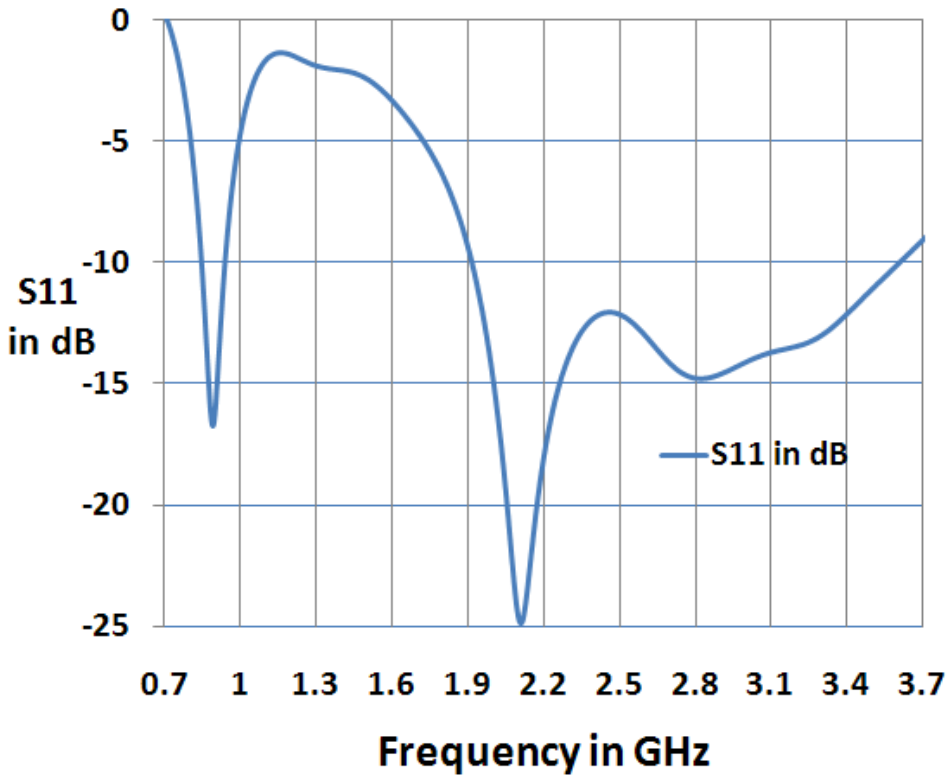

Figure 28: Simulated S11 data for Samsung cellular phone configuration shown in Figure 27 indicating the resonance -10dB resonance from 850-930MHz and 1.9-3.5 GHz

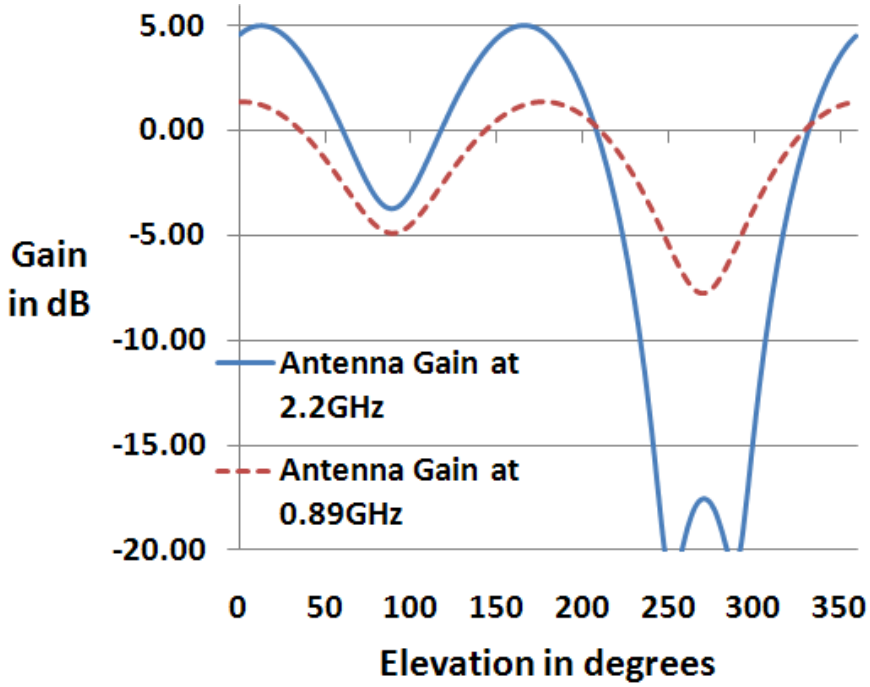

Figure 29: Realized gain in dB at 890 MHz and 2.2 GHz for the antenna optimized in Figure 26. The Gain is plotted in elevation swept 360 degrees around the X axis. The simulated value for total efficiency is 83% at 890MHz and 98% at 2.2 GHz

4.5 Conclusion

This paper has demonstrated the ability to create 3D antennas with randomized shape that are closer to the Chu limit [2] than 1D, 2D, or simpler 3D antennas in the same space using 3D rapid prototyping. The optimized cubical monopole above ground plane showed that plastic coated with a conductive paint was ~6% less efficient than solid metal.

The UHF 3D dipole was optimized to perform over a large bandwidth. At the lowest operating frequency, the antenna has a *ka* of 0.92 and a quality factor of 11.0, almost equivalent to the Goubau antenna [21]. A 3D cavity of random shape from a basic flip phone was filled with a GA optimized antenna. The goal was not to make the antenna small but utilize the space to function in the cell phone frequency bands. The

optimization was able to create an antenna that functions in the frequency ranges used by modern cell phones with efficiency of 83% and above. This research demonstrates the emergence of printing with plastic conductive materials. The latest in 3D rapid prototyping could soon provide an opportunity to pursue even more complicated 3D antenna designs with more imbedded combinations of metal and plastic.

4.6 References

[1] H. A. Wheeler, "Fundamental Limitations of Small Antennas," *Proce. IRE*, vol. 35, pp. 1479–1488, Dec. 1947.

[2] L. J. Chu, "Physical limitations of omni-directional antennas," *J. Appl. Phys*., vol. 10, pp. 1163–1175, Dec. 1948.

[3] H.L.Thal,, "A Reevaluation of the Radiation Q Bounds for Loop Antennas," *IEEE Antennas and Propagation Magazine*, vol.51, no.3, pp.47-52, June 2009

[4] H.L. Thal,, "New Radiation Limits for Spherical Wire Antennas," *IEEE Trans. Antennas Propag.*,vol.54, no.10, pp.2757-2763, Oct. 2006

[5] S. R. Best, "Low Q Electrically Small Linear and Elliptical Polarized Spherical Dipole Antennas," *IEEE Trans. Antennas Propag.*,vol. 53, pp. 1047–1053, Mar. 2005.

[6] S. R Best, "The Radiation Properties of Electrically Small Folded Spherical Helix Antennas" *IEEE Trans. Antennas Propag.,Vol. 52, no. 4*, April 2004 page 953-960

[7] E. E. Altshuler, "Electrically small self-resonant wire antenna optimized using a genetic algorithm," *IEEE Trans. Antennas Propag., vol.50*, no. 3, pp. 297–300, Mar. 2002.

[8] [Online available] *http://www.geneticprogramming.com/coursemainpage.html* [Sep. 2, 2010]

[9] H. Rmili, O. E. Mrabet, J.-M. Floc'h, J.L. Miane, "Study of an Electrochemically-Deposited 3D-Fractal Tree Monopole Antenna," *IEEE Trans. Antennas Propag.*,vol. 55, no. 4, Apr. 2007, pp. 1045-1050

[10] J. Bernard, J. Lewis, J. Adams, et al, "Conformal Printing of Electrically Small Antennas on Three-Dimensional Surfaces", *Advanced Materials,* Vol. 23, Issue 11, pp. 1335–1340, March 18, 2011

[11] C.Pfeiffer, A.Grbic, "Novel Methods to Analyze and Fabricate Electrically Small Antennas" Spokane Washington, *IEEE Antennas and Propag. Soc. Int. Symp., July 3rd – 8th 2011*

[12] Willis B. , Furse C., Sai ; "3D rapid prototyping for small antenna design" Spokane Washington, *Antennas and Propagation Conference July 3rd – 8th 2011*

[13] Willis B. , Furse C. " Rapid prototyping for small 3D antennas", Submitted paper, *IEEE Antennas and Propagation journal [2012.]*

[14] L.Griffiths, C.Furse, "Performing 3-D FDTD Simulations in Less than 3 Seconds on a Personal Computer and its Application to Genetic Algorithm Antenna Optimization," *Applied Computational Electromagnetics Society Journal, Vol. 20, No. 2,* pp. 128-135, July 2005

[15] R.Eberhart, J.Kennedy, "A New Optimizer using Particle Swarm Theory," Micro Machine and Human Science, 1995. MHS '95., *Proceedings of the Sixth International Symposium on , vol., no.,* pp.39-43, 4-6 Oct 1995

[16] [Online Available] *http://www.cst.com/* [Accessed: 11th Dec. 2011].

[17] [Online] Objet Geometries Inc "Connex 500 3D printer"*http://www.objet.com/3DPrinter/Objet_connex500/ 2011*, [Jun 2 2010]

[18] J. Saberin,C. Furse, "Challenges with Optically Transparent Patch Antennas", *IEEE Antennas and Propagation Magazine*, in press

[19] [Online Available] *http://www.spraylat.com/Products/ElectronicMaterials/Technology/ConductiveCoatingTechnology.aspx* [Accessed Sep 15th 2011]

[20] [Online Available] *http://www.mgchemicals.com/products/8331.html* [last accessed Nov 12 2011]

[21] G. Goubau, "Multi-element monopole antenna," *Proceedings of the ECOM-AROWorkshop on Electrically Small Antennas,* Fort Monmouth, NJ, pp. 63-67, October

[22] H. R. Stuart and S. R. Best, "A Small Wideband Multimode Antenna," *2008 IEEE AP-S, Symposium,* Paper 209.2, July 2008.

[23] [Online Available] *http://plastics.dupont.com/plastics/pdflit/americas/delrin/H76836.pdf?GXHC_locale=en_US* [Accessed: 11th Dec. 2011].

CHAPTER 5

COMPARISON OF RAPID PROTOTYPING TECHNIQUES FOR ANTENNAS

Emerging conductive materials are being used to build 3D antennas. In this research, we evaluate methods and materials that can be used to produce 3D antennas. The efficiency and performance of the antennas is shown to be strongly coupled to the conductivity and skin depth of the materials. The conductivities of several materials that could be used in 3D rapid prototyping are measured to determine which materials can be used at which frequencies. Sample monopole antennas are built from solid copper, gold plated copper, Xyloy®, silver paint and copper paint, and the radiation efficiency are measured. The radiation efficiency of the paints compared to within 6% of the solid copper antennas.

5.1 Introduction

3D rapid prototyping holds significant promise for future antenna designs. Most antennas require a combination of dielectric insulator materials and conductive metallic materials. Current methods for 3D rapid prototyping are very effective for insulating materials (plastics), and these shapes can be coated with metallic paint to create

antennas[1], [2]. Conductive materials can be prototyped now, too, although not as easily, and this capability is rapidly advancing. The conductive materials are currently the limiting factor for antenna prototyping. Laser sintering and other methods that produce truly metallic antennas, or methods that plate metal onto plastic designs, can produce antennas with very high conductivity, similar to what is obtained today with the copper antennas most often used. Metallic paints offer a very good, inexpensive, flexible solution for coating plastic objects; however, they are of lower conductivity, thus reducing the performance of the antenna. This paper will evaluate the current state of the art of prototyping with these conductive materials and how it impacts antenna design. In addition, the precision, speed, weight, and cost of the prototyping will be evaluated with the goal of providing information and guidance on the 3D rapid prototyping methods available for today's antenna designers.

The motivation for this research lies in the ability to easily create true 3D antennas which approach the Chu-Wheeler small antenna limit [3], [4]. Small antenna theory says that the performance (Q) of an antenna is limited by the spherical volume encompassing that antenna. Antennas that use more of this volume can have better performance than the simpler 1D and 2D antennas most commonly used. A few attempts at true 3D antennas have been made and have initially demonstrated the performance improvements of these designs. Best [5] demonstrates low Q small spherical dipoles and a small spherical helix [6]. The spherical helix antenna appears to be built from hand-soldered pieces of wire. Similar complicated soldering techniques are used to build 3D wire antennas in [7] and [8]. In [9], a 3D fractal tree is randomly grown by an electrochemically deposited conductor. These antennas all demonstrate the improvements

that may be gained by using the 3D design, especially [10] which uses high dielectric powder surrounding the antenna. The manufacturing methods used for these antennas have been so cumbersome or expensive that 3D antennas were limited to simple geometries (such as horns and dishes). More complex designs were typically regarded as far-fetched and impractical.

Recently, a 3D hemispherical antenna was built by printing a meander-line antenna on a curved glass surface with a silver ink [11]. Another method of transferring a metallic design to a curved plastic or glass surface is direct transfer patterning which uses a stamp to get the desired pattern onto a curved surface [12]. These are relatively easy ways to build a 3D antenna; however, the surface on which the antenna is printed or stamped is limited to relatively simple shapes.

There are several promising and emerging 3D prototyping methods that can be used to create more complicated metallic and nonmetallic shapes, including selective laser sintering (SLS) [13], [14], selective laser melting [14], 3D printing [15], stereolithography [15], [14], electroforming [16], and electron beam melting [16], [17]. The methods also include new procedures such as atomic layer deposition (ALD) [18], laser direct structuring (LDS) [19], and sputtering [20]. These methods can all be used for 3D prototyping of antennas, with more or less ease. SLS and 3D printing (with paint coating) were used to build a 3D antenna designed using a genetic algorithm in [21].

In [21], a complicated antenna design was created with a genetic algorithm (GA) and built using a 3D printed plastic shape coated with metallic paint. The paint has conductivity about 25% less than copper metal, and the paint is thin enough that a single layer is less than the skin depth of the fields. The same antenna was also produced using

SLS to form a solid conductor. The conductivity of this metal is similar to solid copper, and of course, the antenna is thick compared to skin depth. Imperfect conductivity or insufficient skin depth reduce the performance of the antenna as seen in [22], and [21], so the type of paint and number of layers are important design parameters for 3D printed antennas. In this paper, we will further quantify the requirements for conductivity and skin depth, and how well current 3D prototyping methods meet those requirements. The materials investigated in this research are chosen because they are, or have the potential to be, used in rapid prototyping. The materials are compared for their ability to be good conductors as well as their cost, weight, and build time.

This paper reviews 3D prototyping methods available for antenna design with emphasis on the conductive materials. Section 5.2 provides a background on materials and methods and presents additional details on atomic layer deposition (ALD) [18], LDS [19], and sputtering [20]. In Section 5.3, the measured conductivity of several available materials are given, using a standard 4-point probe. Section 5.4 illustrates efficiency measurements completed on many new conductive materials. The measurements are completed using the Wheeler cap method [23]. Results for monopole antennas made from solid copper, solid Xyloy, ALD, copper paint, silver paint, and other materials are compared.

5.2 3D Prototyping Methods and Materials

Rapid 3D prototyping was demonstrated in [21] to create complex 3D antenna shapes. An antenna produced using selective laser sintering (SLS) (solid metal) was compared to an antenna that was 3D printed of a dielectric of plastic and then coated with

metallic paint. The thickness and conductivity of the paint had a measurable effect on the antenna performance, thus confirming observations from [22] and [21] and common sense that maintaining sufficient conductivity and thickness of the metallic part of the antenna is critical to good performance. This section of the paper evaluates methods and materials that can be used to create 3D antennas, considering their conductivity and skin depth. We will review direct transfer patterning, laser direct sintering, silver nano-particle ink, electroless plating, and conductive thermoplastics.

Recently, we demonstrated the ability to create random-shaped 3D antennas and more efficiently use the space available [2], which will allow it to better fit ever-smaller electronic devices. The antenna was optimized by a genetic algorithm, which is basically a 3D extension of previous 2D work [24], [4]. The antennas were then built using 3D rapid prototyping techniques. One was built using Selective Laser Sintering (SLS) to create a solid conductor, and a second was built from plastic using 3D printing. The plastic antennas were then coated with a conductive paint to form a conductive shell. A similar dipole type antenna functioning in the 500MHz band was also built and tested [21]. The lower conductivity of the paint coating reduces the gain of the antenna. The silver painted antenna is ~6% less efficient than the solid SLS antenna. The SLS antenna took ~ 1 day to build and weighed 13.7g. The 3D printed antenna was printed in ~20 minutes and the remainder of a day to paint and dry. The 3D printed antenna weighed 2.5g. The 3D printed antenna with a copper conductive coating is shown in Figure 30.

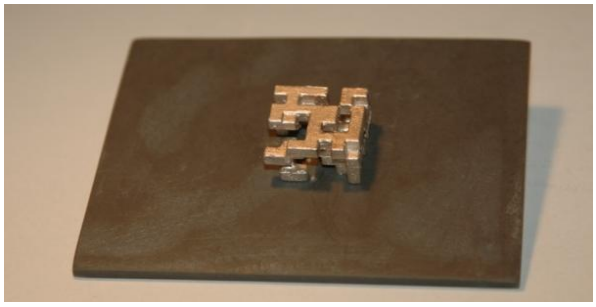

Figure 30: 3D printed cubical antenna above a ground plane, from [25]. © 2012 IEEE. Reprinted with permission.

There are several materials that can be used to produce a conductive layer over a 3D plastic object, including the following: conductive paints [2], [26], [27], conductive adhesives epoxies [28], [29], polymers [30], [31], optically transparent films[22], [32] , thin silicon films [33], [34], nano-fiber [35], [36], powdered metals [37], [38], and conductive fabrics [39], [40], [41], [42].

Direct transfer patterning is one method of producing 3D antennas [12]. The process uses a stamp to get the desired pattern onto a curved surface. It then requires a 6-step process including a plasma etch and gold plate to finalize the design on Polyethylene Terephthalate (PET). In [12], the conductor is thickened by the plating process and in [43], it was found that the transfer of thicker metals proved to be difficult, possibly due to wrinkling of the stamp during metal deposition [43]. The research in [43] shows an array of 10 nm thick, 500 micro meter wide gold lines transferred onto a Polyethylene Terephthalate hemisphere. A sheet resistance of 7 ohms/square for 10 nm gold was estimated from measurements made between several points along the metal stripes. This corresponds to 7×10^{-6} Ohm·cm, consistent with that of conventional gold thin films [43].

Silver nano-particle ink deposited with a 3D printing nozzle has been used to construct spherical antennas [11]. The design uses silver on a glass hemispherical shell. The silver ink requires a 550° degree C sintering temperature and an annealing time of ~24 hours. The silver particles have an average conductivity of 5.2 $X10^{-5}$ Ohm·cm [44]. The weight of this antenna would be ~ the weight of the Pyrex glass hemisphere used as the substrate.

Another emerging process uses atomic layer deposition (ALD) to coat a substrate with a nanometer thick conductive layer. Also, a similar technique allows a thin layer to be plated by element sputtering to create thin conductive films. The nano-fabrication lab at the University of Utah provided us with an antenna made of gold using ALD on a glass substrate. They also provided one built from sputtering using platinum on a glass substrate. Both of these methods apply a thin conductive film, and are typically used in fabricating micro- and nano-electronics. These films can be plated to a desired thickness up to ~200 micrometers. These antennas are manufactured in ~1 day and the weight is equivalent to the glass substrate.

Laser direct sintering (LDS) [19] is similar to other plating techniques and requires a multiple-step process. The plastic where the conductive plating is desired is typically etched with a laser or chemical etchant. The etched area allows the conductive particles from the polymer to adhere to the surface. The metal is then deposited on the etched area using a plating process. The built time is ~ 1 day, and the weight as with other thin layer antennas is equivalent to the plastic substrate.

Electroless plating allows for a conductive layer to be built up by a chemical reaction rather than electrical. The process relies on the presence of a reducing agent

which reacts with the metal ions to deposit metal. The base material may be arbitrary shaped, and the plating does not require line of sight [45]. (Painting requires either line of sight or dipping.)

Two conductive materials used for injection molding are of interest as well. The first is a metal mixture of zinc and aluminum with a melting point at approximately 270° C [46]. The second is a low-temperature carbon fiber melt extrudable thermoplastic. The thermoplastic also requires a 270° degree C melting temp and an 8 hour drying time. This has a resistivity of 0.3 ohms per square [47].

These processes vary in the materials they can use and the resolution and complexity they can provide [48]. Today's resolutions for 3D printing are on the order 0.0006 inches [49], which is common for most low-cost manufacturing methods. One item of note that demonstrates the strong international and economic interest in conductive 3D prototyping is an $80,000 Gada prize (to be given in 2012-2015) that was recently announced for the development of advanced 3D printing [50]. One of the requirements for winning is the ability to print useful conductive materials such as those for circuit boards [50].

5.3 Conductivity Measurements

The conductivity of the metallic components of an antenna have a strong impact on its performance, but many of these values are not provided by the manufacturers. In this section, we describe measurements of monopole antennas built of common conductive materials – silver and copper paints, Xylov (used for conductive injection molding), conductive epoxy solder, ALD, Sputtering, LDS plated plastic, and compared

them to solid copper sheeting that would commonly be used in antenna designs. The materials were characterized using a 4-point probe [51] to measure conductivity and a Wheeler cap [23] to measure radiation efficiency. The goal is to better understand the relationship between the conductivity of the material, the skin depth, and the antenna efficiency at a specific frequency. The primary focus is to evaluate the usability of emerging techniques and lossy conductive materials for antenna design. The data are compared to manufacturer's specifications for conductivity. The measured radiation efficiency is compared to measurements of antennas built of solid copper sheet and to simulated data using lossy materials.

The 4-point probe is used to measure conductivity. Here the thickness of the sample is given by *t*, which is much less than the spacing of the probes, which is ~1.5mm for our equipment. The sheet resistivity is related to the differential resistance:

$$\Delta R = \rho\left(\frac{\partial x}{A}\right) \tag{5.1}$$

and the area of the conductive material being measured

$$A = 2\pi xt \tag{5.2}$$

then solving for resistance:

$$R = \int_{x1}^{x2} \rho \frac{\partial \mathrm{x}}{2\pi \mathrm{xt}} \tag{5.3}$$

and relating it to voltage and current, we substitute in the equivalent of *R* which is given as

$$R = \left(\frac{v}{2I}\right) \tag{5.4}$$

and then solve for the sheet resistivity

$$\rho = \frac{\pi t}{\ln 2}\left(\frac{v}{I}\right) \quad 5.5$$

In general, sheet resistivity Rs = ρ/t and can be expressed as

$$R_S = k\left(\frac{v}{I}\right) \quad 5.6$$

where k=4.53 = $\pi/ln2$. For a semi-infinite thin sheet, the sheet resistivity is given in ohms/square. To convert to ohm-meters, the thickness of the sample must be factored into the equation. R_s is multiplied by the thickness, giving the units of ohm-meters. The conductivity is the inverse of the electrical resistivity and is given in siemens/ meter.

Several materials were measured on the 4-point probe, and the results are shown in Table 9. LDS over plastic was measured with a 40 um layer of gold. Silver and copper conductive paints (3 layers) were sprayed onto a paper substrate. Copper paint was also tested for a single paint layer. The injection molding material Xyloy® was also tested.

These values are compared to a standard piece of 17 um copper sheets that was used to verify the 4-point probe measurements. Silver epoxy is also evaluated, since it is needed in some cases to attach the antennas to the center conductor pin of an SMA connector. The measurements for gold ALD and platinum sputtering were measured on a 4-point probe. Manufacturer's values for other emerging materials have also been included in the table. These have not been tested on the 4 point probe or for radiation efficiency. These materials are silver nano-particle ink from [11], the low-temperature carbon fiber melt extrudable thermoplastic from [47], and direct transfer patterning from [12]. The material in [12] had an additional thickness from being plated, and our information for conductivity was obtained from [43].

Table 9: Measured data from the 4-point probe

Material	Current measured in mV	Thickness micro-meters	Ω /□	Resistivity Ω·m	Conductivity S/m
Gold LDS	0.052	40	0.002	$1.17X10^{-8}$	$8.49\ X10^{7}$
2-layer Copper Paint	6.61	16	0.298	$5.27X10^{-6}$	$1.90\ X10^{5}$
3-layer Copper Paint	1.97	23	0.089	$2.10X10^{-6}$	$4.77\ X10^{5}$
3-layer Silver Paint	1.97	23	0.030	$7.07X10^{-7}$	$1.42\ X10^{6}$
Copper sheet	0.057	17	0.00258	$4.38X10^{-8}$	$2.3\ X10^{7}$
Xyloy	0.024	500	0.00135	$1.69X10^{-7}$	$5.89\ X10^{6}$
Silver Solder (epoxy)	20	125	0.0453	$2.27X10^{-5}$	$4.42\ X10^{4}$

A correction factor was applied to the measurements due to the standard copper sheet measuring ~30% lower than the expected $5.96x10^{7}$ S/m.

The measurements taken had a correction factor applied due to the standard copper sheet measuring ~30% lower than $5.96X10^{7}$. Table 10 presents the data with the correction factor applied. Table 11 provides the skin depth calculations.

Table 12 indicates how the thickness of the material using its standard application method compares to skin depth. Figure 31 then indicates how the copper paint compared to the manufacturer's given data. To reduce loss, the material must have a thickness greater than at least 2 skin depths and preferably more than 4 skin depths.

Table 10: Measured data with corrections, also included is additional data found in the current literature.

Material	Current measured in mV	Thickness micro-meters	Corrected Ω /□	Corrected Resistivity Ω·m	Corrected Conductivity S/m
Gold LDS	0.052	40	0.00089	4.4910^{-9}	$2.22\ X10^{8}$
2 layer Copper Paint	6.61	16	0.114	$2.01X10^{-6}$	$4.97X10^{6}$
3 layer Copper Paint	1.97	23	0.034	$8.0X10^{-7}$	$1.25X10^{6}$
3 layer Silver Paint	1.97	23	0.0114	$2.70X10^{-7}$	$3.71X10^{6}$
Copper sheet	0.057	17	0.00098	$1.67X10^{-8}$	$5.96X10^{7}$
Xyloy	0.024	500	0.00051	$6.48X10^{-8}$	$1.54X10^{7}$
Silver Solder (epoxy)	20	125	0.0179	$8.65X10^{-6}$	$1.16X10^{5}$
Premier Carbon fiber [47]	NA	23	0.25	$5.75X10^{-6}$	$1.73X10^{5}$
Silver nano ink [44]	NA	12	NA	$5.2X10^{-7}$	$1.9X10^{6}$
Direct Transfer patterning [43]	NA	0.01	7	$7X10^{-8}$	$1.43X10^{7}$
Gold ALD	NA	0.035	1.2	$4.2X10^{-8}$	$2.38X10^{7}$
Platinum Sputtering	NA	0.19	1.07	$2.0X10^{-7}$	$4.92X10^{6}$

Table 11: Skin depth calculations given in microns at 0.5, 1.6, 2.6, and 15 GHz for the materials of interest.

Material	Corrected Resistivity Ω·m	Skin depth in microns f=0.5 GHz	Skin depth in microns f=1.6GHz	Skin depth in microns f=2.6GHz	Skin depth in microns f=15GHz
Gold LDS	$4.49X10^{-9}$	1.51	0.84	0.66	0.28
Thin Copper Paint over plastic	$2.01X10^{-6}$	31.9	17.84	13.99	5.83
Copper Paint over plastic	$8.0X10^{-7}$	20.13	11.25	8.83	3.68
Silver Paint over plastic	$2.70X10^{-7}$	11.7	6.54	5.13	2.14
Copper sheet standard	$1.67X10^{-8}$	2.91	1.63	1.28	0.53
Xyloy	$6.48X10^{-8}$	5.73	3.2	2.51	1.05
Premier Carbon fiber	$5.75X10^{-6}$	53.97	30.17	23.67	9.85
Silver nano ink	$5.2X10^{-7}$	16.23	9.07	7.12	2.96
Direct Transfer patterning	$7X10^{-8}$	6	3.33	2.61	1.09
Gold ALD	$4.2X10^{-8}$	4.61	2.58	2.02	0.84
Platinum sputtering	$2.0X10^{-7}$	10.07	5.63	4.41	1.84

Table 12: Skin depth compared to standard conductor thickness for manufacturing; green indicates acceptable thickness for skin depth, yellow indicates marginal, and red indicates insufficent.

Material	Thickness micro-meters	Skin depth in microns f=0.5 GHz	Number of skin depths at 0.5GHz	Skin depth in microns f=2.6GHz	Number of skin depths at 2.6 GHz	Skin depth in microns f=15GHz	Number of skin depths at 15 GHz
Gold LDS	40	1.51	26	0.66	60	0.28	142
Thin Copper Paint over plastic	16	31.9	0.2	13.99	1.1	5.83	2.75
Copper Paint over plastic	23	20.13	1.1	8.83	2.6	3.68	6.2
Silver Paint over plastic	23	11.7	2	5.13	4.48	2.14	10.75
Copper sheet standard	17	2.91	5.5	1.28	13.2	0.53	32
Xyloy	500	5.73	83	2.51	199	1.05	476
Premier Carbon fiber	23	53.97	0.5	23.67	1	9.85	2.3
Silver nano ink	12	16.23	0.75	7.12	1.6	2.96	4
Direct Transfer patterning	0.010	6	0.001	2.61	0.003	1.09	0.0091
Gold ALD	0.035	4.61	0.007	2.02	0.017	0.84	0.041
Platinum sputtering	0.190	10.07	0.01	4.41	0.043	1.84	0.10

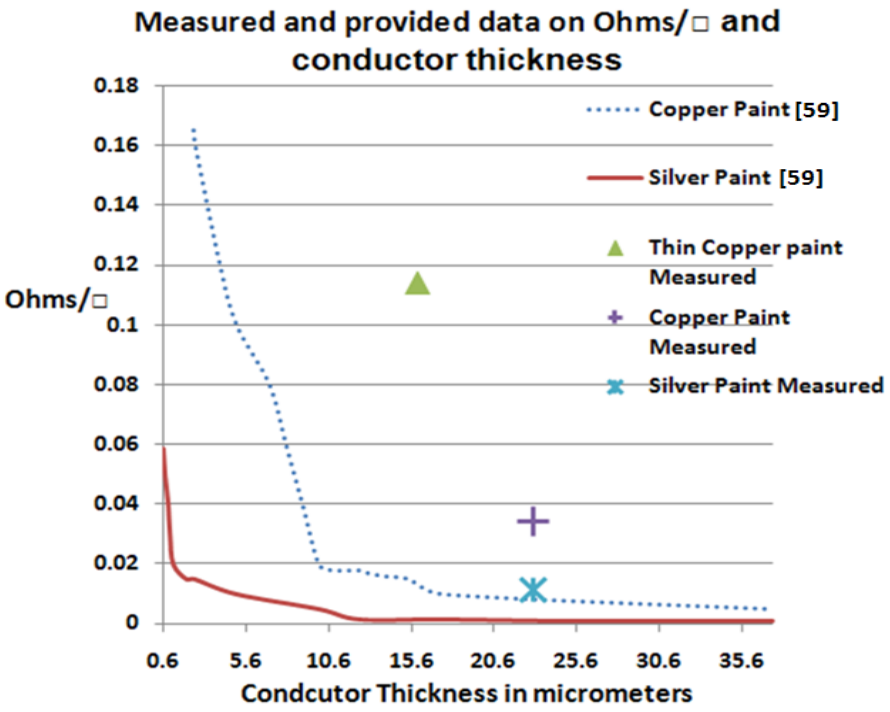

Figure 31: Conductivity of paints as a function of thickness.

The table is highlighted with red indicating less than 2 skin depths, with yellow showing 2-4 skin depths, and with green for more than 4 skin depths. The green indicates that the material and its application thickness are acceptable for that frequency region.

5.4 Radiation Efficiency Measurements

The wheeler cap method is used to measure the radiation efficiency. The wheeler cap is designed such that the antenna above a ground plane has its radiated fields shorted out in the near field region. The shape of the cap in this research is constructed to be a rectangular form. The cap also acts as a resonant cavity and it must be designed such that the cavity resonance falls outside the resonance region of the antenna. The fields created inside the cap are then strictly determined by the radiated fields due to the antenna.

Three types of antennas were fabricated and measured. Each antenna is placed above a copper ground plane that is 91.5mm X 76mm and is fed using a 50 ohm coaxial line with a SMA thread on the back. The center conductor of the SMA extends 0.1 inches past the ground plane. The antennas are soldered onto the conductor with a 0.05 inch gap between the bottom of the antenna and the ground plane.

First, the Xyloy material, silver and copper paints over paper, copper, and gold plating over copper are fabricated into antennas measuring ~6mm wide X 35mm long. 8mm from the bottom, the antenna tapers to a 4mm point. At 1.75 GHz, these are approximately 1/4 wave monopoles above a ground plane. The silver and copper conductive paints (3 layers) are sprayed onto a paper substrate. The antennas are shown in Figure 32. The fabricated monopole above a ground plane is shown in Figure 33. The measured S11 data is presented in Figure 34 and the efficiency is shown in Table 13. A second set of antennas were built from the available materials using LDS over plastic , gold ALD, and platinum sputtering. The efficiency measurements are given in Table 13.

The third set of antennas is built such that at 1.7 GHz, it is a 1/2 wave monopole above a ground plane. The half wave antenna provides a more efficient antenna. Here the total radiation loss is evaluated for the same frequency but a longer antenna size. The antennas are 6mm width and 70mm length, and are metalized with copper paint, silver paint, and copper sheet. The S11 data for the 70 mm antennas are given in Figure 35. The efficiency is given in Table 13. The wheeler cap is designed such that the highest operating frequency of the cap will be outside the resonance region. The cap is 45mm wide and 120mm long [23]. The length allows the same cap to be used to accommodate measurements for antennas that are 35mm long and those that are 70 mm long.

Figure 32: Fabricated antennas from left to right are silver paint, Xyloy®, copper paint, solid copper, and gold plating.

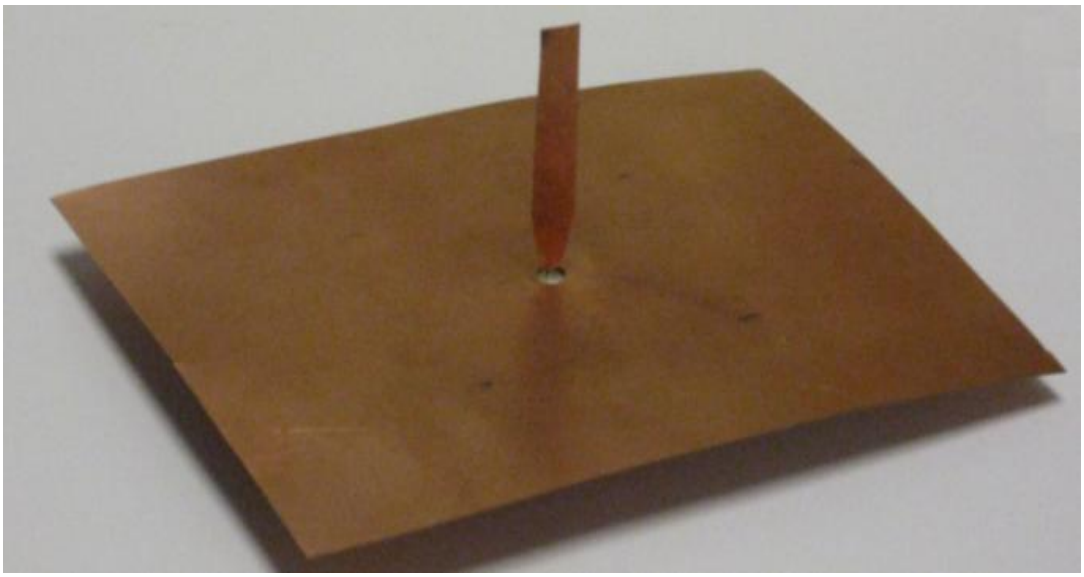

Figure 33: Fabricated monopole antenna above a ground plane for efficiency testing using the wheeler cap.

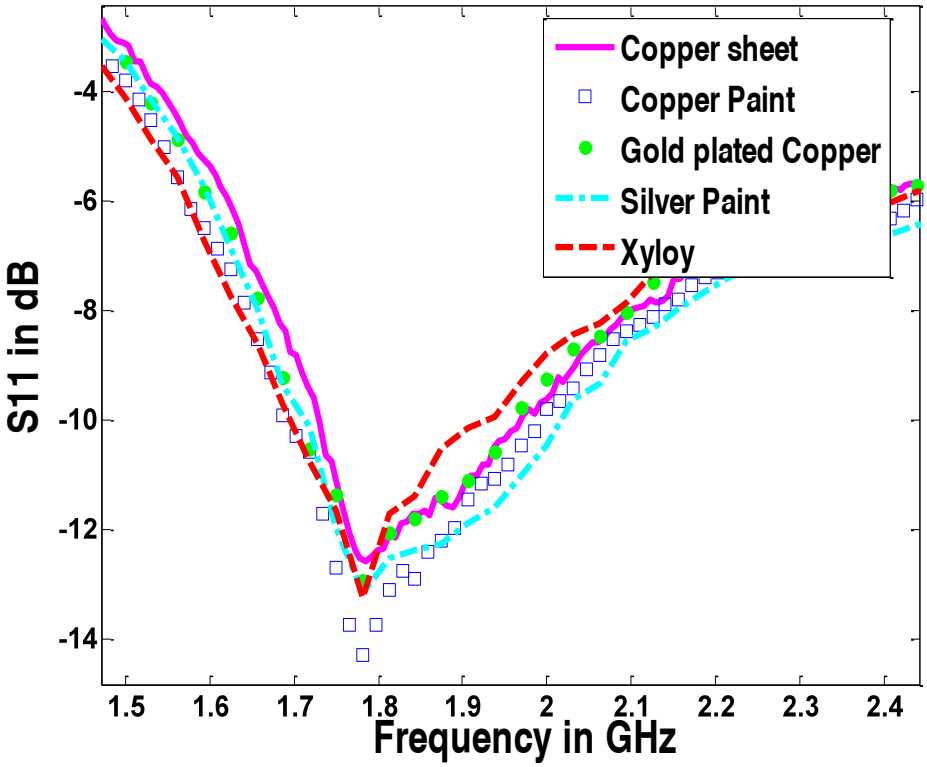

Figure 34: S11 for the 35mm antennas constructed from Xyloy®, 3 layers of silver paint and copper paint over paper, gold plated copper, copper sheet.

Table 13: Measured radiation efficiencies for the measured antennas.

Material and length	Resonant point in GHz	% Radiation efficiency
Gold plating 35mm	1.79	81 %
Silver Paint 35mm	1.79	75 %
Copper Paint 35mm	1.79	74 %
Copper sheet 35mm	1.79	81 %
Xyloy® 35mm	1.79	81 %
Gold LDS 35mm	2.2	86 %
Titanium 25mm	2.8	41 %
Gold ALD 40mm	2.1	39 %
Silver Paint 70mm	1.64	86 %
Copper Paint 70mm	1.64	74 %
Copper sheet 70mm	1.64	94 %

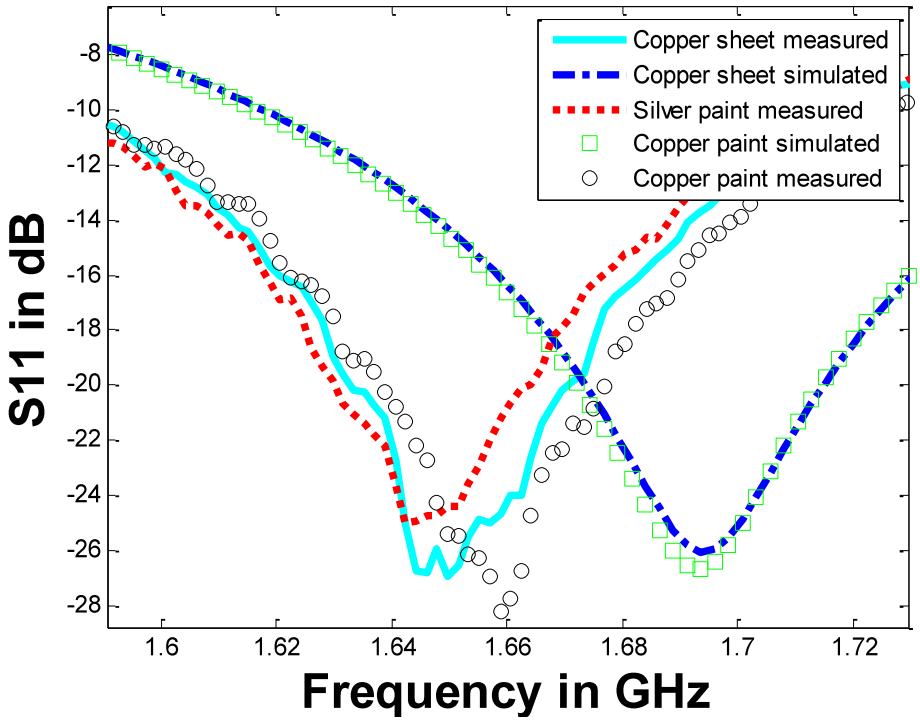

Figure 35: Measured S11 data for the 1/2 wave (70mm) monopole above a ground plane showing the copper sheet, 3 layers of silver paint, and 3 layers of copper paint over paper.

The efficiency measurement is only valid where the antenna has real impedance, and is within the resonance region [52].

To verify the measurements, the 1/2 wave monopole antennas that are 70mm long are then measured for gain in the antenna range. These were chosen because there was the largest difference in efficiency between the painted antennas and the copper sheet. The gain measurements are shown for 1.62GHz in Figure 36 and 1.7 GHz, in Figure 37. The peak gains are given in Table 14.

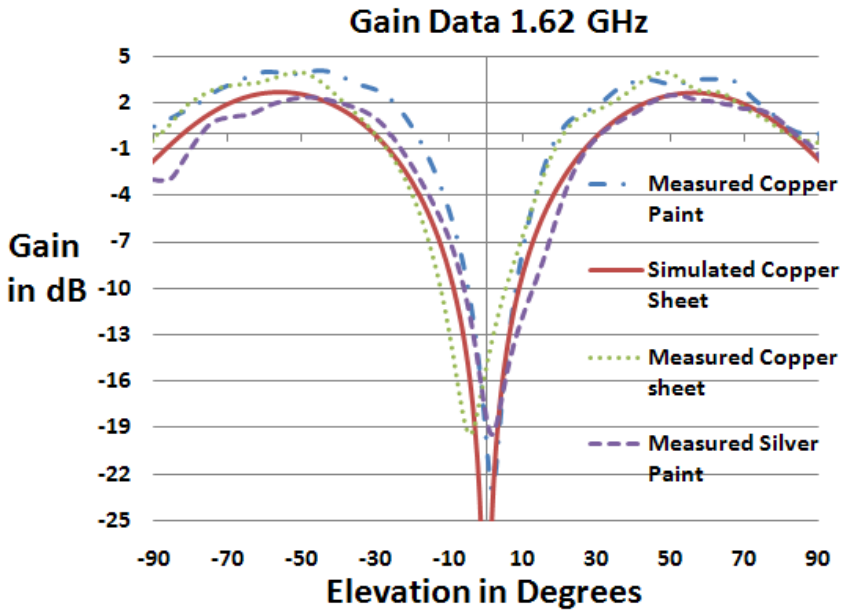

Figure 36: Measured gain at 1.62 GHz for the half-wave monopoles (70mm) above a ground plane for the silver paint, copper paint, and copper sheet. The simulated copper sheet antenna is also included as a reference

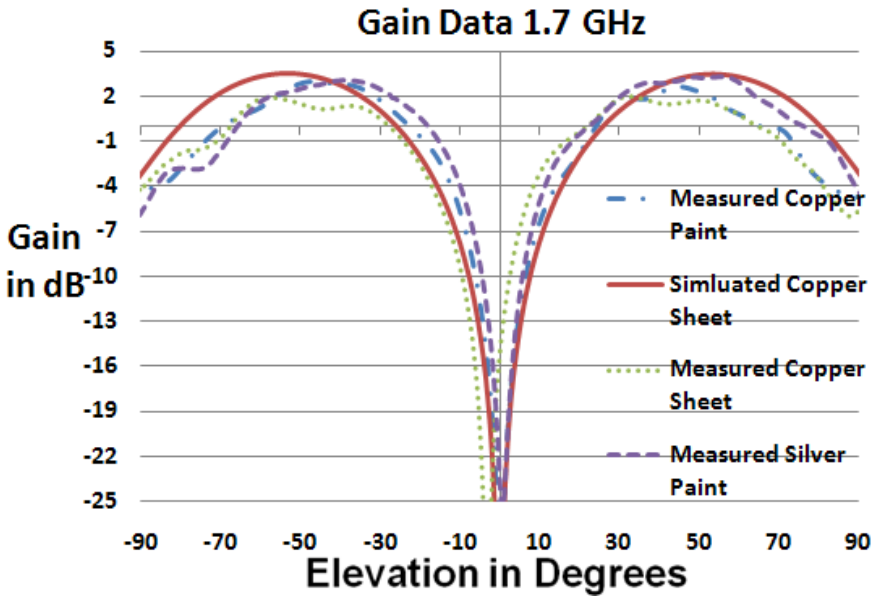

Figure 37: Measured gain at 1.7GHz for the half-wave monopoles (70mm) above a ground plane for the 3 layers of silver paint and then 3 layers of copper paint, both over paper, and copper sheet. The simulated copper sheet antenna is also included as a reference

Table 14: Peak gains for the measured antennas

Material and frequency	Peak Gain
Silver Paint 1.62 GHz	2.53 dB
Copper Paint 1.62 GHz	4.05 dB
Copper sheet 1.62 GHz	3.93 dB
Silver Paint 1.7 GHz	3.26 dB
Copper Paint 1.7 GHz	2.92 dB
Copper sheet 1.7 GHz	1.97 dB

5.5 Conclusions

The ability to use true 3D manufacturing techniques allows antenna designers to create arbitrarily shaped antennas and understand the losses associated with using lower conductive materials and/or thin conductive coatings. The measurements provide a good indication of the conductivity and thickness that is needed for a material to be efficient. We found that for the paints, the thinner the paint was, the lower the conductivity and hence the larger the skin depth. The larger skin depth caused the antenna to have less efficiency. Other materials which may be utilized for antenna fabrication such as Xyloy® and LDS with gold measured at practically the same conductivity and radiation efficiency as a copper. The measured gain of the materials such as paint compared extremely well with the standard copper sheet. Based on the measurements, the larger the painted area is through which the current propagates, the lower the efficiency will be when compared to a standard piece of copper.

5.6 References

[1] B.Willis , C.Furse,"*3D Rapid Prototyping for Small Antenna Design"* Spokane Washington, Antennas and Propagation Conference July 3rd – 8th 2011

[2] B.Willis, *"3D Rapid Prototyping for Space Efficient Antenna Design"* PhD Dissertation, University of Utah , April. 2012

[3] H. A. Wheeler, "Fundamental Limitations of Small Antennas," *Proce. IRE*, vol. 35, pp. 1479–1488, Dec. 1947.

[4] L. J. Chu, "Physical limitations of omni-directional antennas," *J. Appl. Phys*., vol. 10, pp. 1163–1175, Dec. 1948.

[5] S. R. Best, "Low Q electrically small linear and elliptical polarized spherical dipole antennas," IEEE Trans. Antennas Propag., vol. 53, pp. 1047–1053, Mar. 2005.

[6] S. R Best; "The Radiation Properties of Electrically Small Folded Spherical Helix Antennas" IEEE Trans. of Antennas and Propagations, VOL. 52, NO. 4, April 2004 page 953

[7] E.E.Altshuler E. E. Altshuler, "Electrically small self-resonant wire antenna optimized using a genetic algorithm," IEEE Trans. Antennas Propag., vol.50, no. 3, pp. 297–300, Mar. 2002.

[8] John R Koza "Genetic algrothims and genetic programming" Aug 4th 2004 http://www.geneticprogramming.com/coursemainpage.html [Sep. 2, 2010]

[9] H. Rmili, O. E. Mrabet, J.-M. Floc'h, and J.L. Miane, "Study of an Electrochemically-Deposited 3D-Fractal Tree Monopole Antenna," *IEEE Transactions on Antenna and Propagation*, vol. 55, no. 4, Apr. 2007, pp. 1045-1050

[10] E. Altshuler, T. O'Donnell, 'An Electrically Small Multi-Frequency Genetic Antenna Immersed in a Dielectric Powder,' *IEEE Antennas and Propagation Magazine*, vol. 53, no. 5, Oct. 2011, pp.33-40

[11] J. Bernard, J. Lewis, J. Adams, et al, "Conformal Printing of Electrically Small Antennas on Three-Dimensional Surfaces", Advanced Materials Volume 23, Issue 11, pages 1335–1340, March 18, 2011

[12] Pfeiffer C. , Grbic A "Novel Methods to Analyze and Fabricate Electrically Small Antennas" Spokane Washington, *Antennas and Propagation Conference July 3rd – 8th 2011*

[13] [Online] RedEye Express "Open Market Rapid PrototypeQuotes"*http://express.redeyeondemand.com.* 2010 [Oct 12 2010]

[14] [Online]Dalmar Mfg Co "Dalmar plating information site" *http://www.dalmar.net* [Oct 9 2010]

[15] [Online] Z Corporation "The fastest, most affordablecolor3Dprinting"*http://www.zcorp.com/documents/931_9062-ZPrinterBroch.pdf*, 2010 [June 2 2010]

[16] Wohlers, T, 2009, Wohlers Report 2009, Rapid Prototyping, Tooling & Manufacturing State of the Industry, *Annual Worldwide Progress Report, Wohlers Associates Inc.,* Colorado, USA

[17] MTT Manufacturing Technologies group " Direct Metals Manufacturing Technology " *http://www.mtt-group.com/selective-laser-melting.html* Dec. 22 2010 [Oct 9 2010]

[18] M. Leskelä, M. Ritala, *"Atomic Layer Deposition Chemistry:* Recent Developments and Future Challenges" Volume 42, Issue 45, pages 5548–5554, November 24, 2003 [Article first published online: 18 NOV 2003]

[19] [Online] Tyco electronics "Laser Direct Structuring"h*ttp://www.tycoelectronics.com/mid/lasertech.asp*. 2011 [Oct. 9, 2010]

[20] William D. Westwood (2003). *Sputter Deposition,* AVS Education Committee Book Series, Vol. 2.

[21] B. Willis, C. Furse, *" Design and rapid prototyping for 3D space efficient antennas", Submitted paper,* IEEE Trans. Antennas and Propagation [2012.]

[22] J. Saberin and C. Furse, "Challenges with Optically Transparent Patch Antennas", *Submitted to IEEE Antennas and Propagation Magazine*, 2010

[23] W.Wang , Z. Jiang *Design and construction of a wheeler cap test set up;* Masters thesis University of Gävle; 2010-09-23

[24] L.Griffiths, C.Furse, *"Performing 3-D FDTD Simulations in Less than 3 Seconds on a Personal Computer and its Application to Genetic Algorithm Antenna Optimization,"* Applied Computational Electromagnetics Society Journal, Vol. 20, No. 2, pp. 128-135, July 2005

[25] B. Willis, C. Furse*; "Rapid Prototyping for Small 3D Antennas"* [to be published]

[26] A. Moscicki, J. Felba, T. Sobierajski, J. Kudzia, A. Arp, and W. Meyer, "Electrically Conductive Formulations Filled Nano Size Silver Filler for Ink-Jet Technology," *in Proc.,5th International Conference on Polymers and Adhesives in Microelectronics and Photonic*s, October 2009, pp. 40-44.

[27] A. Koptioug, P. Jonsson, J. Sidén, T. Olsson and M. Gulliksson, " On The Behavior of printed RFID Tag Antennas, Using Conductive Paint", *Mid Sweden University, SE-831 25 Östersund, Sweden*

[28] K. I. Rybakov, V. E. Semenov, S. V. Egorov, A. G. Eremeev, I. V. Plotnikov, and Yu. V. Bykov, "Microwave Heating of Conductive Powder Materials", *AIP Journal of Applied Physics*, vol. 99, Issue: 2, Jan. 2006, pp. 023506-1 – 023506-8

[29] M.A. Gayness, R. H. Lewis, R. F. Saraf, and J.M. Roldan, " Evaluation of Contact Resistance for Isotropic Electrically Conductive Adhesives," *IEEE Transactions on Components, Packaging, and Manufacturing Technology* ,vol.18, Issue: 2, May 1995, pp. 299 – 304

[30] R. Malamud and I. Cheremisov, "Anti-Corona Protection of High Voltage Stator Windings and Semi-Conductive Materials for its Realization", in *Proc.,IEEE International Symposium on Electrical Insulation*, Apr. 2000, pp.32-35.

[31] K. Bock, "Polytronics-Electronics and Systems on Flexible Substrates", IEEE VLSI-TSA International *Symposium on VLSI Technology*, Apr. 2005, pp.53-56

[32] R. Gordon, "Criteria for choosing transparent conductors," *MRS Bulletin*, August 2000.

[33] K. Bock, "Polytronics-Electronics and Systems on Flexible Substrates", *IEEE VLSI-TSA International Symposium on VLSI Technology*, Apr. 2005, pp.53-56

[34] A. R. Duggal and L. M. Levinson, "A Novel High Current Density Switching Effect in Electrically Conductive Polymer Composite Materials", *AIP Journal of Applied Physics*, vol. 82, Issue: 11, Dec. 1997, pp. 5532 – 5539

[35] D. Micheli, C. Apollo, R. Pastore, and Mario Marchetti, "Modeling of Microwave Absorbing Structure using Winning Particle Optimization Applied on Electrically Conductive Nano-structured Composite Material", in Proc., XIX *International Conference on Electrical Machines* ,Sept. 2010,pp.1-10.

[36] Y. Li, R. Zhang, L. Shu, W. Lin, O. Hilbreth, H. Hiang, J. Lu, Y. Xiu, Y. Liu, J. Moon, and C.P. Wong, "Nano Materials and Composites for Electronic and Photo Packaging", in Proc., 9th *IEEE Conference on Nanotechnology*, July. 2009, pp.1-3.

[37] Huang, Haiyu; Nieman, Karl; Hu, Ye; Akinwande, Deji; , "Electrically small folded ellipsoidal helix antenna for medical implant applications," *Antennas and Propagation (APSURSI), 2011 IEEE International Symposium on* , vol., no., pp.769-771, 3-8 July 2011

[38] Sigmarsson, H.; Kinzel, E.; Chappell, W.; Xianfan Xu; , "Selective laser sintering of patch antennas on FR4," *Antennas and Propagation Society International Symposium, 2005 IEEE* , vol.1A, no., pp. 280- 283 Vol. 1A, 3-8 July 2005

[39] Y. Ouyang, E. Karayianni, and W. J. Chappell, "Effect of Fabric Patterns on Electrotextile Patch Antennas," *in Proc. IEEE Antennas and Propag. Soc. Int. Symp*., 2005, vol. 2B, pp. 246–249.

[40] A. Tronquo, H. Rogier, C. Hertleer, and L. Van Langenhove, "Applying Textile Materials for the Design of Antennas for Wireless Body Area Networks", Proceedings of the European Conference on Antennas and Propagation, EUCAP 2006, Nice, France, p. 159, November 2006.

[41] P. Salonen, Y. Rahmat-Samii, M. Schaffrath, and M. Kivikoski, "Effect of Textile Materials on Wearable Antenna Performance: A case study of GPS antennas," *in Proc. IEEE Antennas Propag. Soc. Int. Symp*., 2004, vol. 1, pp. 459–462.

[42] A. Tronquo, H. Rogier, C. Hertleer and L. Van Langenhove, "Robust planar textile antenna for wireless body LANs operating in 2.45 GHz ISM band", *IEEE Electronic Letters*, Vol. 42, Issue. 3, February 13,2006, pp. 142-143

[43] X. Xu, M. Davanco, X. Qi, S. R. Forrest, "Direct transfer patterning on three dimensionally deformed surfaces at micrometer resolutions and its application to hemispherical focal plane detector arrays," *Organic Electronics, vol. 9, no. 6, pp. 1122–1127*, December 2008.

[44] B. Y. Ahn, et al. "Omnidirectional Printing of Flexible, Stretchable, and Spanning Silver" Microelectrodes" Sciencemag Science 323, 1590 (2009).

[45] [online available] *http://www.electro-coatings.com/electroless-nickel-plating.php* [last accessed Jan 4th 2012]

[46] [Online]Available:*http://www.coolpolymers.com/XyloyM950.asp* [Accessed on April 6th 2011]

[47] [Online]Available:h*ttp://www.chomerics.com/products/premier.htm* [Accessed on Oct 11 2011]

[48] J.R. Honiball "The Application of 3D Printing in reconstructive surgery", *PhD Dissertation, University of Stellenbosch* , Mar. 2010

[49] [Online] Objet Geometries Inc "Connex 500 3D printer" *http://www.objet.com/3D-Printer/Objet_connex500/ 2011*, [Jun 2 2010]

[50] [Online Available] *http://www.foresight.org/gadaprize.php.* [Accessed: 11th Jan. 2011]

[51] [Online Available] *http://pvcdrom.pveducation.org/CHARACT/4pp.HTM* [Accessed: 21th Jan. 2012]

[52] R. H. Johnston, L. P. Ager and J. G. McRory, *"A New Small Antenna Efficiency Measurement Method*", IEEE Antennas and Propagation Society International Symposium, 1996.

CHAPTER 6

THE FUTURE OF 3D PRINTED ANTENNAS

3D rapid prototyping holds significant promise for future antenna designs and production. This is demonstrated with genetic algorithm optimized 3D antennas and a traditional 14-16 GHz horn printed in plastic metalized with conductive paint. The 3D printed antennas function very similar to comparable designs built from solid metal if the metallic coating is sufficiently conductive and sufficiently thick. In addition to the flexibility that 3D prototyping brings to antenna design, this paper describes how this new and emerging method for building antennas can provide fast and affordable antennas for testing, teaching, and fast turn-around prototyping.

6.1 Introduction

Advances in 3D rapid prototyping are occurring at a fast pace. The use of conductive materials in advanced manufacturing is at the forefront of this progress. This is of great interest and importance to antenna design and allows multiple options for manufacturing conductive parts. The advances in 3D rapid prototyping allow designs that would have been impossible or impractical to build in the past, as well as providing

inexpensive, fast turn-around design of more standard antennas (such as horns and waveguides). This method can provide engineers, educators, and students the ability to design and manufacture virtually any small antenna rapidly and easily.

The challenge for antenna development using rapid prototyping is that typically, the materials used in these methods have higher losses than solid metal. Lossy conductors reduce antenna performance, as seen in [1], and [2].

The motivation for this research is the difficulty in building true 3D arbitrarily shaped antennas. The 3D antennas that are built are done so by hand or by complicated time-consuming processes. A few attempts at true 3D antennas have been made and have initially demonstrated the performance improvements of these designs. The following indicates the mathematical, simulated, and tested results for 3D antennas. Thal has calculated limits for spherical antennas in [3], and [4], indicating that a spherical helix can better approach the small antenna limit set by Chu [5]. Thal provides a baseline for small spherical 3D antennas. Best demonstrates low Q small spherical dipoles [6] and properties of a small spherical helix [7]. The spherical helix antenna is made up of hand-soldered pieces of wire. The design indicates a Q within 1.5 times the fundamental limit and efficiencies at or above 90%. The research in [8] also appears to be manufactured by hand-soldering pieces of wire. Similar complex, hand-soldered antennas are seen in the evolved antenna from the NASA Ames genetic algorithm [9]. A 3D fractal tree is randomly grown by an electrochemically deposited conductor [10]. The novel property of this 3D antenna is the impedance bandwidth improvement over a similar 2D antenna. A 3D hemispherical antenna was recently built by printing a meander-line antenna pattern on a curved glass surface with a silver ink [11]. Another recent 3D spherical

antenna was built using a process called direct transfer patterning. The process uses a stamp to get the desired pattern onto a curved surface. It then requires a 6-step process including a plasma etch and gold plate to finalize the design on Polyethylene Terephthalate (PET) [12]. These antennas all demonstrate the improvements that may be gained by using the 3D design, especially [13] which uses high dielectric powder surrounding the antenna. Unfortunately, the manufacturing methods required to produce these 3D antennas have previously been so cumbersome or expensive that 3D antennas were limited to simple geometries (such as horns and dishes). More complex designs were typically regarded as far-fetched and impractical. But now, cutting edge rapid prototyping creates 3D manufacturing opportunities that have not previously been available in the antenna design world.

Recently, we demonstrated the ability to create random-shaped 3D antennas and more efficiently use the space available [14], which will allow them to better fit ever-smaller electronic devices. The antenna was optimized by a genetic algorithm [15], which is basically a 3D extension of previous 2D work [16] [14]. The antennas were then built using 3D rapid prototyping techniques. One was built using SLS to create a solid conductor, and a second was built from plastic using 3D printing. The plastic antennas were then coated with a conductive paint to form a conductive shell. The 3D printed antenna is shown in Figure 38 and the measured results in Figure 39. To create an efficient antenna when coating, it is important to take into account the desired frequency, the conductivity of the material used, and the required thickness of the coating relative to the skin depth [1].

Figure 38: 3D printed cubical antenna above a ground plane, from [14]. © 2012 IEEE. Reprinted with permission.

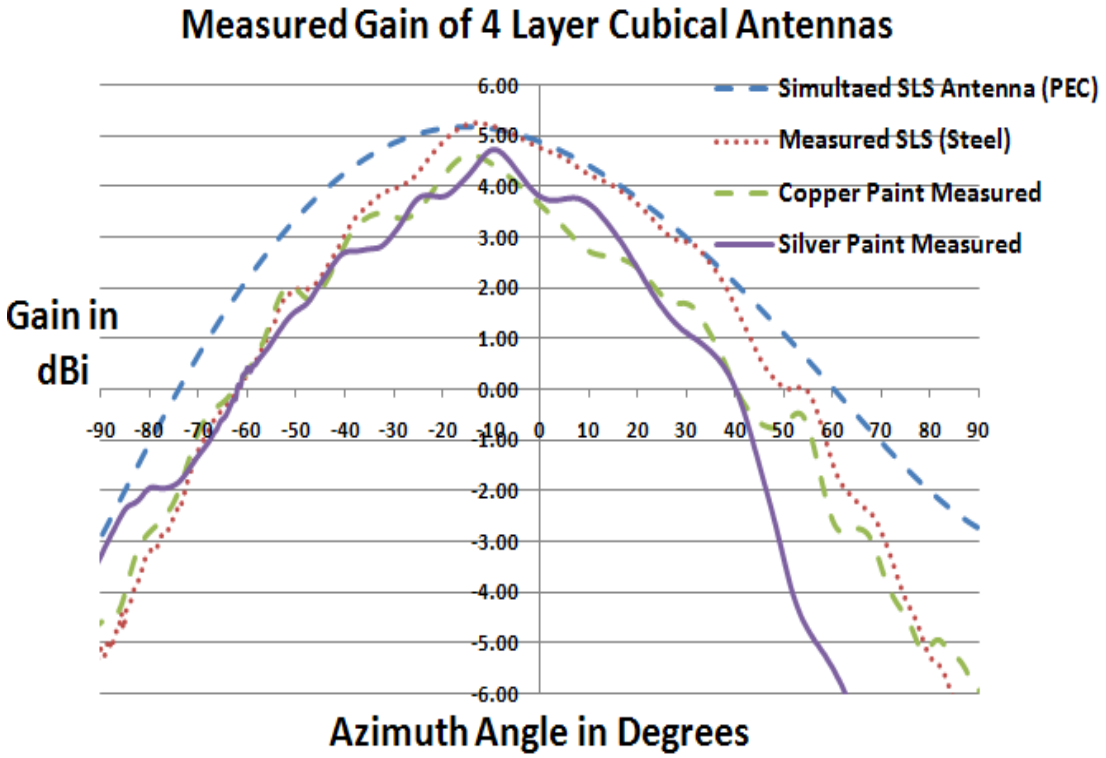

Figure 39: Measured gain for the cubical antenna in Figure 38 compared to the simulated design with perfect conductivity (PEC). The lower conductivity of the paint coating reduces the gain of the antenna. Silver painted antenna is ~6% less efficient than the solid SLS antenna.

A similar dipole type antenna functioning in the 500MHz band was also built and tested [15]. Also a simulation was performed indicating an application in a cellular phone [15].

The 3D antenna created in [14] is just one example of a 3D design and demonstrate that arbitrarily shaped antennas can be built easily. Similarly, we designed and built a 3D dipole type antenna functioning in the 500MHz band where skin depth would pose more of a problem [15]. The measured results for a plastic antenna with 3 layers of silver paint agree accurately with simulated data.

In this paper, we further demonstrate the ease of 3D printing for rapid prototyping antennas by building a simple horn which is shown in Section 6.2. The Ku band horn is replicated similar to a purchased aluminum horn. The new design is 3D printed from plastic and metalized using paint. Section 6.3 presents the use of a low-resolution (~0.01 inches) lower cost 3D printer to build an antenna that is the same 3D arbitrarily shaped antenna geometry as found in [14]. Section 6.4 discusses our thoughts on what we believe the near-term future development is for rapid prototyping using conductive materials.

6.2 3D Printed Horn Metalized with Paint

Previous work has demonstrated the use of 3D printing for complex 3D designs, [14], [15], [1] but that is not the only application of 3D rapid prototyping. This section describes a horn antenna built as a test antenna for testing another antenna. A horn with a special flange connector was required, and we did not have time to wait to order one. So, a Ku band horn was built from plastic using an Objet® Connex 500 3D printer. The horn

is designed similar to the Advanced Technical Materials® Ku band horn (12.4-18 GHz) [17]. The purchased horn has part number 62-442-6. It is interfaced with a WR62 waveguide feed. The length is 5.75 inches, with a width of 2.88 inches and a height of 2.11 inches. Here the average gain is given as 20dB. The printed horn antenna is built from with a length of ~5.75 inches and is a square height and width of ~2.8 inches, and is fed from a waveguide feed. The horns are shown side by side in Figure 40. The plastic horn is measured with no paint, with a single layer of paint, and with 3 layers of paint.

The details of the copper paint are found at [18]. The plastic horn with 1 layer of paint is shown in Figure 41. The ridges from the 3D printing resolution are visible where the paint has not completely covered the plastic. The horn with 3 layers of paint is shown in Figure 42 and the plastic has been completely covered. The horn is measured with no paint, with 1 layer of paint, and with 3 layers of paint. The gain in dB for each measurement is plotted in Figure 43 and compared with the aluminum horn. Horn antenna and other standard type designs have 3D models readily available from such software as Antenna Magus [19]. This software provides a huge searchable database for antennas where the parameters can be modified to function for a specific frequency. The exported model data used in a 3D printer give a design engineer a multitude of models which can be 3D printed. This provides the ability to build any antenna needed for testing, prototyping, or teaching.

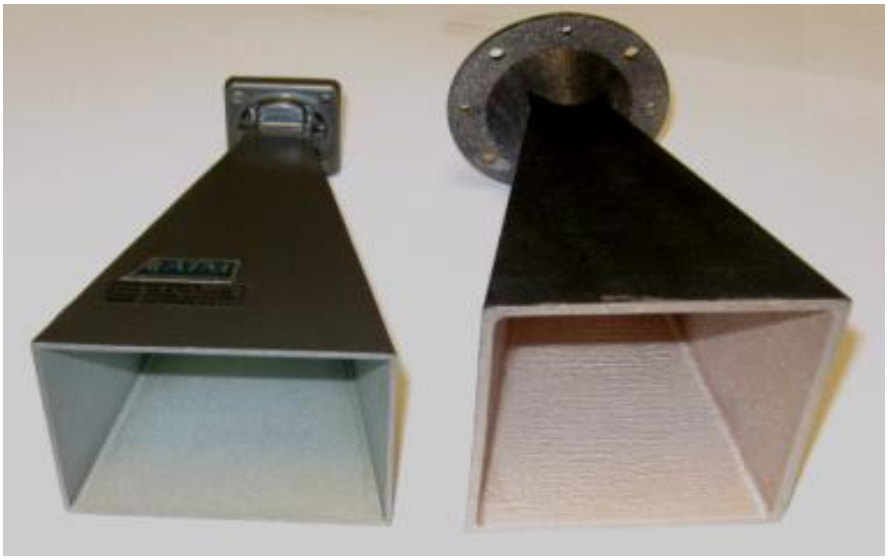

Figure 40: Aluminum horn [16] on left next to a printed plastic horn with paint metallization on right.

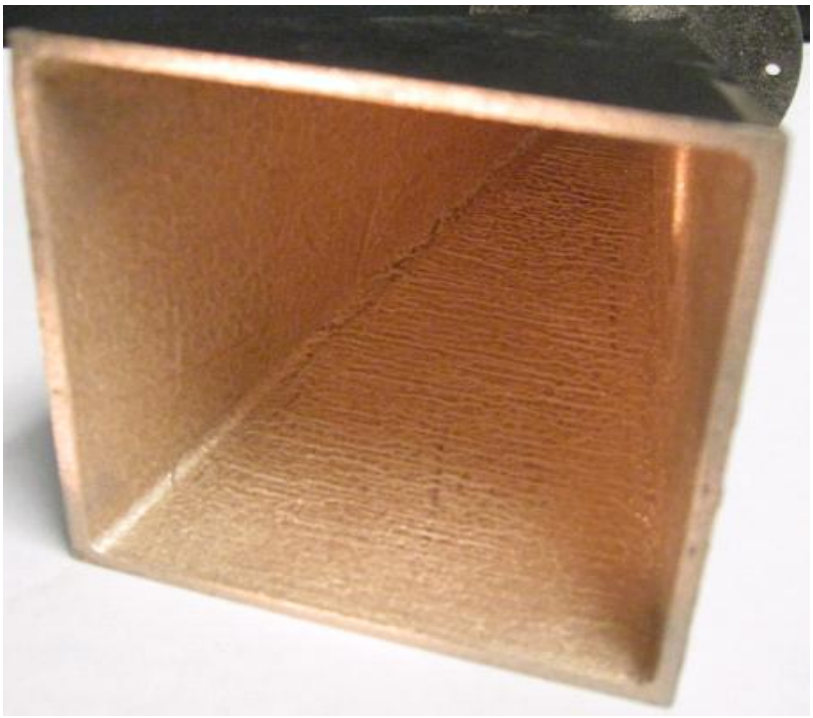

Figure 41: plastic horn with a single layer of copper paint. It is easy to see the plastic ridges due to the 3D printing where the paint has not completely covered the plastic.

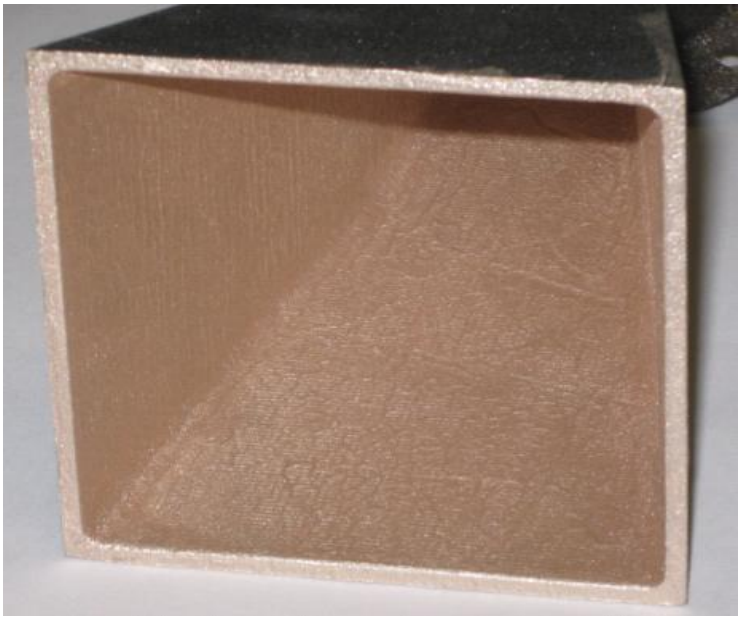

Figure 42: Plastic horn with 3 layers of copper paint. The surface is visibly smoother.

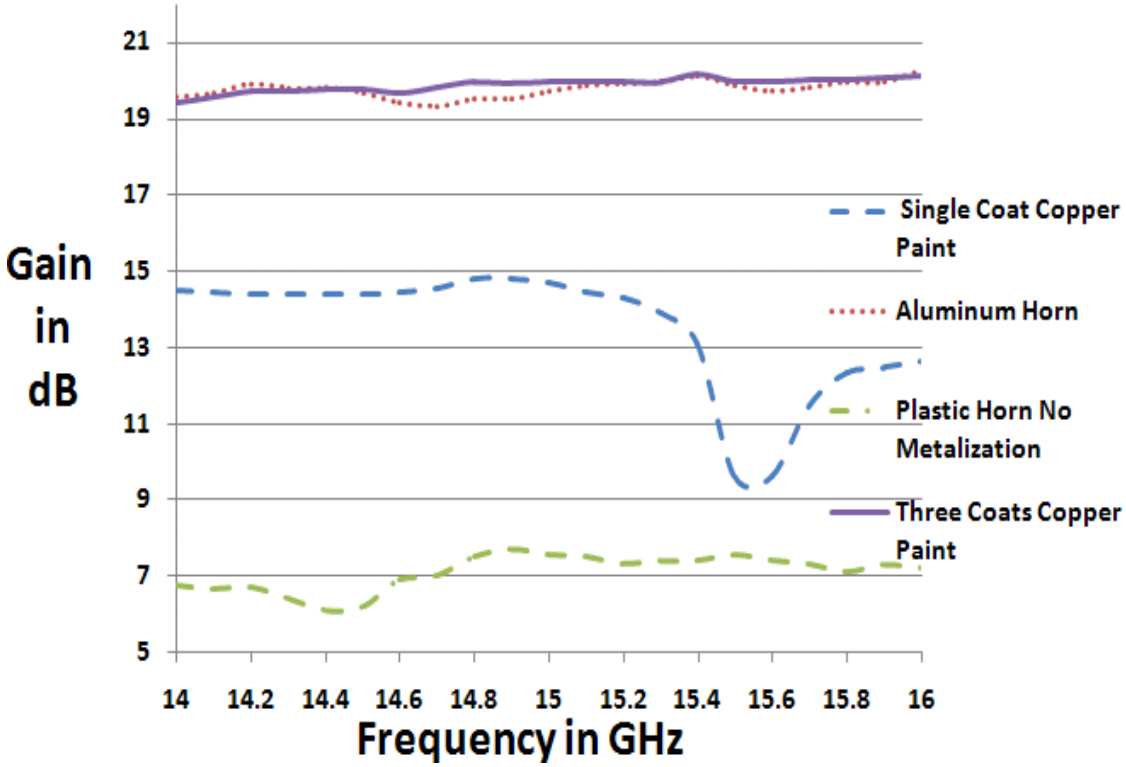

Figure 43: Comparison of plastic horn with 1 layer and 3 layers of paint to an aluminum horn from [17]. © 2012 IEEE. Reprinted with permission.

6.3 Resolution Test of 3D Printed Antenna

In order to compare the resolution of different antennas, we built the same antenna, shown in Figure 44, with high- and low-resolution printers. The high-resolution printer is the Object Connex 500, which uses Vero white plastics and has a resolution of 0.0006 inches. The lower resolution printer (a less expensive 3D printer) is the Dimension® 1200es [20] which uses layer deposition 3D printing and ABS plastic and has a resolution of 0.01 inches. There is a significant emerging market for household 3D printers which are readily available and inexpensive. Most of the home-based 3D printers can be purchased for just over a thousand dollars. They typically use ABS plastic and have resolution in the Z axis better than 0.01 inches [21].

The cubical layered patch antenna from [14] is printed from Vero white plastic using an Object® Connex 500 3D with a resolution of 0.0006 inches. In this research, we print the same antenna design used in [14] with a Dimension® 1200es 3D printer from blue ABS plastic. The surface roughness is definitely noticeable along with the ridges on the side from the separate layers shown in Figure 44 top. The Connex 500 3D print is shown in Figure 44 bottom. The antennas were both metalized using 3 layers of silver paint. The S11 of these antennas is shown in Figure 45.

Figure 45 indicates a slight decrease in bandwidth for the lower resolution antenna. Resolution plays an obvious factor in the design of antennas and manufacturing tolerances limit the tools available for rapid prototyping.

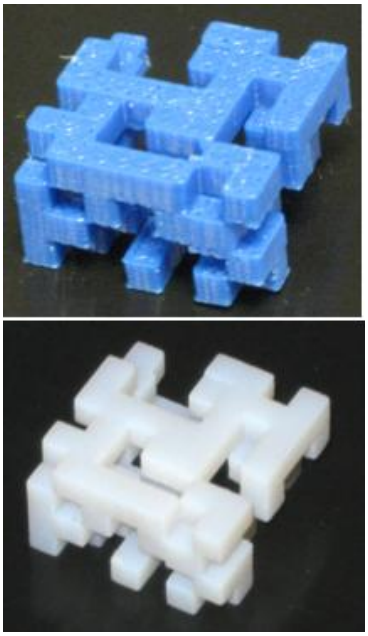

Figure 44: The resolution difference for two 3D printed layered patches is apparent. The top antenna is built from ABS plastic using a Dimension 1200es printer with resolution of about 0.01 inch. The bottom layered patch is in Vero white plastic printed on a Connex 500 and originally tested in [14]. It has a resolution of 0.0006 inch.

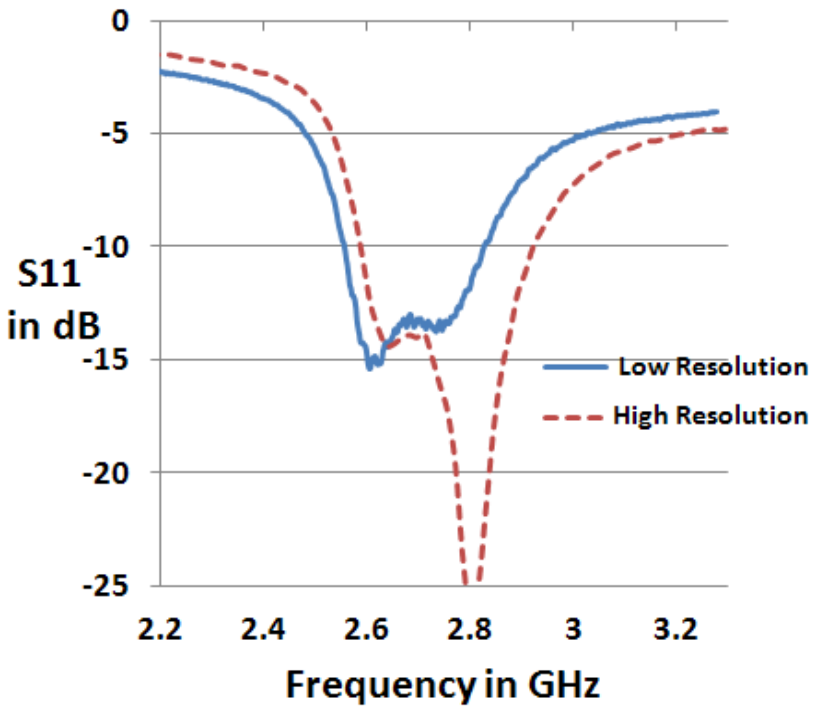

Figure 45: S11 comparison between the antennas in Figure 44.

The 3D printed antennas have frequency limitations due to resolution and the use of a plastic base material coated with a thin conductive layer. The frequency limitations in the low-frequency spectrum are due to the outer conductive layer. The paints currently used have about 25% lower conductivity than standard copper [18]. Figure 46 indicates that there is a large increase in skin depth as the frequencies drop below ~100 MHz. The method of applying a conductive layer to plastic is more valuable when the frequencies are greater than ~100MHz. The paint technology is improving as highly conductive nano-particle metals such as silver are utilized in the low loss paint medium. The improvement in technology will allow higher conductives to be utilized without the need for sintering after their application.

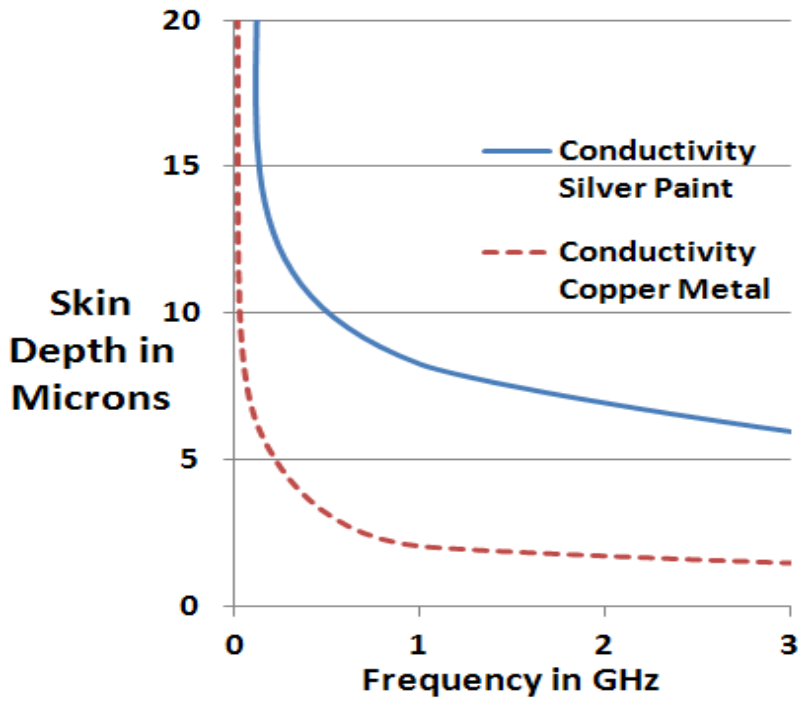

Figure 46: Skin depth for silver paint and copper paint

As the resolution of the antenna decreases (such as shown in Figure 44), the antenna surface roughness increases. This has more impact at higher frequencies than lower frequencies. This surface roughness sets an upper frequency limit on the ability to 3D print effective antennas. The root mean square RMS surface roughness contributes to loss because of the phase errors. Figure 47 indicates the Phase Error Loss (PEL) derived from gain reduction due to reflector anomalies [22].

$$PEL = \left(\frac{-4\pi\varepsilon_o}{\lambda} \right) \qquad 6.1$$

Here the term ϵ_o is the effective RMS tolerance and λ is the wavelength. The loss is plotted for an RMS of 0.5 mm and 1mm. As indicated by Figure 47, the loss falls off rapidly above ~20 GHz.

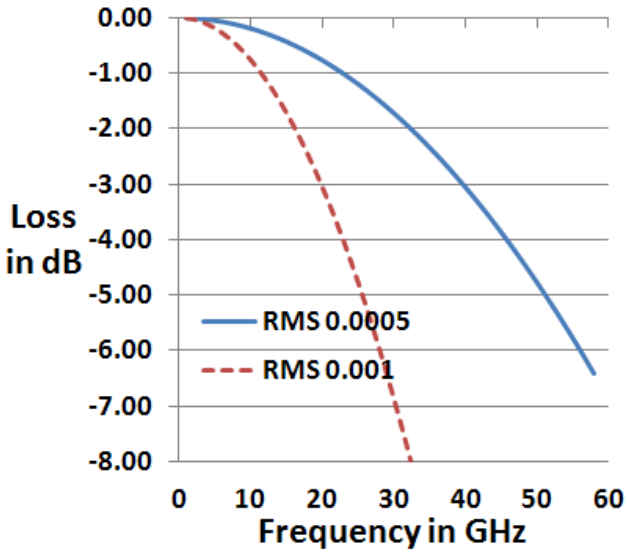

Figure 47: Phase error loss due to RMS of a rough surface, typically used on aperture antennas.

Figure 48 indicates loss calculation for a rough microstrip line. The loss is calculated as a ratio of power absorbed for a rough surface divided by the power absorbed for a smooth surface. The derivation uses periodic rough surface with rectangular grooves [23]. The derivation matches the periodic layers from 3D printing. The Hammerstad equation [23] gives the P_a which is the power absorbed as a ratio of smooth and rough and is only a function of the RMS height h and the skin depth δ.

$$\frac{P_a rough}{P_a smooth} = 1 + \frac{2}{\pi} \arctan 1.4 \frac{h}{\delta} \qquad 6.2.$$

Further research in rough surface scattering has indicated that the actual loss ratio can be greater than 3 and the loss ratio is better defined using a random rough surface and a numerical equation to solve for the loss ratio [24]. Figure 48 illustrates that as the

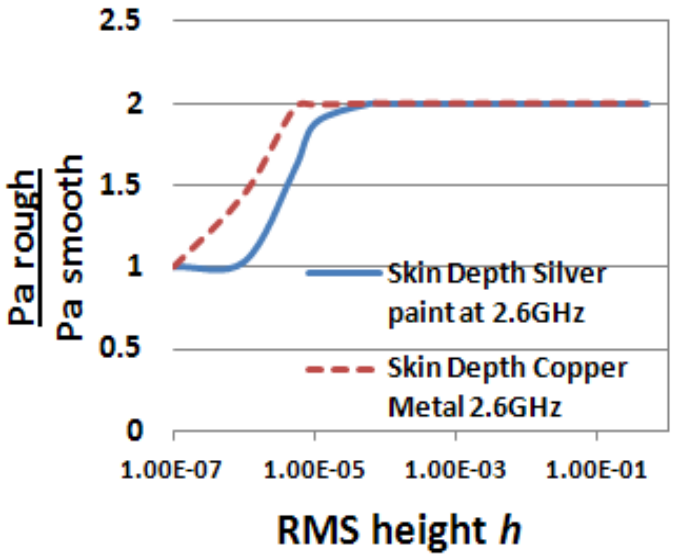

Figure 48: The plot of Hammerstad and Bekkadal equation using skin depth for standard copper and silver paint. The equation is typically used with microstrip circuits. The plot indicates the additional losses seen when using a rough conductive surface.

skin depth increases, the loss due to surface roughness decreases. However, after the RMS value is above $1X10^{-4}$, the power absorbed by the conductor is twice that for a completely smooth conductor surface.

The future for rapid prototyping is to continue to refine the materials and machines used. So resolutions are continually improving.

6.4 Future of 3D Rapid Prototyping

The future in rapid prototyping is a simple manufacturing technique that uses a single process to fabricate complex 3D shapes with both conductive and dielectric materials. As previous work has shown, current methods are already capable of prototyping antennas up to about 15 GHz. With improving resolution, higher frequency antennas can be built. Currently, desktop 3D printers are available for a few thousand dollars which offer 0.005 inch resolution [25].

Another application of 3D prototyping for antennas is rapid design and deployment of test antennas that are required in most laboratories. The rapid prototyping tool paired up with a simple-to-use antenna and waveguide software simulation design tool would allow designers to rapidly build and test new antenna designs or build needed antenna hardware. The simple concept is to have a software package that allows the user to pick a basic antenna such as a directional horn, then let the user change a few variables that will determine the operating frequency, gain, etc. The design would be simulated and verified in software. Once it is verified in software, a CAD model is exported which will allow the rapid prototyping machine to manufacture the antenna for

test and use. The simple manufacturing and design tool allows the user to have an antenna in hand for test in a matter of hours.

This form of rapid 3D prototyping could easily be applied to a more advanced simulation option using a 3D solver similar to CST [26] . The tool would allow an easy build of an optimized complicated antenna design such as the antenna completed in [14] and shown in Figure 44, thus providing an easily built 3D arbitrarily shaped antenna model for test and verification.

The gateway to creating the single-step fabrication process is to use an inexpensive 3D printer with a heated nozzle and low temperature conductive materials. The materials we identified in [1] for injection molding conductive parts. Two such materials are Xyloy® [27] and Premier® [28]. As material prices decrease, the cost to print will follow. Print time is increasing and new modifications for basic 3D printers have dramatically increased the accuracy and extrude rate [25]. The weight of using plastic is a benefit in 3D printing design. As conductive plastic technology is refined, there will be more weight savings with less loss due to conductor.

A logical next step would be to utilize the open source Rep Rap style 3D printer [29] and modify the extruder and nozzle to function with the different materials at a higher temperature. A basic reprap 3D printer is shown in Figure 49. The ABS plastic currently used melts at ~110º C. The Xyloy® and nickel plated carbon fiber melt at ~255-270º C.

The future in rapid 3D prototyping is to easily use conductive materials. We believe 3D printing is an ideal candidate because of its ability to create complex shapes from the inside out.

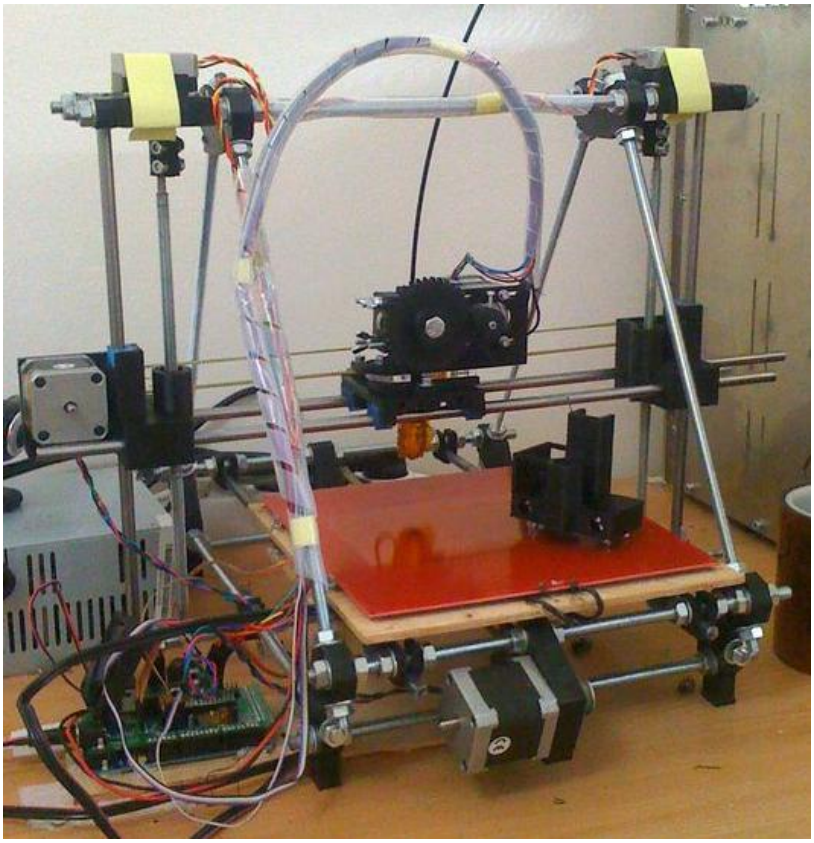

Figure 49: A inexpensive home-built reprap open source 3D printer, from [29]**.** © www.reprap.org

Also, 3D printing currently has the ability to print multiple types of materials in a single build process [12]. This allows items such as dielectric loaded spheres, waveguides, or horns to be built in a single step. Multiple materials would allow the ability to build coaxial connectors right into the antenna. The multiple material options would allow for many complicated designs to be fabricated in a few hours, perhaps minutes. Being able to use multiple materials during the build process is a valuable advantage and opens the door to many possible useful electronic devices and designs. Rapid development allows first article prototyping and test of the antenna before mass production.

6.5 Conclusion

3D rapid prototyping holds significant promise for future antenna designs. This paper demonstrates that a 3D printed Ku band 14-16 GHz horn compares within 0.5 dB to its metal fabricated aluminum counterpart.

One of the important parameters of a 3D build process is its resolution. The resolution of today's printers is typically between 1 mm (less expensive) and 0.5 mm (more expensive) and limits the antennas to use below 15 GHz or 30 GHz, respectively.

In addition, loss in the conductive coating from imperfect conductors and thin layers relative to skin depth can limit the performance of the antenna. Conductive coated printed plastic antennas are frequency limited by skin depth on the low end (~100MHz) and by resolution on the high end (~25GHz).

The gateway to the single-step 3D printing lies in low-temperature injection molding of conductive materials paired with 3D printing. The ability to combine printing of a good conductor and a low loss dielectric opens the doors to many additional antenna designs and to complete systems that include the antenna and its connectors and feed network, perhaps even additional associated circuitry. We can expect to see additional 3D antennas in the near future. These designs have much more flexibility than traditional 1D or 2D designs, can occupy and optimize unused oddly-shaped voids in devices, can improve the performance over their 1D and 2D counterparts, are low cost, low weight, and quick to build. They offer improvements in antennas for aircraft and space vehicles (weight) and consumer devices (filling oddly shaped voids, low cost). The speed, convenience, and low cost of this prototyping method also holds promise for antennas in education and antennas used for testing. There is a tremendous opportunity

to directly couple software used for antenna design directly with the equipment that can build the antenna.

6.6 References

[1] B. Willis, C. Furse, “A Comparison of Rapid Prototyping Build Techniques” Submitted paper, *IEEE Trans. Antennas and Propagation* [2012.]

[2] J. Saberin,C. Furse, “Challenges with Optically Transparent Patch Antennas”, *IEEE Antennas and Propagation Magazine*, in press

[3] H.L. Thal,, "New Radiation Limits for Spherical Wire Antennas," *IEEE Trans. Antennas Propag.*,vol.54, no.10, pp.2757-2763, Oct. 2006

[4] H.L. Thal,, "A Reevaluation of the Radiation Q Bounds for Loop Antennas," *IEEE Antennas and Propagation Magazine*, vol.51, no.3, pp.47-52, June 2009

[5] L. J. Chu, “Physical limitations of omni-directional antennas,” *J. Appl. Phys*., vol. 10, pp. 1163–1175, Dec. 1948.

[6] S. R. Best, “Low Q Electrically Small Linear and Elliptical Polarized Spherical Dipole Antennas,” *IEEE Trans. Antennas Propag.*,vol. 53, pp. 1047–1053, Mar. 2005.

[7] S. R Best, “The Radiation Properties of Electrically Small Folded Spherical Helix Antennas” *IEEE Trans. Antennas Propag.,Vol. 52, no. 4*, April 2004 page 953-960

[8] E. E. Altshuler, “Electrically small self-resonant wire antenna optimized using a genetic algorithm,” *IEEE Trans. Antennas Propag., vol.50*, no. 3, pp. 297–300, Mar. 2002.

[9] [Online available] *http://www.geneticprogramming.com/coursemainpage.html* [Sep. 2, 2010]

[10] H. Rmili, O. E. Mrabet, J.-M. Floc’h, J.L. Miane, “Study of an Electrochemically-Deposited 3D-Fractal Tree Monopole Antenna,” *IEEE Trans. Antennas Propag.*,vol. 55, no. 4, Apr. 2007, pp. 1045-1050

[11] J. Bernard, J. Lewis, J. Adams, et al, “Conformal Printing of Electrically Small Antennas on Three-Dimensional Surfaces”, *Advanced Materials,* Vol. 23, Issue 11, pp. 1335–1340, March 18, 2011

[12] C.Pfeiffer, A.Grbic, "Novel Methods to Analyze and Fabricate Electrically Small Antennas" Spokane Washington, *IEEE Antennas and Propag. Soc. Int. Symp., July 3rd – 8th 2011*

[13] E. Altshuler, T. O'Donnell, 'An Electrically Small Multi-Frequency Genetic Antenna Immersed in a Dielectric Powder,' *IEEE Antennas and Propagation Magazine,* vol. 53, no. 5, Oct. 2011, pp.33-40

[14] B. Willis, C. Furse, " Rapid prototyping for small 3D antennas", Submitted paper, *IEEE Trans. Antennas and Propagation [2012.]*

[15] B. Willis, C. Furse, " Design and rapid prototyping for 3D space efficient antennas", Submitted paper, *IEEE Trans. Antennas and Propagation [2012.]*

[16] L.Griffiths, C.Furse, "Performing 3-D FDTD Simulations in Less than 3 Seconds on a Personal Computer and its Application to Genetic Algorithm Antenna Optimization," *Applied Computational Electromagnetics Society Journal, Vol. 20, No. 2,* pp. 128-135, July 2005

[17] [Online available] *http://www.atmmicrowave.com/wave-horn.html#Standard_Horns*, [last accessed Jan 5, 2012]

[18] [Online Available] *http://www.spraylat.com/Products/ElectronicMaterials/Technology/ConductiveCoatingTechnology.aspx* [Accessed Sep 15th 2011]

[19] [Online Available] *http://www.antennamagus.com/* [Accessed: 11th Feb. 2012] [Online avialabe] *http://www.objet.com/3D-printer/Objet_connex500/ 2011*, [Jun 2 2010]

[20] [Online available] www.dimensionprinting.com; last accessed Nov 16 2011;

[21] [Online Available] *http://3d-printing.com.au/about-us/tech-info* [Accessed Sep 15th 2011]

[22] T.A. Milligan "Modern Antenna Design" McGraw Hill, New York, New York; 1985, pp 233

[23] E. O. Hammerstad and F. Bekkadal, *Microstrip Handbook. Trondheim, Norway: Univ. Trondheim, 1975, pp. 4–8.*

[24] L. Tsang, X. Gu, H. Braunisch, "Effects of Random Rough Surface on Absorption by Conductors at Microwave Frequencies*"; IEEE Microwave and Wireless Components Vol* 16, No. 4, April 2006.

[25] [Online Available] *http://www.desktopfab.com/printers.php* [Accessed: 11th Feb. 2012]

[26] [Online Available] *http://www.cst.com/* [Accessed: 11th Dec. 2011].

[27] [Online Available] *http://www.coolpolymers.com/XyloyM950.asp* [Accessed on April 6th 2011]

[28] [Online Available] h*ttp://www.chomerics.com/products/.htm* [Accessed on Oct 11 2011]

[29] [Online Available] :H*ttp://reprap.org/wiki* [Accessed: 11th Jan. 2012].

CHAPTER 7

SUMMARY AND CONCLUSIONS

Small efficient antenna design is needed for the shrinking size of electrical devices in use today. Rapid prototyping for antenna design is an emerging area that is becoming more relevant as antenna designs continue to better utilize 3D space and grow more complex in shape. The ability to manufacture an antenna of arbitrary 3D shape was introduced in this dissertation along with a comparison of rapid prototyping manufacturing techniques and their effect on efficiency of the antenna.

Chapter 3 has demonstrated that GA design and rapid prototyping can be used as a viable method for manufacturing 3D antennas. Both 3D printed plastic coated with metallic paint and metal antennas produced by selective laser sintering are viable options. The skin depth effects must be taken into account in these designs. Antennas with 3 layers of paint were better than those with 1 or 2. As expected, the 3D designs had lower frequencies and higher bandwidth than a 2D antenna with the same footprint. The GA design has a *ka* of 0.94 when the full-size ground plane is removed. This work will be submitted to the IEEE Transactions on Antennas and Propagation [23].

3D rapid prototyping opens up a wide array of potential antenna designs. This paper demonstrated the use of a GA to optimize the designs, but any good optimization method could also be used. The designs in this paper were limited to simple cubical volumes for convenience. Other, much more complex volumes could be used instead. In addition to flexibility of design, the antennas produced using printed plastics coated with metallic paint are much lighter than metal antennas produced using either SLS or (if it were possible to build them at all) traditional metals.

The use of SLS or 3D printing for antenna designs opens up many options in simple, cost-effective 3D antenna design. Both of these methods can be used to produce antennas that have metal or metal-like bodies, and they can be used above a substrate material (as in this paper) if back radiation is not desired. The conductivity of the paint is sufficiently high that it acts as a good conductor. The challenge is that the paint layer of 8 microns is less than the skin depth at 2GHz. They are also lighter weight than equivalent antennas built of metal. Antennas with a combination of conductors and insulators could be more difficult to build this way. The emerging ability to print conductive materials could soon open up the option to build antennas with a wider variety of distributed materials, perhaps even printing circuits along with the antenna. 3D rapid prototyping provides an opportunity to pursue complicated 3D antenna designs that would otherwise be impractical. It enables a new, wide array of potential antenna designs.

Chapter 4 has demonstrated the ability to create 3D antennas with randomized shape that are closer to the Chu limit [2] than 1D, 2D, or simpler 3D antennas in the same space using 3D rapid prototyping. The optimized cubical monopole above ground plane

showed that plastic coated with a conductive paint was ~6% less efficient than solid metal.

The UHF 3D dipole was optimized to perform over a large bandwidth. At the lowest operating frequency, the antenna has a *ka* of 0.92 and a quality factor of 11.0, almost equivalent to the Goubau antenna [55]. A 3D cavity of random shape from a basic flip phone was filled with a GA optimized antenna. The goal was not to make the antenna small but utilize the space to function in the cell phone frequency bands. The optimization was able to create an antenna that functions in the frequency ranges used by modern cell phones with efficiency of 83% and above. This research demonstrates the emergence of printing with plastic conductive materials. The latest in 3D rapid prototyping could soon provide an opportunity to pursue even more complicated 3D antenna designs with more imbedded combinations of metal and plastic.

Chapter 5 indicates the ability to create antennas using true 3D manufacturing techniques such as 3D printing or selective laser sintering. These true 3D antennas allow designers to create arbitrary shaped antennas. This chapter also focuses on minimizing the losses associated with using lower conductive materials and or thin conductive coatings. The measurements provide a good indication of the conductivity and thickness that is needed for a material to be efficient. We found that for the paints, the thinner the paint, was the lower the conductivity and hence the larger the skin depth. The larger skin depth caused the antenna to have less efficiency. Other materials which may be utilized for antenna fabrication such as Xyloy® and LDS with gold measured at practically the same conductivity and radiation efficiency as a copper. The measured gain of the materials such as paint compared extremely well with the standard copper sheet. Based

on the measurements, the larger the painted area through which the current propagates, the lower the efficiency will be when compared to a standard piece of copper.

Chapter 6 discusses how 3D rapid prototyping holds significant promise for future antenna designs. Then demonstrates that a 3D printed Ku band 14-16 GHz horn compares within 0.5 dB to its metal fabricated aluminum counterpart.

One of the important parameters of a 3D build process is its resolution. The resolution of today's printers is typically between 0.1 inches (less expensive) and 0.0006 inches (more expensive) and limits the antennas to use below 15 GHz or 30 GHz, respectively.

In addition, loss in the conductive coating from imperfect conductors and thin layers relative to skin depth can limit the performance of the antenna. Conductive coated printed plastic antennas are frequency limited by skin depth on the low end (~100MHz) and by resolution on the high end (~25GHz).

The gateway to the single-step 3D printing lies in low temperature injection molding of conductive materials paired with 3D printing. The ability to combine printing of a good conductor and a low loss dielectric opens the doors to many additional antenna designs and to complete systems that include the antenna and its connectors and feed network, perhaps even additional associated circuitry. We can expect to see additional 3D antennas in the near future. These designs have much more flexibility than traditional 1D or 2D designs, can occupy and optimize unused oddly-shaped voids in devices, can improve the performance over their 1D and 2D counterparts, are low cost, low weight, and quick to build. They offer improvements in antennas for aircraft and space vehicles (weight) and consumer devices (filling oddly shaped voids, low cost). The

speed, convenience, and low cost of this prototyping method also holds promise for antennas in education and antennas used for testing. There is a tremendous opportunity to directly couple software used for antenna design directly with the equipment that can build the antenna.

The major contributions of this dissertation are:

5) Introduction of the concept of using 3D rapid prototyping for antenna design. The antennas designed in Chapter 3 [23] are the first of their kind and represent a major shift in antenna design through easy, low-cost 3D manufacturing.
6) Demonstration of the applications where 3D antennas may be most useful. These include the ability to fully utilize the 3D sphere often associated with small antenna theoretical limits. 3D antennas can more closely approach this limit. In addition, the ability to fill random-shaped voids such as those in handheld personal communication devices may provide better antennas for a wide variety of applications[24]. Finally, the advantages of low weight and quick turn-around time are also noted. This information is found in Chapter 4 [24].
7) Evaluation of the impact of conductivity and thickness of the metallic components of the design (typically metal paints or plating) on the efficiency and performance of the antennas [25]. Chapter 5 outlines the requirements as a function of frequency, and describes the frequency range where 3D rapid prototyping is effective today [25].
8) Contemplation and evaluation of the future of 3D rapid prototyping for antenna design is found in Chapter 6 [26]. 3D prototyping is rapidly advancing, and this

chapter evaluates what changes are coming, what changes are needed, and what these changes may mean for future antenna design and manufacture.

In short, this dissertation provides the tools and methods for a new type of 3D antenna manufacturing that has the potential to revolutionize small to moderate scale antenna design by providing the great flexibility in form and design for 3D manufacturing that has to date been available only for 2D (planar) designs. Table 15 shows a comparison of the antennas designed in this research.

Table 15: Comparison of GA optimized antenna designs and manufacuring methods

Antenna Design	ka	Bandwidth	Efficiency	Q
4-layer Cubical Patch 91.5mm length ground plane	4.02	15%	96%	4.4
4-layer Cubical Patch 20.3mm^2 ground plane	0.91	6%	95%	0.70
3-Layer UHF Dipole	0.96	51%	95%	1.385
2-layer cubical patch 20.3mm2 ground plane	0.9326	12%	95%	0.70
1-layer cubical patch 20.3mm2 ground plane	1.05	11%	95%	0.70
Goubau Antenna	0.76	63%	94%	0.75